8-2019

Identifying And Targeting Adaptive Changes To Bet Inhibition In Ovarian Cancer

Christopher LaFargue

IDENTIFYING AND TARGETING ADAPTIVE CHANGES TO BET INHIBITION IN OVARIAN CANCER

by

Christopher John LaFargue, M.D

APPROVED:

_____
Anil K. Sood, M.D.
Advisory Professor

_____
Menashe Bar Eli, Ph.D.

_____
Wei Hu, M.D., Ph.D.

_____
Kwong K. Wong, Ph.D.

_____
Prahlad T. Ram, Ph.D.

APPROVED:

_____
Dean, The University of Texas
MD Anderson Cancer Center UTHealth Graduate School of Biomedical Sciences

IDENTIFYING AND TARGETING ADAPTIVE CHANGES TO BET INHIBITION IN OVARIAN CANCER

A

THESIS

Presented to the Faculty of

The University of Texas

MD Anderson Cancer Center UTHealth

Graduate School of Biomedical Sciences

in Partial Fulfillment

of the Requirements

for the Degree of

MASTER OF SCIENCE

by

Christopher John LaFargue, M.D.
Houston, Texas

August, 2019

Dedication

To my son Jack LaFargue; through hard work, anything is possible.

Acknowledgements

I would like to thank my parents Craig and Linda for always pushing me to strive for excellence. I am forever grateful to my wife Ashley for your unwavering support no matter how busy I am or how many late nights I have to work. I am thankful to my children Brooke, Bella, and "squeezy" Jack for always being there to put a smile on my face.

Thank you Dr. Sood for your scientific mentorship during my research years of fellowship. I never imagined that I could develop the skills to think like a translational scientist in only two years. Nor did I ever think I would be able to read Cancer Cell papers and actually understand them. I have always believed that through hard work comes excellence, and your guidance and direction is certainly a testament to that.

Thank you to Alejandro and Shaolin for not only always being there to help me with an experiment or answer the same question for the 10th time, but for teaching me not be afraid of the mice. Thank you Mangala for being a friend and an ear to listen. You are an excellent scientist and are wise beyond your years. Lastly, I would like to thank everyone in the lab who helped me develop as a scientist over the past two years, I am beyond appreciative.

IDENTIFYING AND TARGETING ADAPTIVE CHANGES TO BET INHIBITION IN OVARIAN CANCER

Christopher John LaFargue, M.D.

Advisory Professor: Anil K. Sood, M.D.

Abstract

Purpose: To identify combination strategies using Bromodomain and Extra-Terminal Domain (BET) inhibitors in a mechanism driven fashion to maximize anti-tumor activity, and to determine the efficacy of BET inhibitor combinations in pre-clinical ovarian cancer mouse models.

Experimental Design: We used a novel, previously uncharacterized pan-BET inhibitor, CN210, for all *in vitro* (MTT, apoptosis, protein expression, reverse phase protein array (RPPA) analysis and *in vivo* (orthotopic mouse model)) experiments. The poly (ADP-ribose) polymerase (PARP) inhibitor olaparib, as well as the mechanistic target of rapamycin (mTOR) inhibitors rapamycin and INK-128 were also used. Statistical analyses of *in vitro* and *in vivo* experiments were performed using either Student *t* test or Mann-Whitney test with a p value < 0.05 considered significant (sig). RPPA data was analyzed by Cluster 3.0 using median value and the heat maps were generated by Java Treeview.

Results: Eight ovarian cancer cell lines were screened using MTT assays with CN210 to determine the most and least sensitive. HeyA8 and OVCAR8 ip1 cells displayed the greatest degree of sensitivity whereas OVCAR4 and OVCAR5 cells were the most resistant. We next examined the previously reported synergistic combination of olaparib and BETi and found only modest effects using *in vitro* and *in vivo* applications. RPPA analysis was then performed on all four cell lines after CN210 treatment revealing that activation of the mTOR pathway appeared to be an early adaptive response to BET inhibition. Decreased cell viability and increased apoptosis were seen with the addition of an

mTORC1 or dual mTORC1/2 inhibitor to CN210 compared with CN210 alone. Notably, we found that decreased Akt activation and increased Rictor activation after CN210 treatment served as a possible marker for the increased response seen with CN210 and INK-128 combination. Lastly, we demonstrated a significant reduction in tumor weight using CN210/INK-128 combination treatment in an orthotopic ovarian cancer mouse model.

Conclusions: RPPA analysis identified mTOR activation as an early adaptive change to BET inhibition in ovarian cancer cells. Combination of BET and dual mTORC1/2 inhibitors led to robust anti-tumor responses, supporting the inclusion of these drugs into future clinical trials.

Table of Contents

List of Figures

List of Tables

Introduction

Epidemiology and treatment of ovarian cancer

Ovarian cancer is the deadliest gynecologic malignancy in the developed world. It is estimated that in 2019 there will be 22,530 new cases of women with ovarian cancer, and 13,980 deaths resulting from this disease in the United States (1). The three main histologic types of ovarian cancer are epithelial, germ cell, and sex-cord stromal, with the epithelial type accounting for ~90% of all ovarian cancers. As the overwhelming majority of women afflicted with ovarian cancer will have an epithelial histology, the focus of the work presented here will be primarily concentrated on this specific type. Although both the incidence and mortality for epithelial ovarian cancer in the United States has decreased over the past 15 years (2), it still remains the 5th leading cause of cancer death in women (1). One significant reason for such a large mortality rate relative to the incidence is that epithelial ovarian cancer is often diagnosed at an advanced stage (Stage 3 or 4). In fact at the time of diagnosis, 37% of women will already have stage 3 disease, and 28% have stage 4 (2). The reasons for this unfortunate characteristic of ovarian cancer are primarily two-fold. First, typical symptoms of ovarian cancer such as abdominal bloating, feeling full quickly, diarrhea/constipation, and vague abdominal discomfort, overlap with many common and benign gastrointestinal disorders. As such, these symptoms are often attributed to non-worrisome diseases and may be ignored for a long period of time without further clinical evaluation. Second, despite numerous well-intentioned efforts (3-5), there remains no valid screening test for ovarian cancer in the general or "low-risk" population. Accordingly, although women diagnosed with stage I ovarian cancer have a five year survival rate of 83-89%, the majority will be diagnosed at an advanced stage with five year survival rates ranging from 18-46% (2, 6). It is now well known that women who harbor a genetic mutation in either the *breast cancer susceptibility gene 1 (BRCA1)* or *breast cancer susceptibility gene 2 (BRCA2)* are at a substantially increased risk for ovarian cancer, and fall into a separate category than the general population (7).

For women who do not have a genetic predisposition to ovarian cancer, historical risk factors have included age >50, early menarche or late menopause, infertility, and nulliparity (8).

Table 1. Five year overall survival in ovarian cancer patients by FIGO Stage at diagnosis (2, 6). This figure contains information obtained from Torre, L. A., B. Trabert, C. E. DeSantis, K. D. Miller, G. Samimi, C. D. Runowicz, M. M. Gaudet, A. Jemal, and R. L. Siegel. 2018. Ovarian cancer statistics, 2018. *CA Cancer J Clin* 68: 284-296; and Heintz, A. P., F. Odicino, P. Maisonneuve, M. A. Quinn, J. L. Benedet, W. T. Creasman, H. Y. Ngan, S. Pecorelli, and U. Beller. 2006. Carcinoma of the ovary. FIGO 26th Annual Report on the Results of Treatment in Gynecological Cancer. Int J Gynaecol Obstet 95 Suppl 1: S161-192.

FIGO Stage at Diagnosis	5 Year Overall Survival (%)
All stages	47
Ia	89
Ib	86
Ic	83
IIa	70
IIb	65
IIIa	46
IIIb	41
IIIc	32
IV	18

The primary treatment of epithelial ovarian cancer is surgical cytoreduction with the intent to remove all visible disease, followed by adjuvant platinum and taxane chemotherapy. Surgical cytoreduction involves removing the uterus, bilateral fallopian tubes and ovaries, omentum, and any other organ that can be safely removed which contains tumor (small or large intestine, spleen, diaphragm, section of liver). The time to recurrence (progression-free survival, or PFS) and time to death (overall survival, or OS) are the longest in women who have no visible disease remaining at the conclusion of their initial operation (9). Although there are a variety of factors that affect the recurrence rate of ovarian cancer, ultimately 70% of women with advanced stage disease will develop relapsed disease and require further treatment (10).

Until recently, the treatment of recurrent epithelial ovarian cancer was relatively simple, with only a handful of available chemotherapeutic agents to choose from. The mainstay treatments consisted of retreatment with a platinum agent (if deemed platinum-sensitive), paclitaxel, topotecan, liposomal doxorubicin, and gemcitabine (10). As shown in Figure 1, 2014 marked a turning point in the treatment of both primary and recurrent ovarian cancer. New classes of drugs such as angiogenesis inhibitors, PARP inhibitors, and immunotherapies have now attained FDA approval, with different and complex indications for each of them. In light of this emergence of novel therapies, the number of women currently living with ovarian cancer along some spectrum of its disease course is a remarkable 225,000, far exceeding the annual incidence of 22,530 mentioned above. While these novel therapies offer significant promise for many women, they too are limited by the development of adaptive resistance, in which the cancer cells acquire new ways to render the drugs ineffective (11). Recurrent ovarian cancer is almost never a curable disease, and the majority of women will spend the remainder of their life switching from one drug to another once progression occurs. This unfortunate course of the disease underscores the importance of developing novel therapies that can prolong the duration of time spent living with cancer without sacrificing quality of life.

Figure 1. Evolution of ovarian cancer drug approvals (12, 13). This figure was adapted with permission from Anil K. Sood, MD. It also contains information obtained from Administration, F. D. 2019. Drugs@FDA; and Kelland, L. 2007. The resurgence of platinum-based cancer chemotherapy. *Nat Rev Cancer* 7: 573-584.
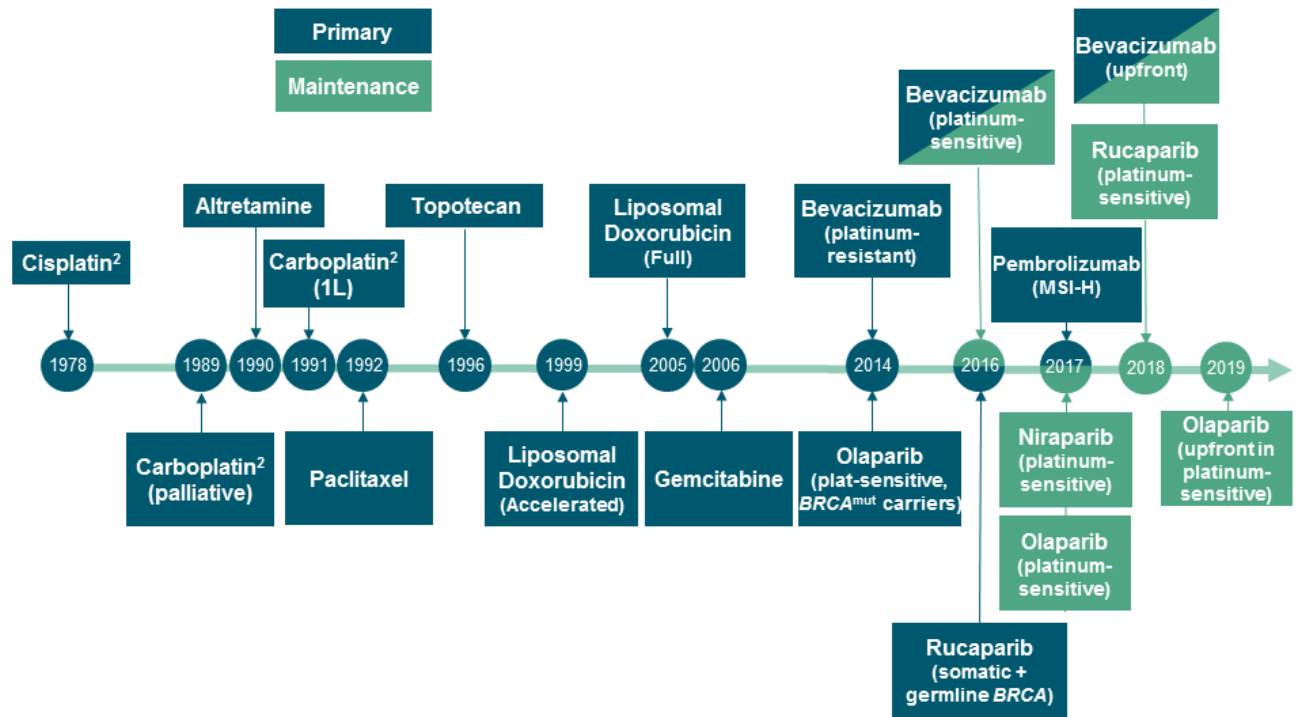
Therapy predicting tool and application in ovarian cancer

Since the completion of the human genome project nearly 20 years ago, combined with the high-throughput advances of genomic sequencing today, the field of targeted cancer therapy has become the mainstay for the development of new cancer treatments (14). The concept behind targeted cancer therapy lies in developing anti-cancer drugs that specifically target altered cellular pathways in each individual cancer, rather than treating all patients with a standard or "one shoe fits all" chemotherapy. For example, even though two women may both have epithelial ovarian cancer, if their underlying tumors have different molecular alterations, then each woman would receive a treatment specifically tailored to their abnormal cellular pathway. While there has been a myriad of new anti-cancer drugs developed using this methodology, only few have shown meaningful impact on patient survival and been incorporated into clinical practice (14). Rather than discarding these "failed" drugs altogether, efforts were undertaken to repurpose them for use in other cancer types or against alternative aberrant pathways through the development of the therapy predicting tool (TPT).

Figure 2. Overview of the therapy prediction tool (15). This figure was adapted from Villar-Prados, A., S. Y. Wu, K. A. Court, S. Ma, C. LaFargue, M. A. Chowdhury, M. I. Engelhardt, C. Ivan, P. T. Ram, Y. Wang, K. Baggerly, C. Rodriguez-Aguayo, G. Lopez-Berestein, S. Ming-Yang, D. J. Maloney, M. Yoshioka, J. W. Strovel, J. Roszik, and A. K. Sood. 2019. Predicting Novel Therapies and Targets: Regulation of Notch3 by the Bromodomain Protein BRD4. *Mol Cancer Ther* 18: 421-436. It was printed with permission from Elsevier, the owner of Molecular Cancer Therapeutics, through license number 4582190290701.
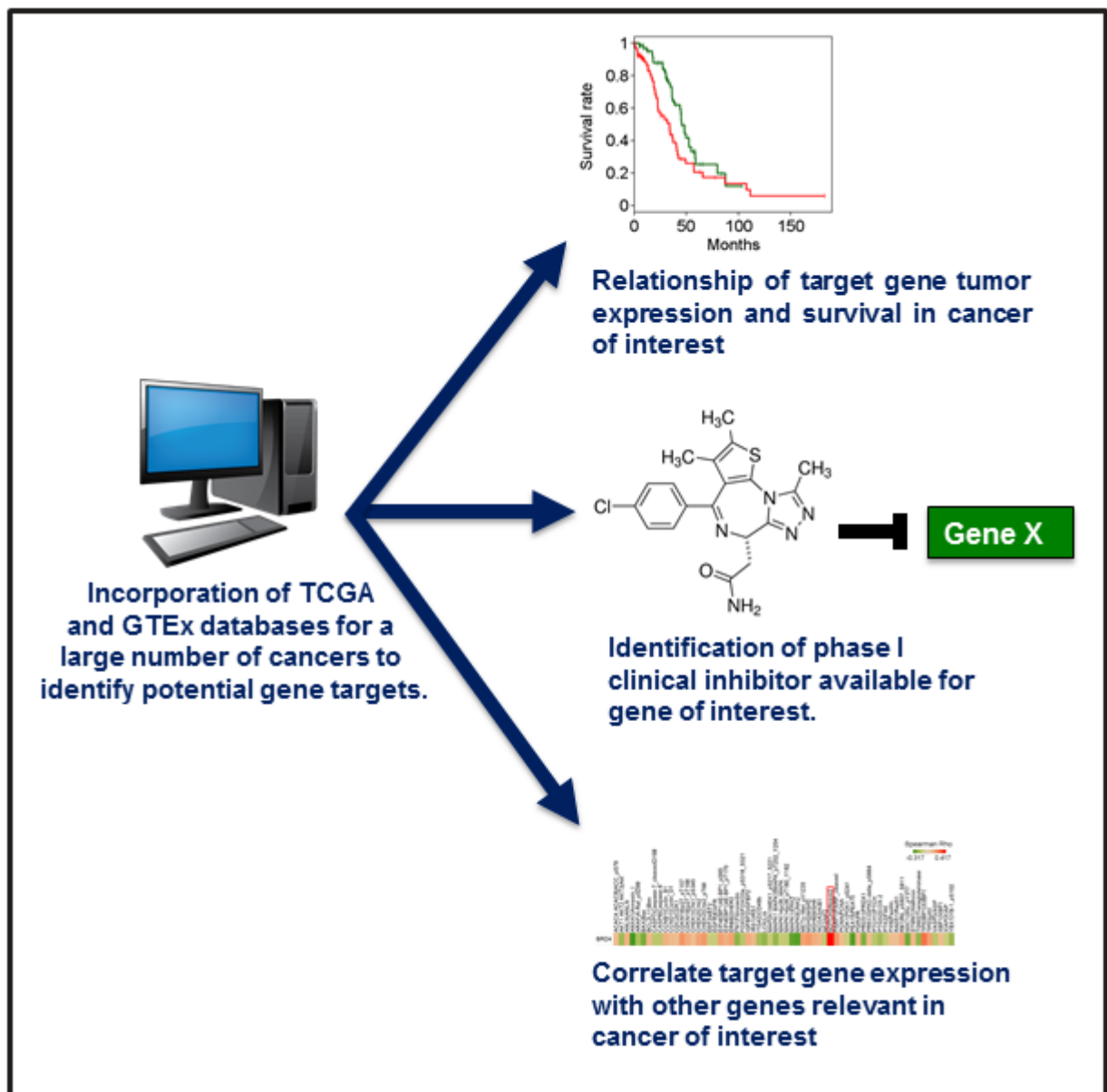
In brief, the TPT is an algorithm that uses publically available gene and protein expression datasets (such as The Cancer Genome Atlas and the Genotype-Tissue Expression project) to identify genes or proteins that are differentially expressed between normal and cancer cells, and that also confer a difference in patient survival (15, 16) (Figure 2). Previous research has demonstrated the utility of applying the TPT to repurpose targeted cancer therapies for use in ovarian cancer (15). Specifically, BRD4 (a member of the bromodomain and extra-terminal domain (BET) proteins) was found to be overexpressed in ovarian cancer compared to normal ovarian tissues (Figure 3A), and ovarian cancer patients with high levels of BRD4 had significantly worse overall survival (15) (Figure 3B). These and other findings led to the conclusion that inhibitors of the BET family of proteins (BETis) may have potential clinical use in the treatment of ovarian cancer.

Figure 3. Overexpression of Brd4 in ovarian cancer. (A) GTEx analysis comparing expression of Brd4 in ovarian cancer (red box) to expression in normal ovarian tissue (blue box). (B) Overall survival curves for patients with ovarian cancer from TCGA datasets comparing high Brd4 expression (red curve) to low Brd4 expression (green curve) in patient tumors (*P* <0.02) (15). This figure was adapted from Villar-Prados, A., S. Y. Wu, K. A. Court, S. Ma, C. LaFargue, M. A. Chowdhury, M. I. Engelhardt, C. Ivan, P. T. Ram, Y. Wang, K. Baggerly, C. Rodriguez-Aguayo, G. Lopez-Berestein, S. Ming-Yang, D. J. Maloney, M. Yoshioka, J. W. Strovel, J. Roszik, and A. K. Sood. 2019. Predicting Novel Therapies and Targets: Regulation of Notch3 by the Bromodomain Protein BRD4. *Mol Cancer Ther* 18: 421-436. It was printed with permission from Elsevier, the owner of Molecular Cancer Therapeutics, through license number 4582190290701.

BET proteins and their role in cancer

The bromodomain and extra-terminal domain family of proteins consist of Brd2, Brd3, Brd4, and Brdt, and function as epigenetic readers during the process of gene transcription. Specifically, they bind to acetylated histone residues and other nuclear proteins at gene promoters and enable mRNA transcription to proceed by releasing the stall of RNA polymerase II at the transcription start site (17-19). All four proteins share two conserved N-terminal bromodomains (BD1 and BD2) which serve as the location for binding to acetylated regions (17, 18). Once BET proteins are recruited to the promoter site through this interaction, they interact with various other proteins and transcription factors involved in the gene transcription process (p-TEFb, Mediator complex, Jmjd6, TWIST, p53, c-Jun, AP2), most notably RNA polymerase II, to allow transcription to continue (Figure 4A) (17, 18). BET proteins are located primarily at promoter and enhancer regions, and even more so at super-enhancers, which are regions comprised of multiple enhancers that display a high density of Mediator complex and master transcription factors (18-20). This is particularly important as the genes regulated by super-enhancers encompass the fundamental cell identity and also tend to be the genes most downregulated when BET proteins are inhibited (21-23). BET proteins play a critical role in cellular growth, as demonstrated by the embryonic lethality that results with homozygous deletion of Brd2 or Brd4 (24-27).

Figure 4. Mechanism of BET proteins and their inhibitors. (A) BET proteins bind to acetylated histones at promoter or enhancer regions and recruit factors such as P-TEFb and MEDIATOR complex. Interactions between these factors, in addition to interaction with RNA Polymerase II, releases the stall of RNA Pol II at the transcription start site allowing transcription to proceed. (B) In the presence of BET inhibitors, BET proteins are no longer able to bind to acetylate histones or other factors at promoter regions, preventing the transcription of the specific downstream genes. RNA Pol II, RNA polymerase II. AC, acetylated histone. TSS, transcription start site.
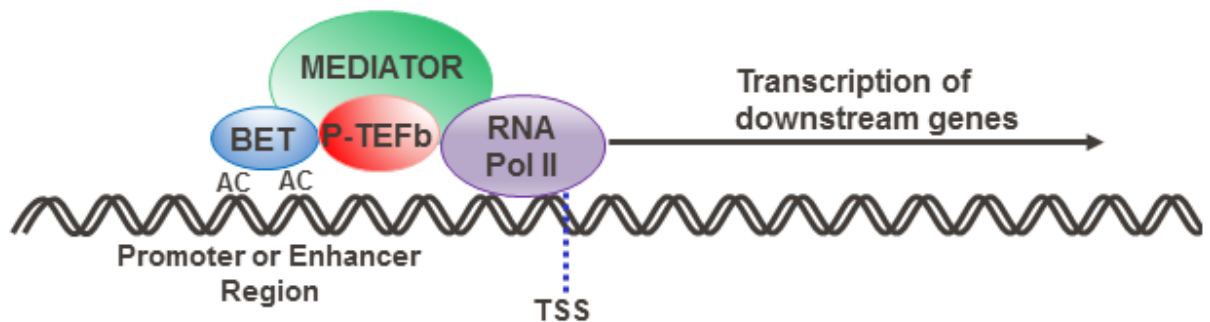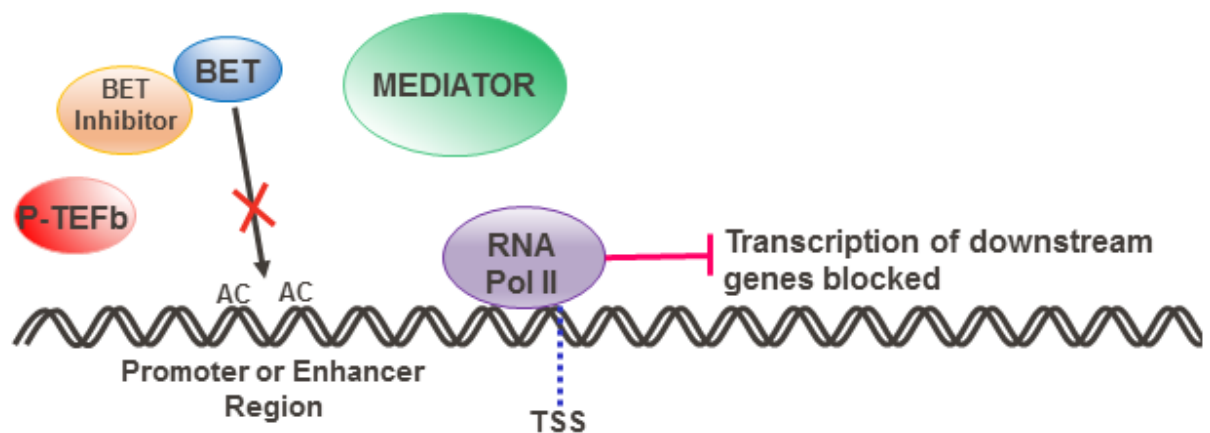
Multiple small molecule inhibitors of BET proteins (BETis) have been synthesized and studied in the pre-clinical setting for their use as anti-cancer therapy. BETis function by binding to specific bromodomains within the BET family, preventing the binding to acetylated histones and other critical transcription factors. As the BET proteins are sequestered by BETis, the transcriptional machinery is

no longer able to release the stall of RNA polymerase II leading to termination of the specific downstream transcript (Figure 4B). The primary rationale for targeting BET proteins in cancer cells derives from three main findings. First, various human cancers demonstrate overexpression of Brd2 and Brd4, as mentioned above (15, 20, 28). Second, genetic expression profiling of various tumors has revealed BET proteins as essential genes that neoplastic cells require for their continued survival (28-31). Lastly, NUT midline carcinoma (NMC) is a type of undifferentiated squamous cell carcinoma defined by a genetic translocation between either the *BRD4* or *BRD3* gene and the *NUT* gene on chromosome 15q14 (32, 33). The resulting Brd4-NUT or Brd3-NUT fusion protein blocks cellular differentiation and treatment using a small-molecule inhibitor of Brd4, JQ1, demonstrated an anti-proliferative effect in patient-derived xenograft models (17). In addition, JQ1 treatment of both leukemia and multiple myeloma cell lines resulted in a significant decrease in *MYC* expression, which is known to play a significant role in the neoplastic processes of both cancers (31, 34, 35). BET proteins play a crucial role in the survival of various cancer types, and mechanisms to inhibit their effect have demonstrated promising anti-tumor activity.

The preclinical findings regarding the use of BETis as anti-cancer agents have led to the initiation of multiple phase I clinical trials. OTX015 has been tested in acute leukemia, non-Hodgkin's lymphoma, NMC, castration-resistant prostate cancer (CRPC), non-small cell lung cancer (NSCLC), and glioblastoma (36-40). The highest response rates were found in NMC ranging from 33-50%, while in the hematologic malignancies response rates ranged from 0-12%, and no responders were identified in the remaining solid tumor groups (36-40). Despite the fact that there were no responders in the remaining solid tumor groups, five patients with CRPC and two patients with NSCLC had prolonged stable disease (37). CPI-0610 was tested in non-Hodgkin's lymphoma with two complete and one partial response (41). GSK525762 and TEN-010 are two additional BETis that were tested in patients with NMC and demonstrated a 20-67% response rate (42, 43). Lastly, BAY1238097 was examined in eight patients with stage IV solid tumors and showed no responses, however the study

was terminated early due to dose limiting toxicities (DLTs). Although this last study was terminated due to DLTs, the other studies above report that BETis are generally well-tolerated with predominant side-effects including bone marrow suppression (anemia, neutropenia, thrombocytopenia), gastrointestinal disturbance (diarrhea), fatigue, and bilirubin increase (36-43). While it appears that the strongest signal from BETi use lies in patients with NMC or hematologic malignancies, it is important to consider the paucity of data in patients with other solid tumors.

Poly (ADP-ribose) polymerase (PARP) inhibitors in ovarian cancer

The PARP family of proteins (PARP1, PARP2, PARP3) are part of the cellular DNA repair machinery that function in the repair of single-stranded DNA breaks (SSBs) that occur within cells on a regular basis (44). When PARP is inhibited or inactive, the cell is unable to repair these SSBs which causes a stall at the replication fork during DNA replication and the subsequent progression to a double-stranded DNA break (DSB) (45, 46). The cell is able to repair these DSBs however, using the high-fidelity homologous recombination DNA repair (HRR) pathway (45, 46). It is known that ~10-20% of women will harbor germline mutations in either *BRCA1* or *BRCA2*, which are integral proteins in the HR repair pathway (47-49). Without the ability to repair DSBs, cells either die or allow potentially oncogenic genetic aberrations to pass unchecked through the cell cycle. PARP inhibitors (PARPis) rely on the principle of synthetic lethality in which the deficiency of two or more mechanisms results in cellular death, whereas the deficiency of only one mechanism does not (44, 50). Women with germline *BRCA1/2* positive ovarian cancer lack one functional copy of either BRCA1 or BRCA2 in every cell in their body, while their tumor cells lack any functional copies. PARPis exploit this phenomenon as the SSBs and subsequent DSBs that will occur in normal cells are able to be repaired by the remaining functional copy of BRCA1 or BRCA2, while the resulting DSBs in tumor cells will lead to cell death (44, 51).

Currently, there are three FDA approved PARPis used in the treatment of epithelial ovarian cancer (52-54). All three (olaparib, rucaparib, and niraparib) are indicated for the maintenance treatment of recurrent cancer if patients demonstrate a complete or partial response to a platinum agent, regardless of *BRCA1/2* mutation status. In women who have *BRCA1/2* mutated ovarian cancer, rucaparib and olaparib are approved in the recurrent setting after 2 or 3 prior lines of failed chemotherapy. Most recently, olaparib gained FDA approval for maintenance use in women who have either germline or somatic mutated *BRCA1* or *BRCA2* ovarian cancer, if they demonstrate response to first-line platinum-based chemotherapy. The approval for the maintenance treatment of recurrent cancer is interesting as it includes not only women who harbor *BRCA1/2* mutations, but also those with *BRCA1/2* WT or homologous recombination repair "proficient" tumors. In the clinical trials which led to this indication for each of the PARPis (55-57), although the greatest benefits were seen in women who had *BRCA1/2* mutated tumors, there was still a clear survival benefit in women who did not. This has driven the question as to why these women still showed a response as the primary mechanism is thought to be based on synthetic lethality, as mentioned above. One possible explanation is derived from an alternative mechanism of PARPis that entails "trapping" PARP proteins at DNA damage sites which can itself lead to mitotic catastrophe and cell death (58). Yet, despite such profound clinical responses seen across the various indications, emerging drug resistance remains a concerning threat to the majority of patients treated (59, 60).

mTOR signaling in cancer

The mechanistic target of rapamycin (mTOR) signaling pathway is one of the integral cellular networks controlling cell growth and proliferation. mTOR is a serine/threonine protein kinase that associates with various proteins to form two distinct protein complexes, mTORC1 and mTORC2 (61). While both complexes contain mTOR and share the same three proteins, only the mTORC1 complex contains regulatory-associated protein of mammalian target of rapamycin (Raptor) and proline-rich

Akt substrate 40 kDa (PRAS40); whereas the mTORC2 complex contains rapamycin-insensitive companion of mTOR (Rictor), protein observed with rictor 1 and 2 (protor1/2), and mammalian stress-activated map kinase-interacting protein 1 (mSin1) (61). Importantly, the individual mTOR complexes display different degrees of sensitivity to rapamycin, with mTORC1 being exquisitely sensitive and mTORC2 being resistant, aside from long term treatment. Both mTORC1 and mTORC2 respond to growth factors, however mTORC1 also responds to stimuli such as energy levels, stress, and oxygen availability. The primary downstream pathways of mTORC1 involve cell growth, cell cycle progression, autophagy, and cellular metabolism; whereas the downstream pathways of mTORC2 involve cell survival, cytoskeletal organization, and also cellular metabolism (61).

Both mTOR complexes are closely regulated through the phosphoinositide 3-kinase/protein kinase B (PI3K/Akt) signaling pathway (Figure 5). Stimulatory signals (such as insulin) that activate PI3K lead to the phosphorylation of Akt, which then directly phosphorylates the tuberous sclerosis 1 / tuberin (TSC1/TSC2) complex. TSC1/2 functions as a GTPase-activating protein (GAP) for the Ras homolog enriched in brain (Rheb), which directly activates mTORC1 when bound to GTP. When TSC1/2 is phosphorylated it is unable to exchange Rheb-GTP for Rheb-GDP, leaving Rheb-GTP to activate mTORC1 (62). Akt also independently activates mTORC1 through the phosphorylation of PRAS40, an mTORC1 inhibitor, leading to its dissociation from Raptor and the remainder of the mTORC1 complex (63-65). Once activated, mTORC1 can interact with a multitude of proteins to control various key cellular processes. Perhaps the most important of these is the control of protein synthesis which it activates through the eukaryotic translation initiation factor 4E (eiF4E)-binding protein 1 (4E-BP1) and S6 kinase 1 (S6K1) (66). Negative cellular growth signals lead to the inhibition of mTORC1 and occur through both an indirect method involving TSC1/2 and also a direct method via phosphorylation of Raptor which results in allosteric inhibition of mTORC1 (67, 68). The stability of the raptor/mTOR complex is dependent on the nutrient state of the cell; high energy states weaken the interaction and lead to increased cell growth through phosphorylation of S6K1, whereas low

nutrient states strengthen the interaction which suppresses the catalytic activity of mTOR (69).

mTORC2 is directly regulated by PI3K via the mSin1 subunit that inhibits mTORC2 in the absence of

insulin. When insulin growth factors activate PI3K, the generation of PIP_3 relieves this auto-inhibition

and mTORC2 is able to activate its downstream targets (70). Akt can also directly phosphorylate

mSin1, providing an additional mechanism of mTORC2 activation (71). Interestingly, activated

mTORC2 will then phosphorylate other kinases, including Akt at the serine473 residue, which is a

critical step to achieve maximal activation of Akt and its downstream effectors (cell survival and

proliferation) (72). The mTORC2 specific protein Rictor is also required for proper mTORC2

functioning, as knockdown models demonstrated a significant decrease in the activation of Akt (72,

73). Adding more complexity to the mTOR pathway, mTORC2 is also itself regulated by mTORC1

through a negative feedback loop between mTORC1 and PI3K signaling (74, 75).

Figure 5. Overview of the mTOR pathway (61). This figure was obtained from Laplante, M., and D. M. Sabatini. 2012. mTOR signaling in growth control and disease. *Cell* 149: 274-293. It was printed with permission from Elsevier, the owner of Cell, through license number 4583231368660.
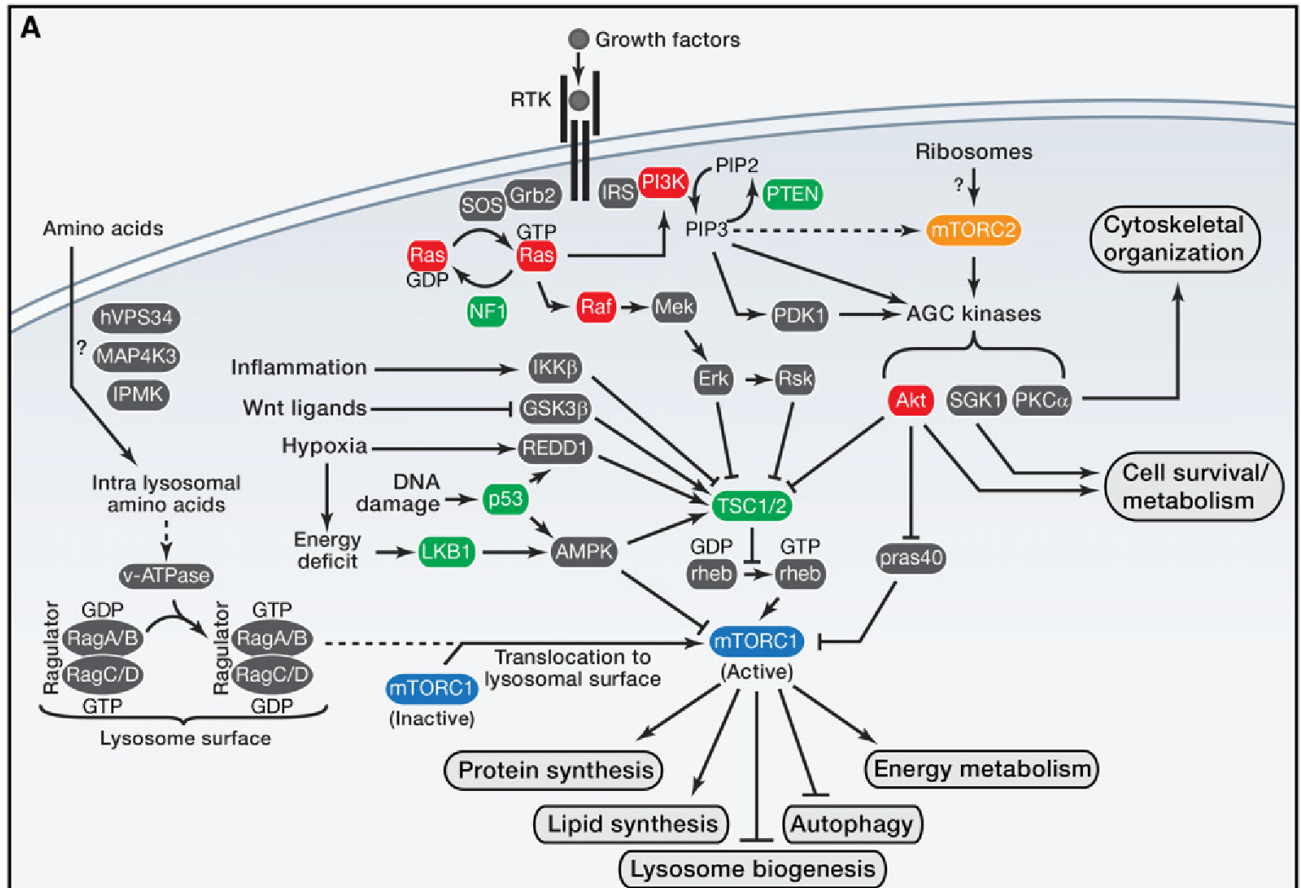
Deregulation of the mTOR pathway plays a critical role in the development of malignant cells. Mutations in the regulatory components of the pathway such as PI3K/Akt activation, or loss of *Pten*, *p53*, or *Tsc1/2,* all have been reported to promote mTORC1 activation (61, 76). Additionally, overexpression of the mTORC2 substrate Rictor has been observed in many gliomas, and ectopic expression of Rictor in glioma cells led to an increased malignant phenotype (77, 78). As such, efforts have been undertaken to target the mTOR pathway for anti-tumor use. Rapamycin analogues, termed "rapalogs", have been developed with the goal of inhibiting mTORC1. As mentioned above, rapamycin leads to the acute inhibition of mTORC1, however inhibits mTORC2 only after long-term exposure. Given the various roles that mTORC1 and mTORC2 play in normal cellular functioning, this becomes an important point when designing rational anti-cancer agents. Rapamycin works primarily through the formation of a complex with the intracellular 12-kDa FK506-binding protein (FKB12) that interacts with and inhibits mTOR only when part of the mTORC1 complex (79, 80). There are currently two FDA approved rapalogs for the treatment of human cancers. Temsirolimus is approved for the first-line treatment of metastatic renal cell carcinoma (RCC) (81). Everolimus is approved for second-line treatment of metastatic RCC after sunitinib or sorafenib failure, neuroendocrine tumors of either pancreatic, lung, or gastrointestinal origin, postmenopausal hormone-receptor positive HER2-negative breast cancer (in combination with exemestane), and for renal angiomyolipoma and tuberous sclerosis complex (82). Given the numerous feedback loops regulating the mTOR pathway described above, efforts have also been made to inhibit both mTORC1 and mTORC2 complexes. These dual inhibitors (termed mTOR kinase inhibitors) function as ATP-competitive catalytic inhibitors of mTOR and therefore block the total kinase activity of mTOR in both mTORC1 and mTORC2. Pre-clinical data has shown them to produce a wider and stronger inhibition of the downstream mTORC pathways (83-89). Among others, sapanisertib (MLN01288 or INK-128) is an example of such a drug which is currently being tested in a phase-1 clinical trial in patients with advanced non-hematologic malignancies (NCT02412722).

mTOR inhibitors in ovarian cancer

Aberrant expression of various components of the mTOR pathway has also been identified in ovarian cancer. Specifically, genetic mutations of *PTEN (90), PIK3CA (91), PIK3R1 (92), Akt1/2 (93, 94)*, and *mTOR (95)* have been reported in ovarian cancer patients, with an incidence ranging from 1.9-13.3%. Both mTORC1 and mTORC2 were found to be constitutively active in multiple ovarian cancer cell lines and knockdown of either Raptor or Rictor (discussed above) led to a significant inhibition of cell proliferation (96). Blockade of both PI3K and mTOR using the dual inhibitor BEZ235 was superior than rapamycin (mTORC1 blockade only) in decreasing cell proliferation as well as phosphorylation of S6, 4E-BP1, and Akt (96). Additionally, inhibitors of the PI3K/Akt/mTOR pathway display a greater anti-tumor effect in ovarian cancer cells with high Akt/mTORC1 activity compared to those with low activity (97-99).

In light of the promising pre-clinical data surrounding PI3K/Akt/mTOR pathway inhibitors, multiple phase I and phase II clinical trials have been performed examining use in ovarian cancer patients. While many of the trials have yet to be reported, GOG170-I, which examined temsirolimus monotherapy therapy in patients with persistent or recurrent epithelial ovarian cancer, displayed an overall response rate of 9.3% (98). Notably, patients with increased baseline mTORC1 activity had higher response rates than those who did not (11.8 vs. 5.9%) (98). More recently, results were reported for the phase Ib clinical trial examining the use of the dual mTOR inhibitor vistusertib with weekly paclitaxel in high-grade serous ovarian cancer (HGSOC) and squamous cell non-small-cell lung cancer (NSCLC) (100). In the HGSOC cohort, response rates were impressive at 52% (RECIST criteria) and 64% (CA125 criteria) (100). These encouraging results suggest that certain ovarian cancer patients stand to benefit from inhibition of the PI3K/Akt/mTOR pathway. Future studies are needed to test these agents in larger trials and to examine their potential in combination use with other targeted therapies.

BET inhibitors in ovarian cancer

BET inhibitors have also recently been examined for their potential use in ovarian cancer. As described above, Brd4 was found to be overexpressed in ovarian cancer relative to normal ovarian tissue (15), suggesting that targeting Brd4 and other BET proteins may result in anti-tumor activity. While it appears that the primary oncologic driver for BETi-sensitive NMC and hematologic malignancies is the overexpression of MYC, ovarian cancer cells displayed a profound downregulation of FoxM1 pathway genes when exposed to JQ1 (101). Interestingly, previous analysis of TCGA data revealed that the FoxM1 transcription factor network was activated in 87% of high-grade serous epithelial ovarian cancer cases (102). Furthermore, promoter analysis of FoxM1 using chromatin immunoprecipitation (ChIP) revealed an accumulation of Brd4, suggesting that disruption of the promoter region through BET inhibition leads to a decrease in FoxM1 expression (101). Brd4 has also been implicated in the expression of *ALDH1A1*, which plays a key role in the development of resistance to platinum agents in the treatment of epithelial ovarian cancer (103). Treatment using JQ1 was able to prevent the continued growth of cisplatin-resistant epithelial ovarian cancer cells in both *in vitro* and *in vivo* settings (104). Additionally, the PD-L1 encoding gene *CD274* was found to be directly regulated by Brd4, linking BET proteins to immune-mediated tumor evasion (105). Normal cells express PD-L1 on their cell surface to prevent auto-immune destruction, as the interaction with the PD-1 receptor on T-cells triggers cell death. Tumor cells will often express PD-L1 to exploit this phenomenon and evade the host immune system. Tumors from ovarian cancer mouse models treated with JQ1 showed a decrease in the expression of PD-L1 (105), suggesting a possible role for BETi combination with immune-checkpoint blockade drugs. A phase I clinical trial (NCT03292172) is currently underway examining the combination of the BETi RO6870810 and the anti-PD-L1 antibody atezolizumab in advanced ovarian and triple negative breast cancer. BETis have also demonstrated a synergistic effect with MEK inhibitors to decrease cell proliferation and survival in ovarian cancer cells (106).

Dual targeting of BET and PARP proteins has also generated considerable excitement in the treatment of epithelial ovarian cancer. Multiple studies have shown that the addition of BETis to PARPis results in synergistic anti-tumor activity in ovarian cancer cells and mouse models (107-109). Moreover, it has been previously reported that BETis act synergistically with PARPis in HRR pathway *proficient* ovarian cancer cells (109), thus providing a potential avenue for patients who may not experience the full benefit of PARPis. Specifically, they reported that inhibition of BET proteins suppresses transcription of *BRCA1* and *RAD51* (another key protein in the HRR pathway), essentially transforming the cells to HRR pathway *deficient* which sensitizes them to PARPis (109). Furthermore, the authors showed a synergistic decrease in tumor weight and ascites volume using both the Brd4 inhibitor JQ1 and olaparib in a *BRCA1/2* WT orthotopic ovarian cancer mouse model. Downregulation of the cell-cycle checkpoint regulator WEE1 and the DNA-damage response factor TOPBP1 after JQ1 treatment has also been described as a mechanism for the synergy between BETis and PARPis in HRR proficient ovarian cancer cells (108). An additional mechanism for the induction of HRR deficiency in HRR proficient ovarian cancer cells includes the depletion of the DSB resection protein CtIP (C-terminal binding protein interacting protein) (107). Interestingly, JQ1 treatment has also been shown to reverse multiple mechanisms of resistance to PARPis in ovarian cancer cells (107). These preclinical data suggest that clinical trials incorporating the combination of BETis and PARPis would likely demonstrate a positive signal.

Despite the enormous excitement surrounding the use of BET inhibitors in cancer therapy, there remain multiple issues that prevent them from obtaining widespread clinical use. First, BET inhibitors appear to have the highest efficacy in NMC, a malignancy driven by either a Brd4-NUT or Brd3-NUT fusion protein. It is safe to assume that there will be very few cancers with this same genetic pathophysiology, possibly hindering the rationale for use in other malignancies. Second, although BET inhibitors do show activity in other tumor types, the response rates are still low (0-12%). Third, BET inhibitors have only been tested in a minority of solid tumors, perhaps masking an

astounding response in so-far unexamined cancer types. Last, and perhaps most important, resistance to BET inhibitors in ovarian cancer has recently been described, mediated by adaptive kinome reprogramming (110). In order to circumvent many of these issues, it is absolutely necessary to determine how cancer cells respond to BET inhibition and to investigate whether these changes reveal other proteins that can be targeted to maximize anti-tumor activity.

Hypothesis and specific aims

Hypothesis: Adaptive changes to BET inhibition in ovarian cancer will identify rational drug combinations.

Specific Aim 1: To identify early adaptive changes to BET inhibition in ovarian cancer cells and to develop combination strategies to maximize anti-tumor activity.

Specific Aim 2: Assess the biological effects of combining BET inhibitors with either PARPis or mTOR inhibitors in murine orthotopic models of ovarian cancer.

Materials and Methods

Reagents and antibodies

For the *in vitro* experiments, we used the BETi CN210, kindly provided by ConverGene; olaparib was purchased from LC Laboratories (#O-9201), rapamycin was purchased from Selleck Chemicals (#S1039), and sapanisertib (INK-128) was purchased from Selleck Chemicals (#S2811). The inhibitors were re-suspended in dimethyl sulfoxide (DMSO; #D2650; Sigma-Aldrich) to make a working stock of 100 mM (olaparib) or 10mM (CN210, rapamycin, and INK-128). The control for all our *in vitro* experiments was DMSO diluted to 1:1,000. For immunoblots, the following antibodies were used: c-MYC (#5605; Cell Signaling Technology; 1:1,000), AKT (#4691; Cell Signaling Technology; 1:1000), p-AKT (Ser473) (#4060, Cell Signaling Technology; 1:1000), Raptor (#2280, Cell Signaling Technology; 1:1000), p-Raptor (Ser792) (#2083, Cell Signaling Technology; 1:1000), mTOR (#2983 Cell Signaling Technology; 1:1000), p-mTOR (Ser2481) (#2974, Cell Signaling Technology; 1:1000), p70 S6 Kinase (#2708, Cell Signaling Technology; 1:1000), p-p70 S6 Kinase (Thr389) (#9234, Cell Signaling Technology; 1:1000), Rictor (#2114, Cell Signaling Technology; 1:1000), and p-Rictor (Thr1135) (3806, Cell Signaling Technology; 1:1000).

Cell line maintenance

All cell lines were maintained in 5% CO_2 at 37 °C. Ovarian cancer cells (HeyA8, OVCAR3, OVCAR4, OVCAR5, OVCAR8 ip1, ID8, SKOV3ip1, Kuramochi, and COV362) were obtained from the American Type Culture Collection (ATCC) and the University of Texas MD Anderson Cancer Center Characterized Core Line Core Facility. OVC432 was gratefully obtained from Dr. Ronny Drapkin (Dana Farber Cancer Center). Kuramochi, HeyA8, OVCAR3, OVCAR4, OVCAR8, OVCAR432, and SKOV3ip1 cells were maintained in RPMI 1640 supplemented with 10% fetal bovine serum (FBS) and 0.2% gentamicin sulfate (#50146970; Fisher). OVCAR5, COV362, and ID8 were

maintained in D-MEM media supplemented with 10% fetal bovine serum and 0.2% gentamicin sulfate. All *in vitro* experiments were conducted at 60-70% cell confluence.

The identity of the cell lines used was validated through short tandem repeat DNA analysis performed by the Characterized Cell Line Core Facility. Mycoplasma detection was performed using the ATCC PCR Universal Mycoplasma Detection Kit (#30-1012K).

Cell viability assay

Cells were seeded in a 96-well plate and treated for 72 hours with increasing concentrations of CN210, olaparib, rapamycin, and INK-128. Combination groups contained the same concentrations as the individual drugs at each specific concentration level. For the majority of the cell lines tested, 3,000 cells were deposited into each well. After 72 hours, 50 ul of 1.5 mg/ml solution of MTT (#M2128; Sigma Aldrich) dissolved in PBS was added to each well, followed by incubation for 2.5 hours at 37°C. The media + MTT solution was then removed, 100 μL of DMSO was added to dissolve the MTT by-product, and the absorbance at 540 nm was recorded for each well. Each concentration point was replicated in experimental quadruplicates with the OD average of the four being used for analysis. Combination indexes were calculated by using the program CompuSyn, version 1.0, 2004.

In Vitro Apoptosis assay

Cells were plated in a 6-well plate in their respective media to reach 60-70% confluence after 24 hours, typically requiring 50,000 cells per well. After 24 hours, the supernatant was removed from each well and replaced with 3 ml media containing the desired concentration of each drug. Combination groups contained the same concentrations as the individual drugs being tested. Each experimental condition was repeated in experimental duplicates. DMSO was used as a control in a

1:1000 dilution, and untreated cells were used for FITC and PI control staining. After 48 hours, the media was collected into individually labelled tubes. Each well was then washed twice with sterile PBS and the cells were trypsinized until detached from the plastic surface. Two mL of media was then added to each well to neutralize the trypsin and the cells were then added to their respective tubes containing the originally collected media. Cells were then centrifuged at 2000 rpm for 3 minutes and the supernatant was discarded. Cell pellets were then washed with cold, sterile PBS x2. Using the FITC Annexin V Apoptosis Detection Kit I (catalog number 556547, BD Pharmingen, BD Biosciences), cells were then incubated with both FITC-labeled Annexin V and PI according to the manufacturer's protocol. Cells were then incubated in the dark at room temperature (RT) for 30 minutes with gentle vortex every 10 minutes. Annexin V and PI control cells were only incubated with either Annexin V or PI, respectively. Cells were then transferred to flow cytometry tubes and analyzed at the MD Anderson South Campus Flow Cytometry Core. The resulting percent of apoptotic cells in each group was then used for statistical purposes. All experiments were repeated twice at a minimum, aside from Figure 10.

Immunoblotting

Cells were treated with either 10 uM CN210 or DMSO (1:1000) dissolved in serum containing media for 48 hrs. To exclude the potential effect of FBS on protein expression changes, cells were either plated and treated for 24 hours in SFM or plated in SFM for 6 hours followed by the addition of 10uM CN210 dissolved in SFM for the remaining 18 hours.

Cells were then washed twice with PBS and lysed with radioimmunoprecipitation assay buffer (RIPA) including protease and phospho-preotease inhibitors. To determine protein concentrations, we used a Pierce BCA Protein Assay Kit (#23225; Thermo Fisher Scientific). Either 20 or 40 ug of total cell lysate was then loaded and separated on Mini-PROTEAN TGX Gels (B#456-1084, BIO-

RAD). Proteins were transferred to a nitrocellulose membrane (Bio-Rad Laboratories, Hercules, CA) at 90V for 90 minutes, blocked with 5% milk for one hour, and then incubated with primary antibody at 4°C overnight. Membranes were then washed three times x10 minutes with Tris-buffered saline including 0.1% Tween-20 (TBS-T), and incubated with horseradish peroxidase-conjugate anti-Rabbit (#7074, Cell Signaling Technologies, 1:2000), or Mouse (GE Healthcare, NA931V, 1:2000) for two hours. The membranes were then washed again three times x10 minutes in TBS-T, developed using Western Lightning Plus ECL (#NEL105001EA; Perkin Elmer), and visualized using x-ray film (#F-BX57; Phenix). Membranes were re-probed multiple times with different primary antibodies. In order to remove the previously bound antibodies, membranes were washed with Restore PLUS Western Blot Stripping Buffer (#46430; Thermo Fisher Scientific) for 10 min and then rinsed in TBS-T followed by washing twice x5 minutes. The membranes were blocked again for one hour using 5% milk, and then incubated with primary antibody overnight 4°C.

Reverse Phase Protein Arrays (RPPA)

HeyA8, OVCAR8 ip1, OVCAR5, and OVCAR4 cells were treated with 1 uM CN210 for 48 hours. After the elapsed treatment time, cells were washed twice with PBS and lysed using RIPA buffer including protease and phospho-protease inhibitors. Protein concentration was determined as above and the lysate was diluted to a concentration of 1.5 ug/ul. Next, the lysate was mixed with 4x sample buffer (40% glycerol, 8% sodium dodecyl sulfate, and 0.25 M Tris, pH 6.8) that did not contain bromophenol blue, and then finally mixed with β-mercaptoethanol in a 1:10 ratio. The samples were submitted to the MD Anderson RPPA Core Facility and run using a panel of 304 antibodies. Each experimental condition was performed and submitted as biological duplicates. Full details of the specific protocol used by the RPPA Core Facility can be found on their website (111).

In Vivo models

All mice used in this study were female athymic (NCr-nude) mice purchased from Taconic Farms (Hudson, NY). Mice were treated and cared for in accordance to the guidelines set forth by the United State Public Health Service policy on Human Care and Use of Laboratory Animals and the American Association for Accreditation of Laboratory Animal Care. All mouse experiments were also supervised and approved by the University of Texas MD Anderson Cancer Center Institutional Animal Care and Use Committee. Mice were approximately 6-8 weeks old at the time of tumor injection.

Tumor cells were grown to 60-70% confluency in their indicated media. Prior to injecting tumor cells into mice, the cells were washed twice with PBS, and harvested using trypsin-EDTA. After the addition of FBS-containing media to neutralize the trypsin, cells were then counted and centrifuged at 1500 rpm for 5 minutes followed by resuspension at the desired concentration in Hanks' balanced salt solution (HBSS; Gibco, Carlsbad, CA) prior to injection. OVCAR5 (1×10^6 cells in 200 uL) or SKOV3 ip1 (1×10^6 cells in 200 uL) cells were then injected into the peritoneal cavity of each mouse.

For the CN210 and olaparib experiment, mice were treated daily via oral gavage using 100 mg/kg CN210 and/or 50 mg/kg olaparib. In order to deliver CN210 orally, we dissolved CN210 powder in a 30% solution of Kolliphor (#42966-1 kg; Sigma-Aldrich) diluted in water and adjusted with 1.05 equivalents of 0.1 N HCl for dosing. Sonication was performed, if necessary, to ensure complete dissolution of the CN210. For experiments containing olaparib, we first created a 86 mg/ml stock concentration dissolved in DMSO. 349 uL of the stock solution was then added to 2051 uL of 15% (2-Hydroxypropyl)-β-cyclodextrin (#H107; Sigma-Aldrich) in PBS, to create a final concentration of 12.5 mg/ml. 100 uL was then given via oral gavage for a total delivery of 50 mg/kg. The control group for the CN210/olaparib experiment received 200 ul of a 50/50 mixture of both solvents used to dissolve CN210 and olaparib. For experiments containing INK-128 (1 mg/kg), the compound was dissolved in order with 30% PEG400 (#202398; Sigma-Aldrich) + 0.5% Tween80 (#P5188; Sigma-

Aldrich) + 5% propylene glycol (#P355-1; Fisher Scientific) in deionized water for a working concentration of 0.25 mg/ml.

Toxicity was observed after 14 days of daily treatment in the CN210/INK-128 combination group, manifesting primarily as weight loss and skin effects (scale development). All groups were given 4 days without treatment, and after resolution of toxicity, treatment was restarted in all groups at every other day frequency. Necropsy was performed in the CN210/olaparib experiment on D35 (28 days of treatment) or if mice became moribund. Necropsy was performed in the CN210/INK-128 experiment on D42 (35 days of treatment) or if mice became moribund.

Statistical analysis

Statistical analyses of *in vitro* and *in vivo* experiments were performed using GraphPad Prism 7. Standard statistical comparison tests such as Student *t* test, *t* test with Welch's correction, and Mann-Whitney test were used to analyze the data. Importantly, when triplicate values were compared, normality and variance were determined and the appropriate statistical test was used. When only duplicate values were available, a t-test without Welch's correction was used as normality and variance could not be ascertained. For these analyses, a P value < 0.05 was considered significant. Results are presented as the mean ± standard deviation of the mean, aside from where indicated.

For both *in vivo* experiments, we calculated that 10 mice per group would allow for detection of a 50% decrease in tumor weight and nodules at a power of 80%, with a confidence of 95%. As there was poor tumor uptake in the control group of the CN210/olaparib combination *in vivo* experiment (~43%, 3/7), all mice in every group without any identifiable tumor were excluded from the analysis of tumor weight or number of tumor nodules. For the CN210/INK-128 combination *in vivo* experiment, there was sufficient tumor uptake in the control group (90%) and all mice in every group were included in the statistical analysis whether tumor was present or not.

For statistical analysis of the RPPA data, the median of the expression fold-change from three individual replicas in each condition was plotted in the heat map as log 2 value. The p values associated with pathways in IPA analysis were calculated using the right-tailed Fisher Exact Test. Fold change data that did not meet significance ($P < 0.05$) was not included. The data was then analyzed by Cluster 3.0 (112) using median value and the heat maps were generated by Java Treeview (113). Furthermore, an additional heat map was created using GraphPad Prism 7 for only the mTOR pathway related proteins. Fold change was calculated by dividing the average expression of CN210 treated cells by the average expression of the DMSO treated cells. Student t test was performed to determine if the fold change was statistically significant. Fold changes that had $P > 0.05$ were not included in the additional heat map.

Results

Sensitivity of ovarian cancer cell lines to BET inhibition

To determine the sensitivity to BET inhibition in ovarian cancer cell lines, MTT assays were performed using the novel BET inhibitor, CN210. CN210 is a "non-specific" or "pan" small-molecule BET inhibitor that reversibly binds to the bromodomains of all four BET proteins, thereby preventing the normal interaction with acetylated histones or transcription factors. Although JQ1 has been extensively used in previously published research, it is known to have multiple off-target effects which limits its integration into the clinical setting. To circumvent this, we collaborated with ConverGene Science who developed CN210 as a novel BET inhibitor with limited off-target effects, making its translation into humans more feasible.

Initially, a panel of eight ovarian cancer cell lines were screened using CN210 cell viability assays. As shown in Figure 6, the IC_{50}s ranged from 3.5 uM to 100.7 uM. To best determine the adaptive changes to BET inhibition in ovarian cancer cells, we decided to compare the cells displaying high levels of sensitivity to those displaying resistance. OVCAR5 and OVCAR4 cell lines were identified as the most resistant to BET inhibition with IC_{50}s of 100.7 uM and 20.8 uM, respectively (highlighted in red). Similarly, HeyA8 and OVCAR8 ip1 cell lines were identified as the most sensitive to BET inhibition with IC_{50}s of 4.9 uM and 3.5 uM, respectively (highlighted in blue). Notably, OVCAR8 ip1, HeyA8, and OVCAR5 cells possess *KRAS* mutations, in contrast to OVCAR4 cells.

Figure 6. Effect of the BET inhibitor CN210 on ovarian cancer cell lines. (Left) Table displaying individual and average IC_{50} values for each cell line. (Right) Representative cell viability curves for the most sensitive and resistant cell lines. Error bars represent the SD. NC; not calculable. M; molar.

IC_{50} for CN210 (uM)						Avg. (uM)
OVCAR 5	NC	180	460	NC		320
OVCAR 432	10.7	36.9	17.1			21.6
OVCAR 8 ip1	7.5	2.6	5.8	3.7	1.7	2.1	3.9
OVCAR 3	59.3	7.4	2.31			23
ID 8	18.8	NC	19			18.9
OVCAR 4	28.4	26.4	20.1	19.8	23.2	23.6
HeyA8	3.3	9.6	7.7			6.9
SKOV3 ip1	9.5	13.3	16.1	6.7		11.4

CN210 Sensitive

CN210 Resistant
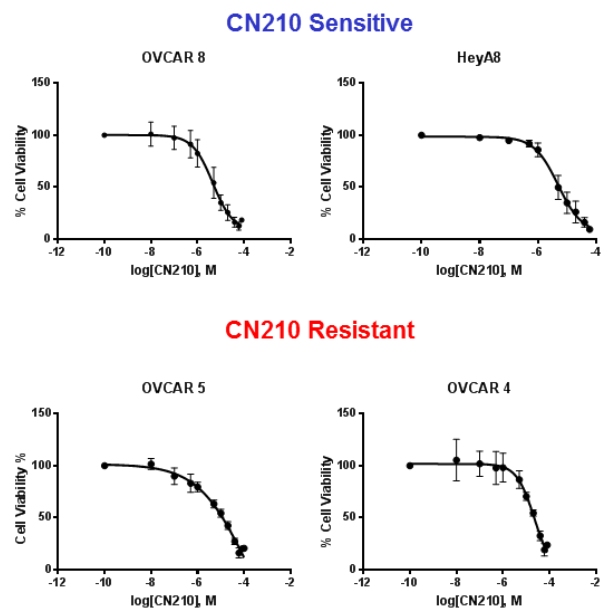
As mentioned above, BET proteins have been reported at high levels at the promoter and enhancer regions of cMYC in hematologic malignancies. Furthermore, BET inhibition was previously shown to cause significant downregulation of cMYC in NMC and hematologic cancer cells. To determine whether BET inhibition had an effect on cMYC levels in ovarian cancer, we examined cell lysates for cMYC expression after 48 hours of DMSO or CN210 (10 uM) treatment. HeyA8 and OVCAR4 cells showed a substantial decrease in cMYC levels after CN210 treatment, whereas a slight increase was observed in OVCAR8 ip1 cells, and no effect was seen in OVCAR5 cells (Figure 7). Interestingly, the two cell lines determined to be the most sensitive to BET inhibition had opposite effects on cMYC expression levels when treated with CN210. This may imply that the alteration of cMYC expression due to BET binding at the cMYC promoter is not relevant for the overall BETi response in ovarian cancer cells. It is important to note however, that the basal expression of cMYC in HeyA8 and OVCAR8 ip1 cells was substantially different, perhaps masking the true effect of BET inhibition on cMYC expression in these cell lines.

Figure 7. Effect of BET inhibition on cMYC expression in ovarian cancer cells.
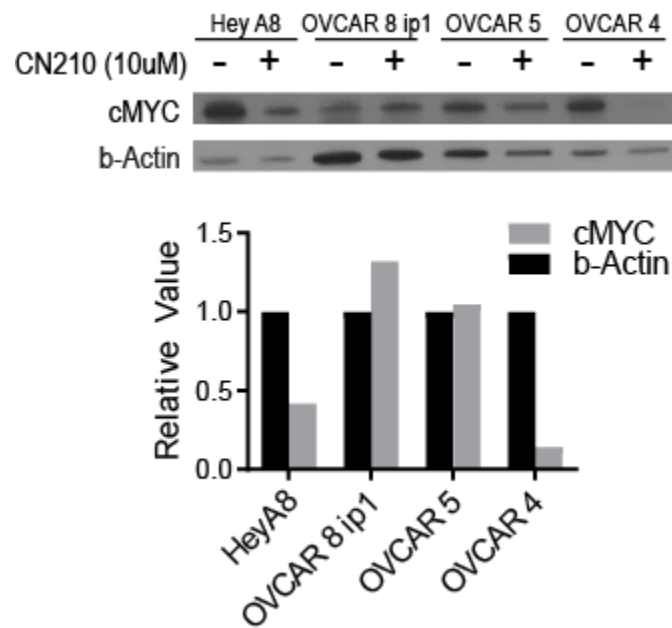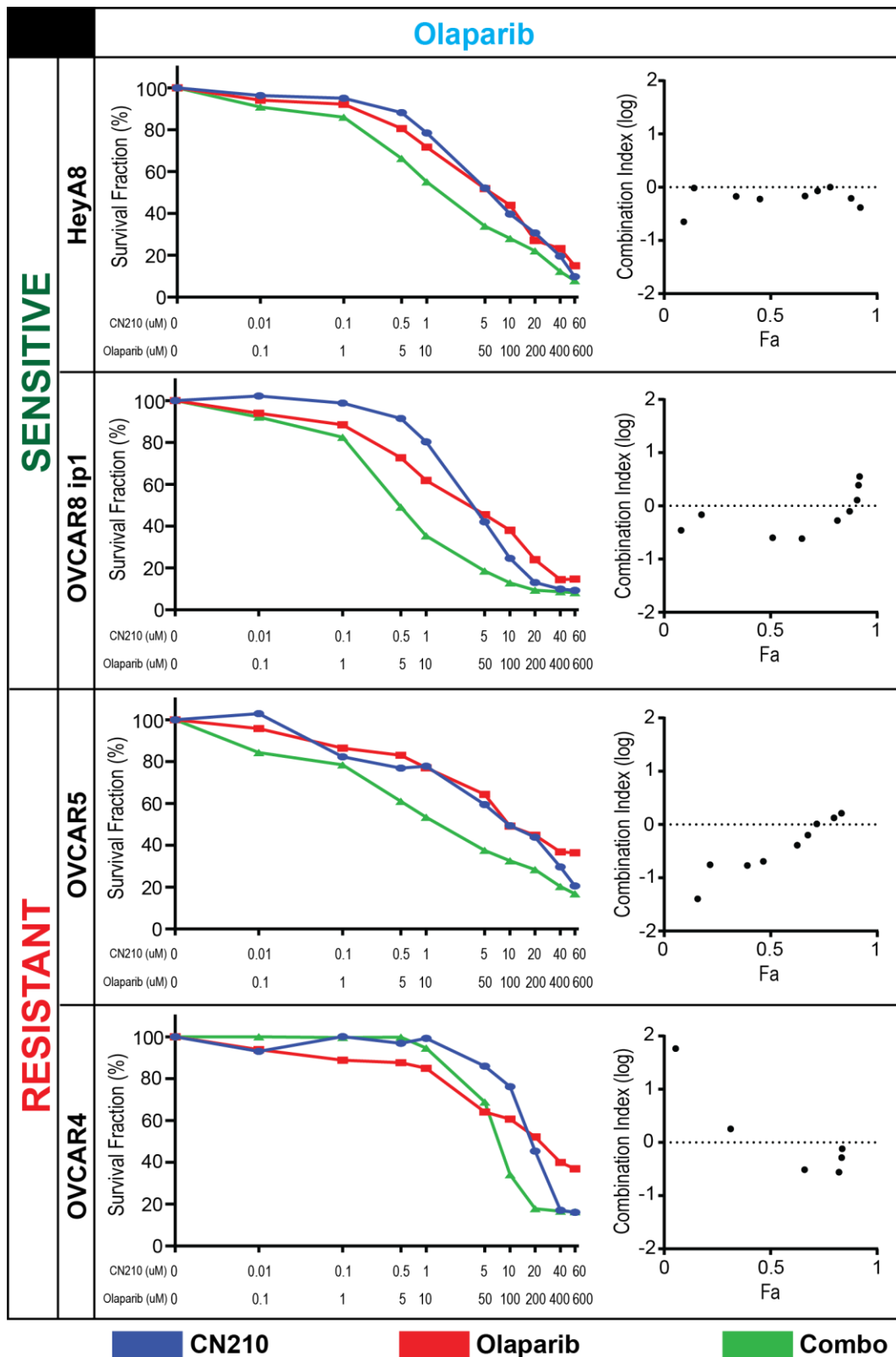
Effect of CN210 and olaparib combination on ovarian cancer cells

The combination of BET and PARP inhibitors has been recently shown to have a synergistic treatment effect in ovarian cancer cells (107-109). To determine whether this effect was reproducible using our specific BET inhibitor, we next performed combination MTT assays with our CN210-resistant and sensitive cell lines using CN210 and olaparib (Figure 8). We found that in our two CN210-sensitive cell lines (HeyA8 and OVCAR8 ip1), there was a synergistic effect at most but not all individual concentrations. Synergism, as represented by the distance between the green combination treatment line and the two individual drug treatment lines, was most pronounced between CN210 concentrations ranging from 0.5 uM to 10 uM, while concentrations lower or higher than this had only minimally increased effects. The CN210-resistant OVCAR5 cells also displayed synergism at the same range of concentrations, while OVCAR4 cells had a predominantly antagonistic effect.

The plots on the right hand side of figure 6 display the log combination indexes (log-CIs) at each individual concentration for the cell lines. Each point represents the degree of increased effect in the combination group compared to individual groups at each individual concentration. The further the values lie below zero, the stronger the synergistic effect at that specific concentration. Values located on the line signify an additive effect, whereas values above the line signify an antagonistic effect. Examining the log-CIs for each cell line reveals that olaparib displayed a synergistic effect with CN210 in all four cell lines, however the degree to which synergism occurred differed at various concentrations. Every point aside for the two additive ones were in the synergistic range for HeyA8 although most were only slightly below zero. OVCAR8 ip1 cells also had points in the synergistic range however antagonist interactions were seen at higher concentrations. For the CN210 resistant cell lines, OVCAR5 cells displayed substantial synergism between CN210 and olaparib at the majority of concentrations tested, however similar to OVCAR8 ip1 cells, antagonistic effects were seen at higher concentrations. OVCAR4 cells had the least amount of synergism between the two drugs as

only 6 of 9 nine possible data points even fit on the graph, two of them being in the antagonistic range,

and four of them being only slightly synergistic.

Figure 8. Effect of CN210 and olaparib combination on cell viability in CN210-resistant and sensitive ovarian cancer cell lines.

To determine if the synergistic decreases in cell viability were caused by an increase in apoptosis, we next examined the effect of CN210 and olaparib combination using apoptosis assays (Figure 9). In both of the CN210-sensitive cell lines there was an increase in apoptosis after CN210 and olaparib individual treatments, however only olaparib treatment in HeyA8 cells resulted in a statistically significant increase. Combination of the two drugs led to an increase in apoptosis compared to DMSO control, however significance was only reached in HeyA8 cells. Notably, there was a statistically significant increase in apoptosis between the combination group and each individual drug in the HeyA8 cell line, signifying an enhanced effect when both drugs were combined. The effect of combination treatment was less pronounced in the CN210-resistant cell lines. In OVCAR5 cells, olaparib treatment produced a significant increase in apoptosis compared to DMSO, while CN210 or the combination group did not. The latter finding is likely due to the wide standard deviation of the combination group in the OVCAR5 cell line. In OVCAR4 cells, each individual group and the combination group resulted in a significant increase in apoptosis compared to DMSO. Importantly, although there was a significant increase seen between CN210 and DMSO, the absolute difference between these two groups was small. Furthermore, OVCAR4 cells had a surprisingly higher amount of apoptosis after CN210 treatment than what would be expected from the MTT data for this cell line. Lastly, although there was no difference between the olaparib group and the combination group in OVCAR4 cells, there was a significant difference between the CN210 group and the CN210/olaparib group, suggesting the effect in the combination group was driven primarily by olaparib.

Figure 9. Effect of CN210 and olaparib combination on apoptosis in CN210-resistant and sensitive ovarian cancer cell lines. Error bars represent the SD. Significance reported for each group compared to DMSO control, except where indicated. *, P <0.05; **, P <0.01; and ***, P <0.001 as determined by the Student *t* test. ns, non-significant.
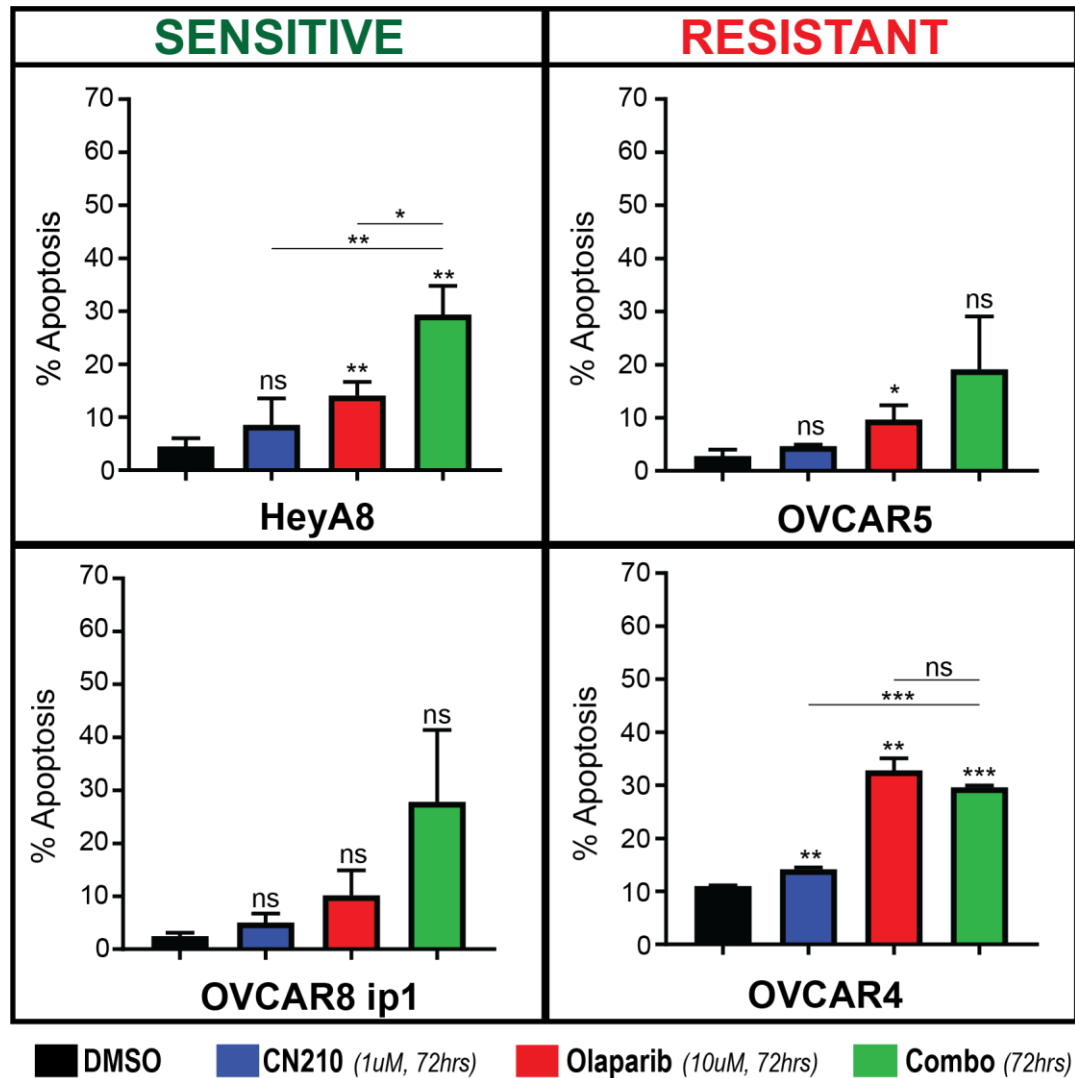
Considering that only one cell line (HeyA8) displayed a significant increase in apoptosis in the combination group vs. either individual drugs, we next sought to determine if an enhanced effect could be achieved through varying the treatment time and concentrations used. We chose to use the OVCAR5 cell line as both the CN210 and combination group did not show a significant increase in apoptosis compared to control. It stands to reason that this cell line would be the most likely to benefit from varied concentrations, especially considering the IC_{50} of CN210 in OVCAR5 cells was ~100 uM and the previous conditions were examined at only 1 uM CN210. The amount of apoptosis in OVCAR5 cells was substantially increased by both increasing the concentration of CN210 and also harvesting the cells after 24 or 48 hours, as compared to the original 72 hours (Figure 10). Cells treated for 48 hours expectedly had larger amounts of apoptosis than cells treated for 24 hours. When OVCAR5 cells were treated at 50% of the IC_{50}, ~25% and 80% of cells had undergone apoptosis at treatment times of 24 and 48 hours, respectively. Cells treated with CN210 at the IC_{50} displayed ~75% and 95% apoptosis at 24 and 48 hours, respectively. Varying the concentration of olaparib from 20 to 50 uM (compared to 10 uM originally) did not substantially change the amount of apoptosis for this drug. Perhaps most interesting was that neither changing the concentrations, nor changing the amount of treatment time, was able to produce an enhanced effect between CN210 and olaparib. Considering that this enhanced effect was seen in HeyA8 cells however, the results from Figure 9 suggest that a combination effect between CN210 and olaparib is cell-specific, and is not dependent on drug concentration or treatment.

Figure 10. **Effect of varied concentration and treatment time of CN210 and olaparib combination on apoptosis in OVCAR5 cells.** Error bars represent the SD between experimental duplicates only. No intergroup comparisons were calculated as biological replicates were not performed for this experiment.
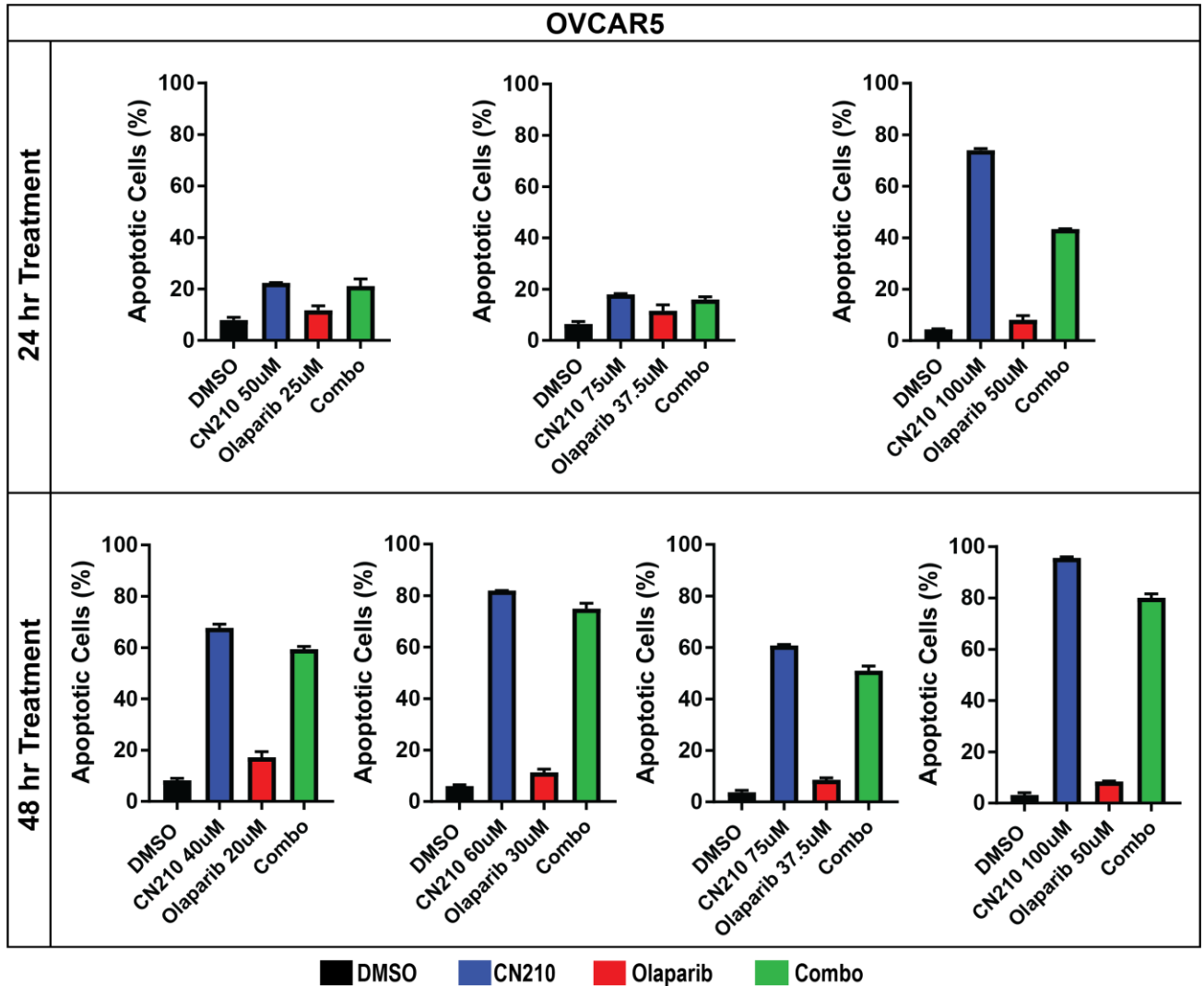
Effect of CN210 and olaparib combination in BRCA mutated ovarian cancer cells

As described above, olaparib and other PARPis exert their anti-tumor activity through the concept of synthetic lethality, in which they exploit the lack of a functional homologous recombination pathway found in cells that harbor *BRCA* mutations. To determine whether the homologous recombination pathway contributed to the ability of CN210 to synergize with olaparib, we examined the effect of combined treatment in ovarian cancer cells lines containing *BRCA* mutations. Kuramochi is a high-grade serous ovarian cancer cell line which harbors a *BRCA2* missense mutation (114). COV362 is also a high-grade serous ovarian cancer cell line which harbors a *BRCA1* splice-site mutation (114). Figure 11 displays the effect of CN210 and olaparib combination in both Kuramochi and COV362 cell lines. Interestingly, there was a substantial lack of a synergistic effect in both cell lines compared to the four *BRCA* WT cells discussed above. Kuramochi cells demonstrated a synergism between CN210 and olaparib at higher concentrations (CN210 10 uM and 20 uM), as represented by the log-CIs, however COV362 cells did not show any meaningful synergistic effects.

Examining the effect of combined treatment on apoptosis in COV362 cells revealed that olaparib produced a significant increase in apoptosis compared to DMSO, whereas neither CN210 nor the combination group did (Figure 12). Furthermore, there was only ~15% apoptotic cells after 48 hours treatment of olaparib at a concentration of 100 uM. Considering that there was ~20% apoptosis in OVCAR5 cells after 48 hours of 20 uM olaparib treatment, this suggests that the *BRCA1* mutation may in fact hinder the ability of cells to undergo apoptosis in this particular cell line. In the Kuramochi cell line, CN210, olaparib, and the combination group all significantly increased the amount of apoptosis compared to DMSO control, however the combination group did produce an effect greater than the individual drugs themselves. We found it surprising that in both *BRCA* mutated cell lines, the response to olaparib was not as pronounced as expected given their efficacy in human patients.

Figure 11. Effect of CN210 and olaparib treatment on cell viability in *BRCA* mutated cell lines.
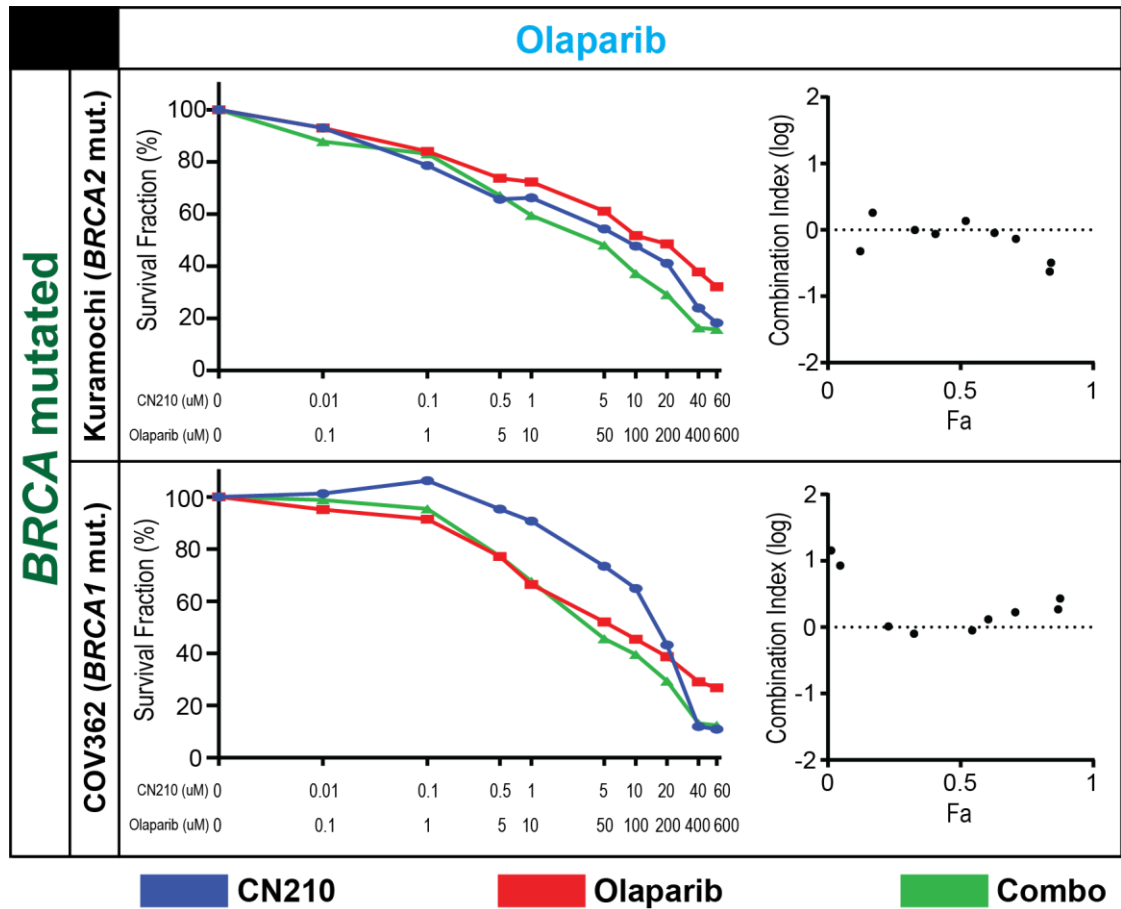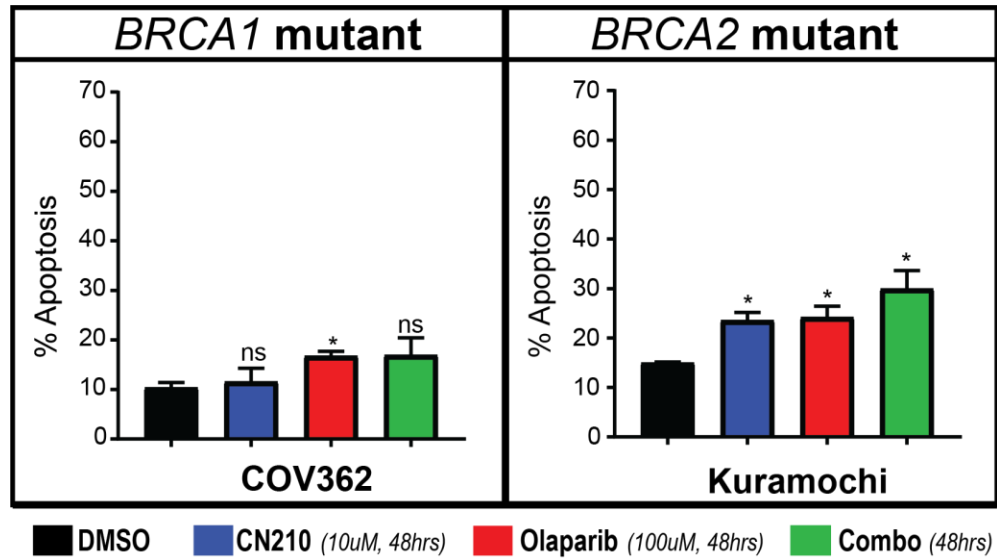
Figure 12. Effect of CN210 and olaparib treatment on apoptosis in *BRCA* mutated cell lines.

Error bars represent the SD. Significance reported for each group compared to DMSO control. *, P <0.05 as determined by the Student *t* test. ns, non-significant.

Effect of BETi and PARPi combination In Vivo

To determine whether PARP inhibition could increase the effect of BET inhibition *in* vivo, we treated an orthotopic ovarian cancer mouse model with either control, 100 mg/kg CN210, 50 mg/kg olaparib, or a combination of CN210/olaparib. We used the human ovarian cancer cell line OVCAR5 and injected $1x10^6$ cells intraperitoneally into nude mice to emulate the normal growth environment of human ovarian cancer (Figure 13A). After 28 days of treatment, there was no difference in mouse weight across all groups (Figure 13B). While it appeared that there was a decrease in tumor weight in the combination group compared to control, this finding was not statistically significant. Furthermore, there was no apparent difference in tumor weight between control and either CN210 or olaparib treatment alone (Figure 13C). Similarly, all three treatment groups had less tumor nodules than control, however this was not statistically significant (Figure 13D). Although previously published literature has reported a large amount of synergy between PARPis and BETis, both our *in vitro* and *in vivo* data did not support this conclusion.

Figure 13. Effect of CN210 and olaparib combination treatment in an OVCAR5 ovarian cancer cell mouse model. (A) Schematic overview of *in vivo* experiment. (B-D) Mouse weight, tumor weight, and number of tumor nodules at necropsy across all treatment groups. Error bars represent the SEM. All comparisons between groups in each panel were non-significant.
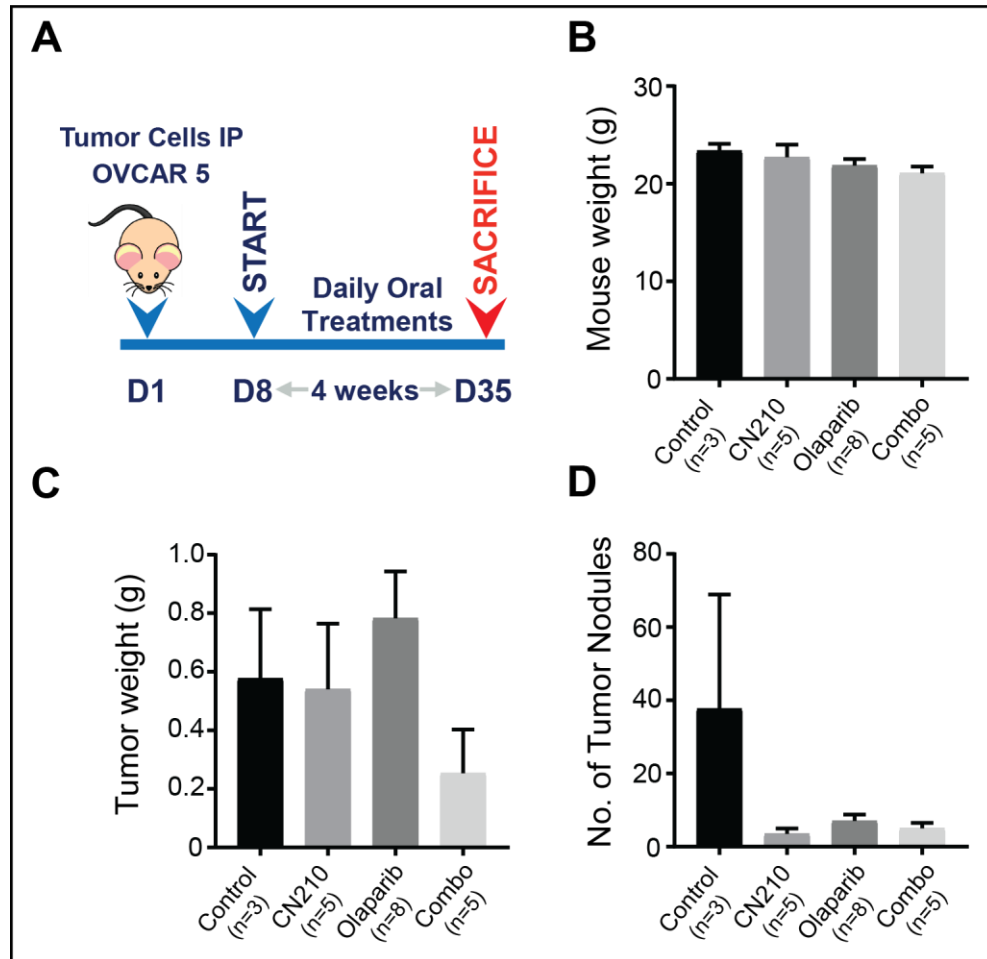
RPPA analysis of CN210-resistant and CN210-sensitive ovarian cancer cell lines

Given that we did not observed the kind of effects that have been reported with the combination of BETis and PARPis in prior studies (107-109), we next sought to determine the adaptive changes to BET inhibition in ovarian cancer cells. We used RPPA analysis to measure the protein expression of genes that were altered after CN210 treatment in both our CN210-sensitive and resistant cell lines (Figure 14 and Figure 15).

Figure 14. Differential expression of proteins and phosphorylated proteins in CN210-sensitive cell lines after CN210 treatment, as detected via RPPA. Heat map of proteins which were significantly different after CN210 treatment (1 uM) for 48 hours compared to DMSO control.
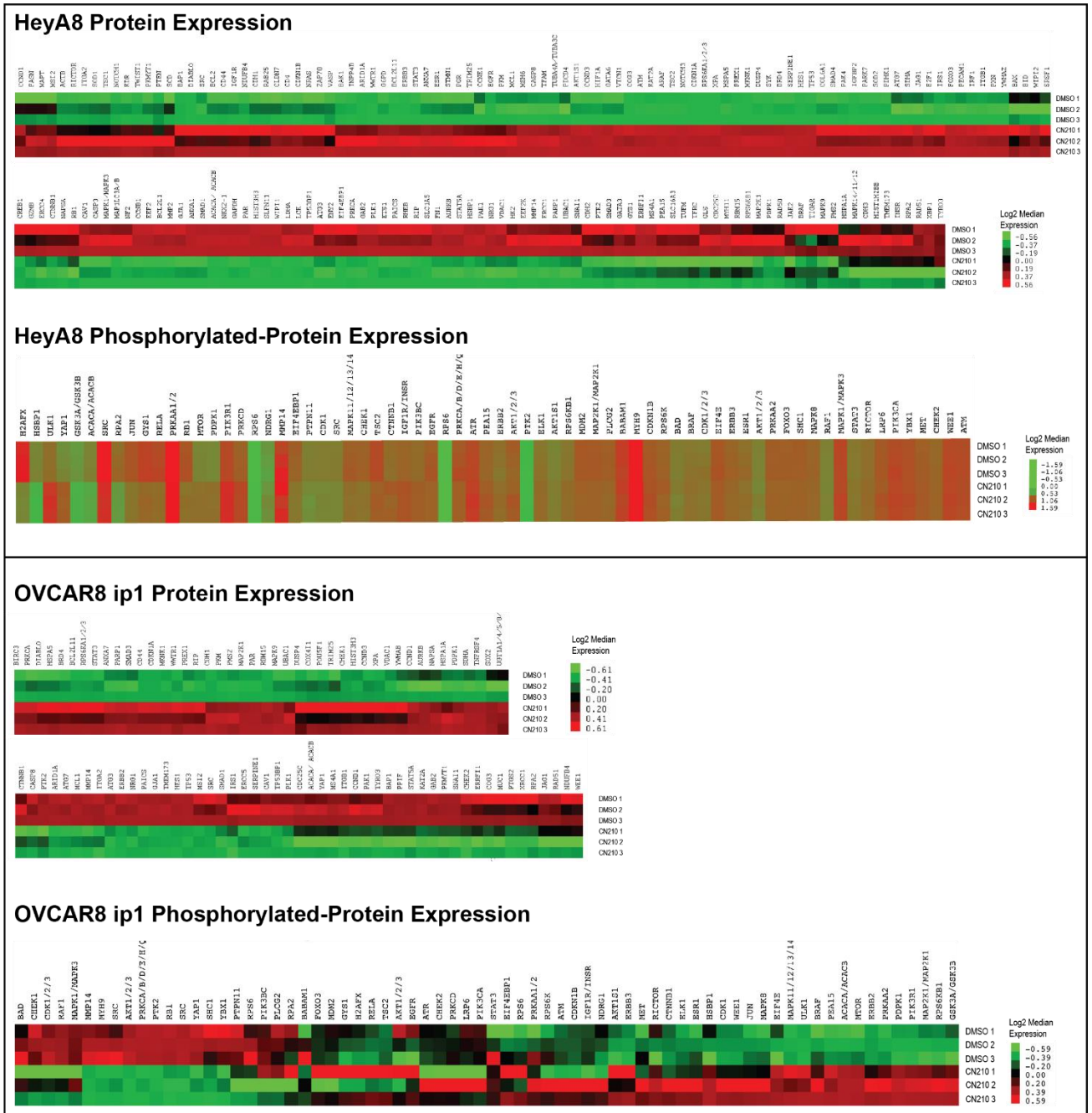
Figure 15. Differential expression of proteins and phosphorylated proteins in CN210-resistant cell lines after CN210 treatment, as detected via RPPA. Heat map of proteins which were significantly different after CN210 treatment (1 uM) for 48 hours compared to DMSO control.
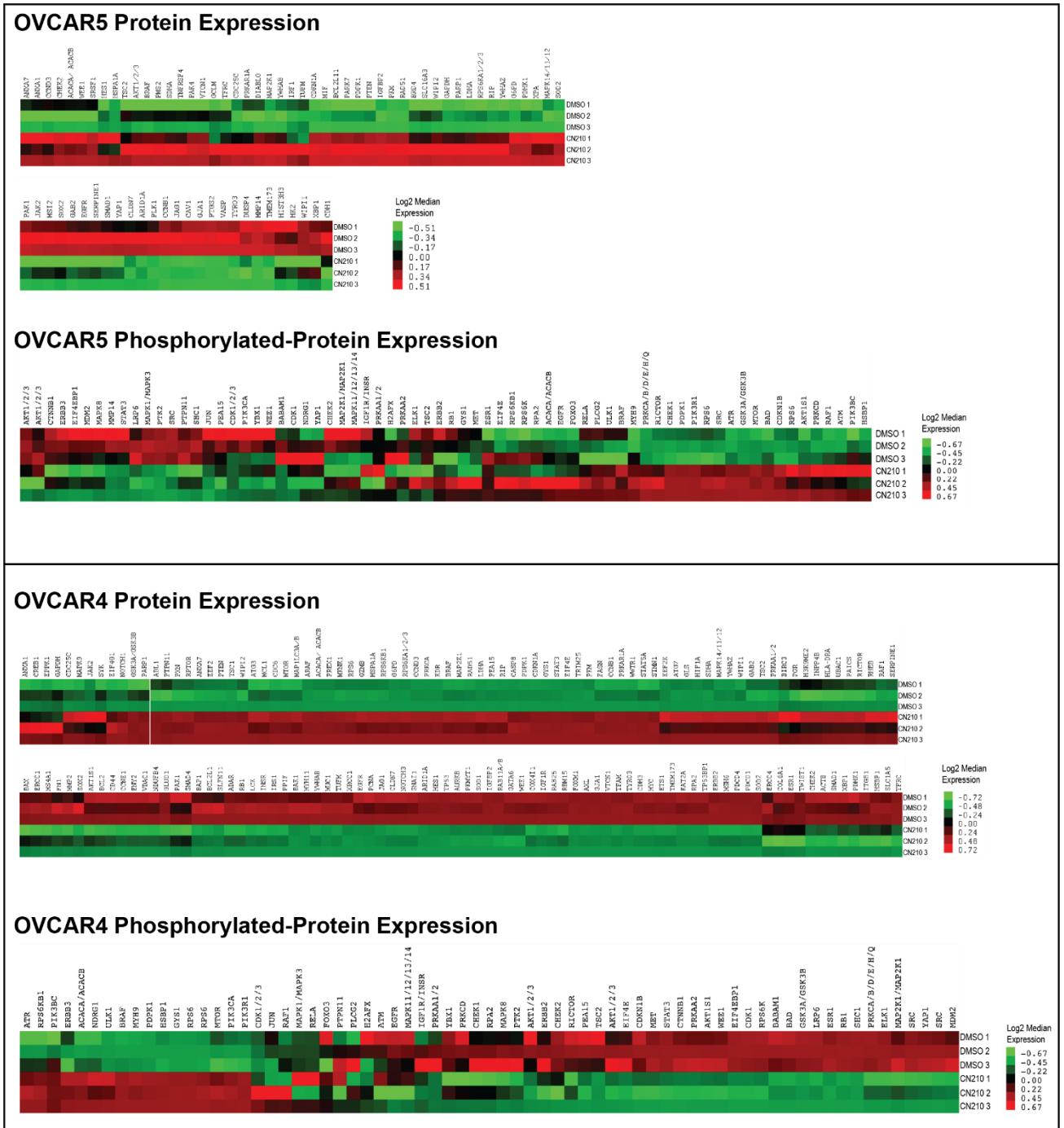
Protein and phosphorylated protein changes were then uploaded into Ingenuity Pathway Analysis (IPA) to perform a network analysis. Interestingly, regulation of eIF4 and P70S6K signaling were highly upregulated in this analysis, suggesting activation of the mTOR pathway after CN210 treatment (Figure 16).

Figure 16. IPA analysis of RPPA data comparing all four treated cell lines to controls. IPA readout of RPPA data showing upregulation of eIF4 and p70S6K signaling after CN210 treatment. Shade of bars signifies up or downregulation of specific pathway (dark orange-strongly upregulated, dark blue-strongly downregulated). -log(p-value) at top signifies strength of association with greater number corresponding to stronger association.
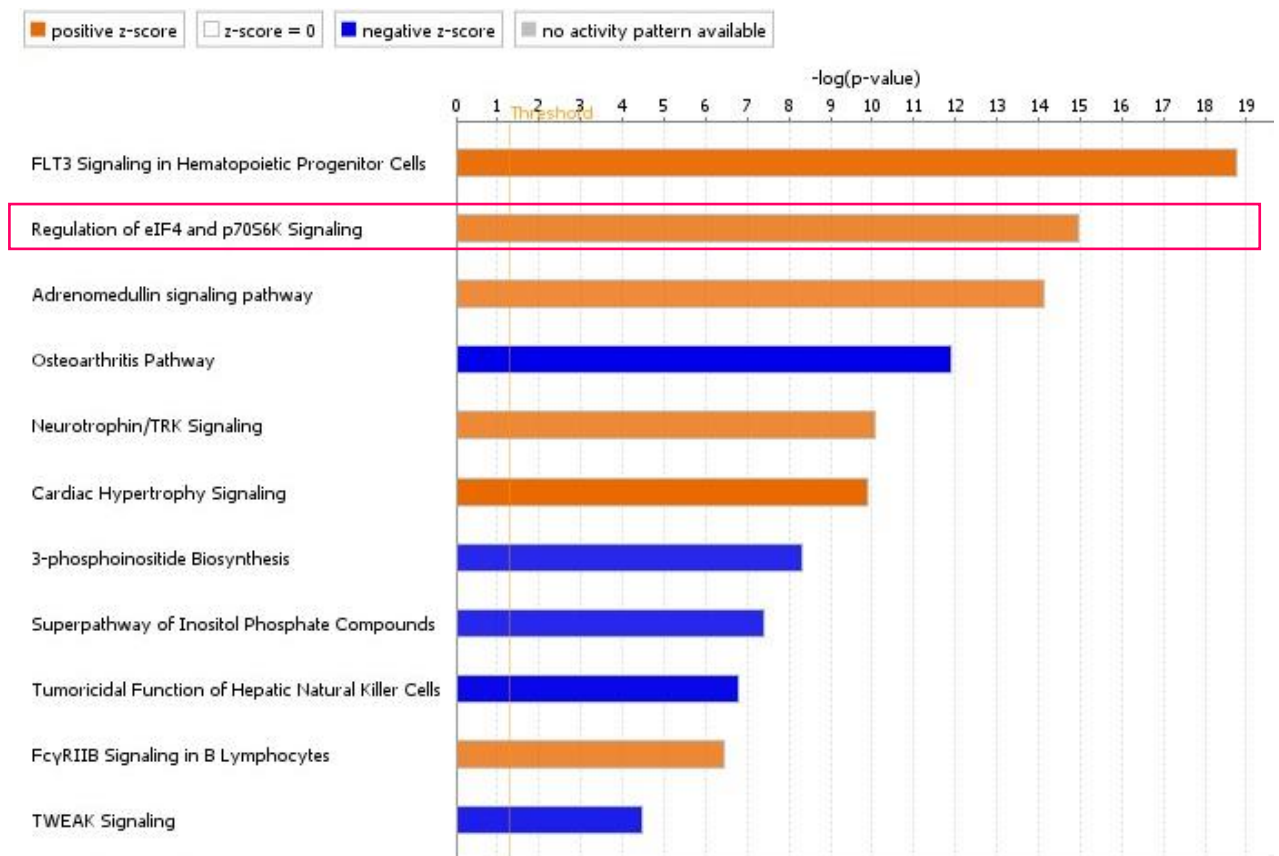
Next we analyzed our RPPA results using IPA in the context of protein expression changes after CN210 treatment between CN210-sensitive and resistant cells. Although both groups displayed an upregulation of mTOR pathway components (eIF4 and P70S6K signaling), the effect was more pronounced in CN210-sensitive cells (Figure 17). This was an interesting finding given that one might expect CN210-resistant cells to use mTOR pathway upregulation as an escape mechanism to cell death.

Figure 17. IPA analysis of RPPA data comparing CN210-sensitive cells to CN210-resistant cells after treatment with CN210. Darker shading signifies stronger association with orange corresponding to upregulation and blue corresponding to downregulation.
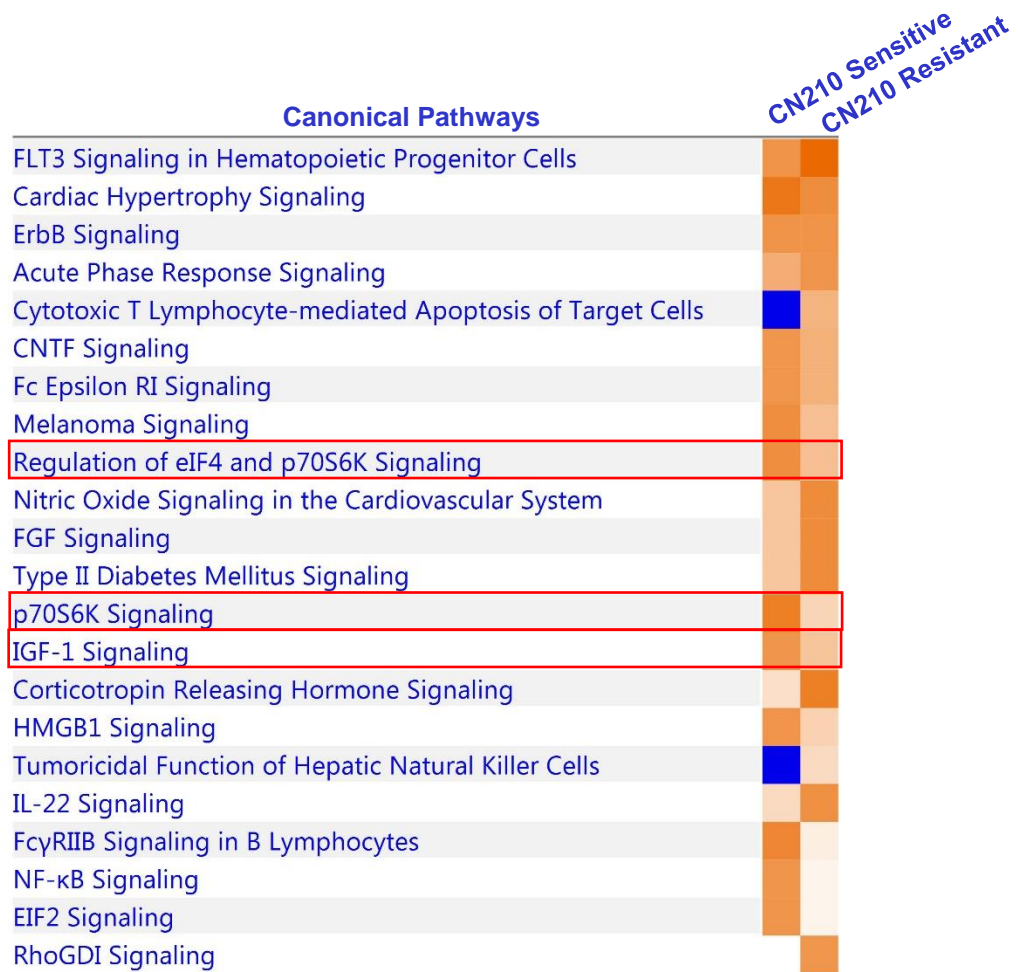
Considering that components of the mTOR pathway were upregulated in all four cell lines after CN210 treatment, we next examined the expression of individual proteins within only the mTOR pathway to determine whether the effect extended throughout. Using the IPA pathway analysis tool and selecting proteins within the mTOR pathway revealed an upregulation of multiple other key proteins including mTORC2, S6K1, Rictor, Akt, RPS6, and p70S6K (Figure 18).

Figure 18. IPA pathway generator of specific mTOR related proteins. RPPA data examined was all CN210 treated cells vs. control. Red proteins signifies an increased expression after CN210 treatment, while green signifies decreased expressed. Lines connecting the individual proteins signify a direct interaction. Red box highlights the specific upregulated mTOR pathway proteins.
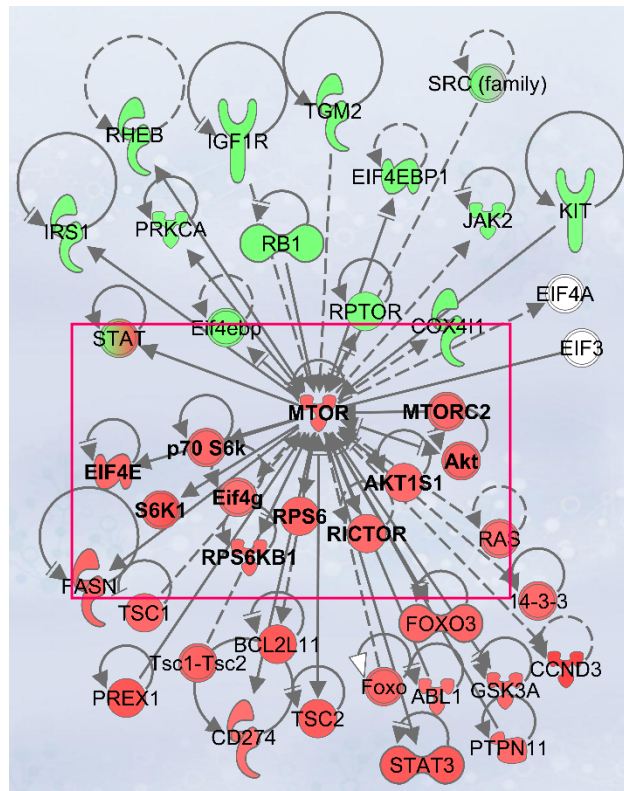
The IPA software uses RPPA data to generate pathways from actual experimental results in combination with expected changes in proteins based on those results. To examine the expression changes of only those proteins involved in the mTOR pathway from our RPPA dataset, an additional heat map was created (Figure 19). Although not every protein resulted in a statistically significant fold change after CN210 treatment, analysis of those that did revealed a global activation of many mTOR pathway components. Specifically, activation of PI3K, mTOR, and S6K was observed in all cell lines after CN210 treatment. Activation of Rictor was seen in HeyA8 and OVCAR5 cell lines. Interestingly however, CN210 treatment resulted in decreased activation of Akt in OVCAR8 ip1 and OVCAR5 cell lines, and decreased total Raptor in HeyA8 and OVCAR8 ip1 cell lines.

Figure 19. mTOR pathway specific protein expression changes after CN210 treatment from RPPA data. Red and green shading correspond to increased (fold change >1.0) and decreased expression (fold change <1.0) after CN210 treatment, respectively. Only values that were considered statistically significant (P < 0.05 as determined by the Student t test) were included, expression changes that were not significant are denoted by an X. (Top) Heat map using a gradient with gray as the baseline of 1.0. (Bottom) Binary heat map displaying overall direction of protein expression change after CN210 treatment.
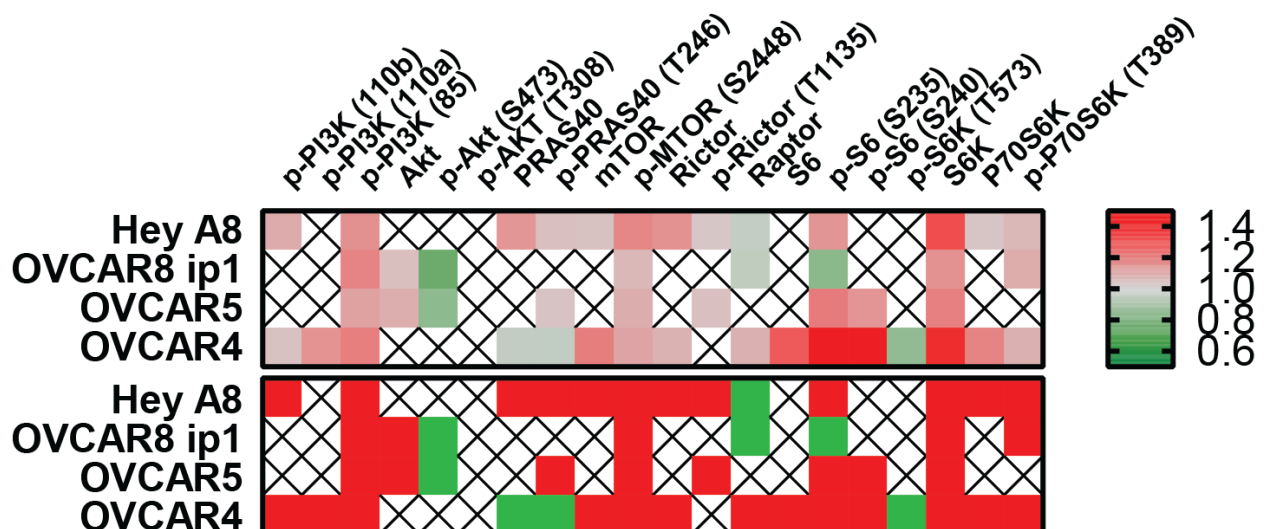
Importantly, we show that CN210 treatment resulted in upregulation of the entire PI3K/Akt/mTOR pathway. It appears that expression of mTORC2 is increased after CN210 treatment as evidenced by the increase in activated and total Rictor. Furthermore, downstream components of the mTOR pathway such as S6 and P70S6K were also found to be increased after BET inhibition. Our RPPA data revealed that activation of the mTOR pathway appears to be an early adaptive change to BET inhibition and could possibly serve as an additional target to increase the anti-tumor activity of BET inhibitors.

Combined Effect of BET and Rapamycin in ovarian cancer cells

Based on our findings that BET inhibition of ovarian cancer cells leads to mTOR pathway activation, we next examined the effect of CN210 and mTOR inhibitors on cell viability. As discussed above, rapamycin is an mTORC1 specific inhibitor which functions by forming a complex with FKBP12 which can inhibit mTOR when it is a part of mTORC1 but not mTORC2. The combination of CN210 with rapamycin produced only modest evidence that there was synergy between the two compounds (Figure 20). HeyA8 cells appeared to have the most promising synergistic interaction as evidenced by all points on the logCI graph being negative (far below 0). Although the remaining cell lines demonstrated synergistic interactions at certain specific concentrations, there was no strong evidence that rapamycin synergized with CN210 on a global scale. Furthermore, the inherent sensitivity of the cell lines to CN210 did not appear to play a role in whether synergy between CN210 and rapamycin occurred.

Figure 20. Effect of CN210 and rapamycin combination on cell viability in CN210-resistant and sensitive ovarian cancer cell lines.
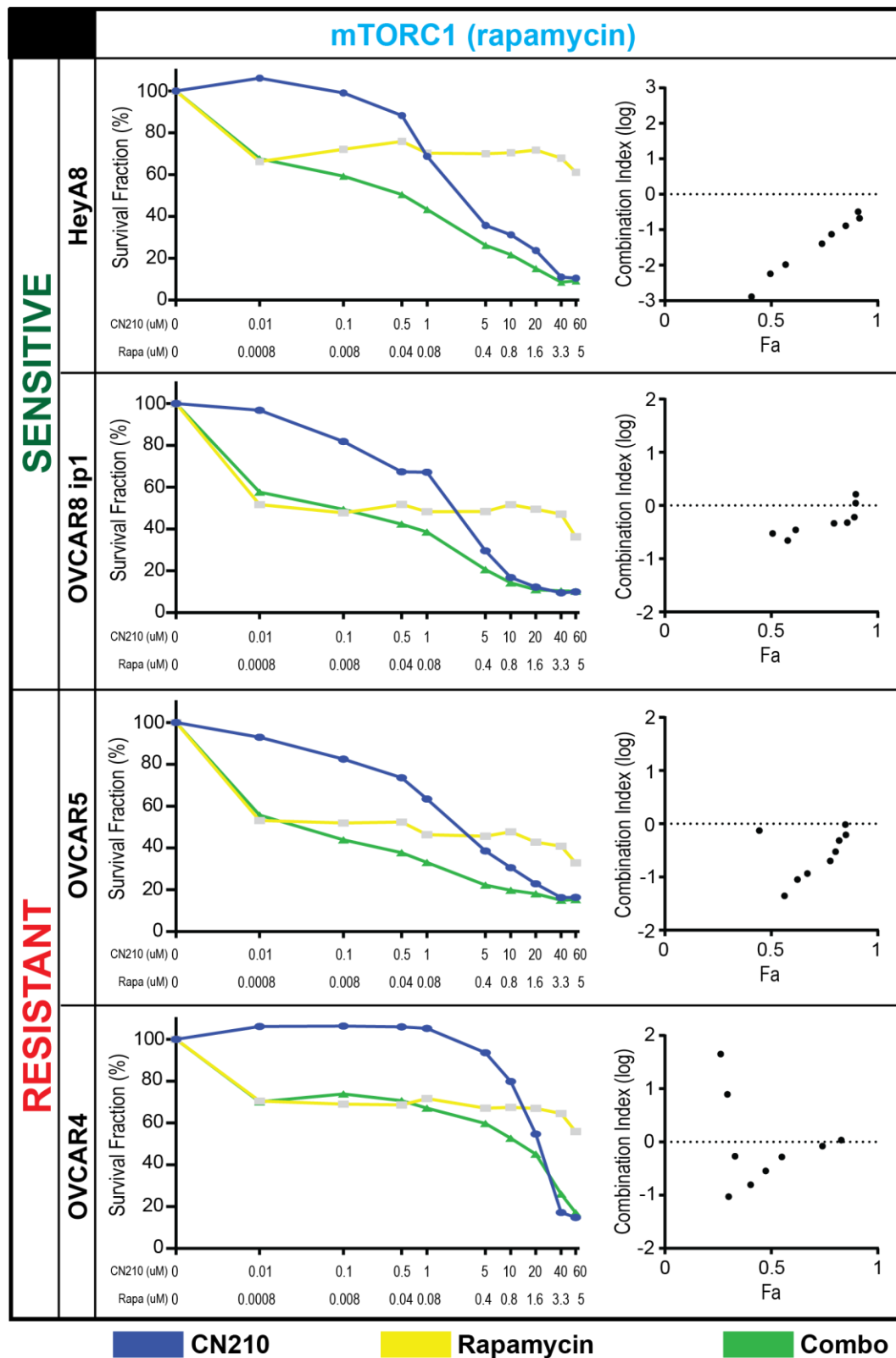
Extending upon the findings from the cell viability analysis, we next analyzed the effect of CN210 and rapamycin combination on apoptosis (Figure 21). All cell lines except OVCAR4 cells showed a significant increase in apoptosis after CN210 treatment vs. DMSO. Importantly, the concentration of CN210 used here was 10 uM (increased from the 1 uM used in the olaparib experiments) and the treatment time was 48 hours (decreased from the 72 hours used above). This is likely the explanation for why the cell lines displayed a more robust response to CN210 inhibition. Rapamycin treatment alone did not result in a significant increase in apoptosis compared to DMSO in any of the cell lines. All of the cell lines except for OVCAR4 displayed a significant increase in apoptosis after combined treatment compared to DMSO. Only OVCAR8 ip1 had any evidence of a potentially enhanced effect with combination treatment, and even this absolute increase amount was minimal. These findings suggest that inhibiting mTORC1 only, either alone or in combination with CN210, is not an effective method to increase cell death.

Figure 21. Effect of CN210 and rapamycin combination on apoptosis in CN210-resistant and sensitive cell lines. Error bars represent the SD. Significance reported for each group compared to DMSO control, except where indicated. *, P <0.05; **, P <0.001; and ***, P <0.0001 as determined by the Student *t* test. ns, non-significant.
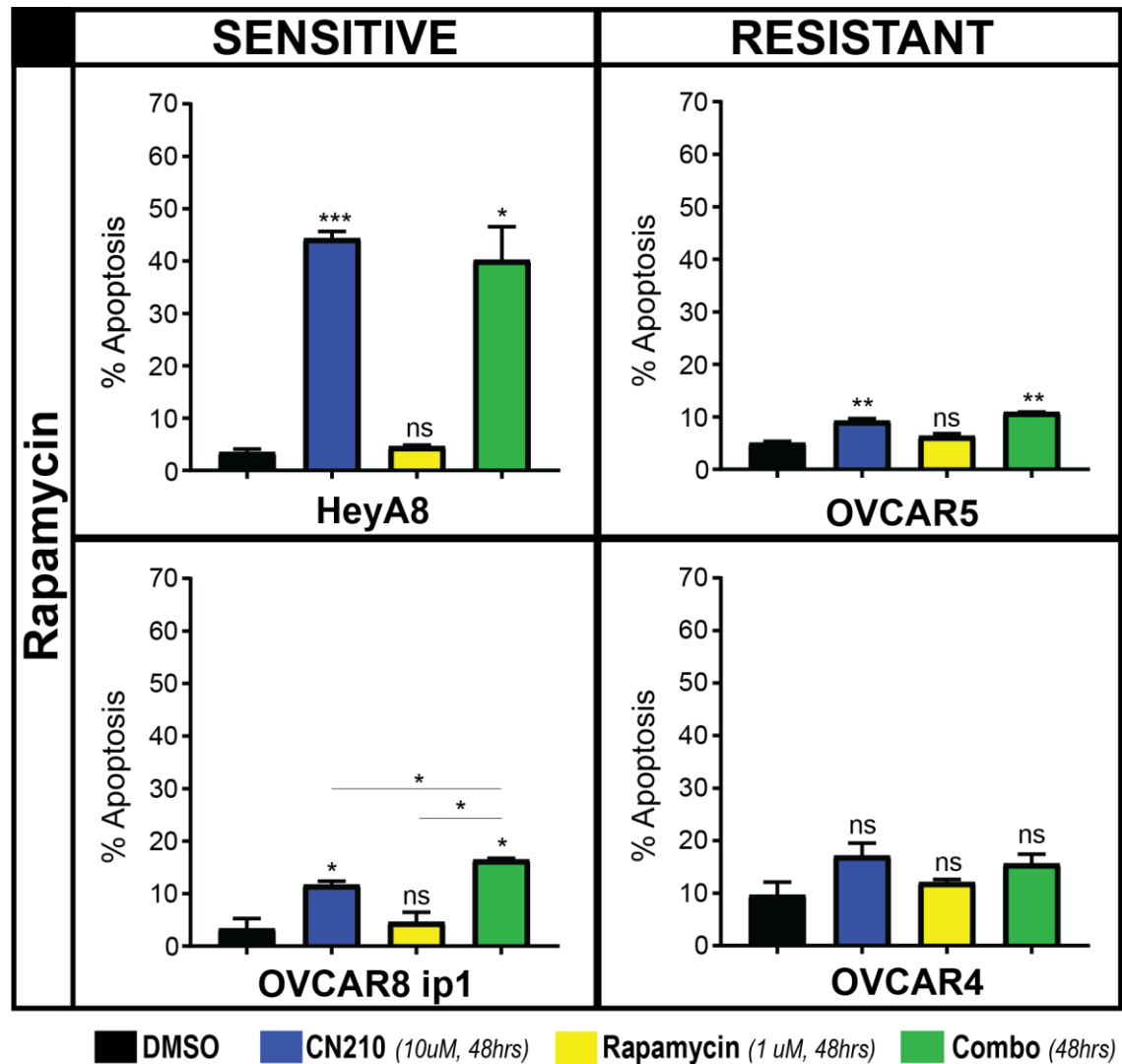
Combined Effect of BET and INK-128 in ovarian cancer cells

Next, we examined the effect of combining CN210 with a dual mTORC1/2 inhibitor. As mentioned above, INK-128 is a dual mTORC1/2 inhibitor which functions as an ATP-competitive inhibitor of mTOR, blocking the phosphorylation of all downstream targets of mTORC1 and mTORC2. Combination of CN210 with INK-128 produced synergistic decreases in cell viability in both CN210-sensitive (HeyA8, OVCAR8 ip1), as well as CN210-resistant (OVCAR5) cell lines (Figure 22). In these three cell lines, the combination curves (green) lie below the individual drug curves (blue/purple) at every concentration point, suggesting a global synergistic or at least enhanced effect in decreasing cell viability. This is also represented in the logCI graphs showing that the majority of the points for these three cell lines are far below zero. The logCI values for OVCAR4 cells suggest an antagonistic interaction between CN210 and INK-128 at 50% of the concentrations tested, as can also be seen in the cell viability curve.

Figure 22. Effect of CN210 and INK-128 combination on cell viability in CN210-resistant and sensitive ovarian cancer cell lines.
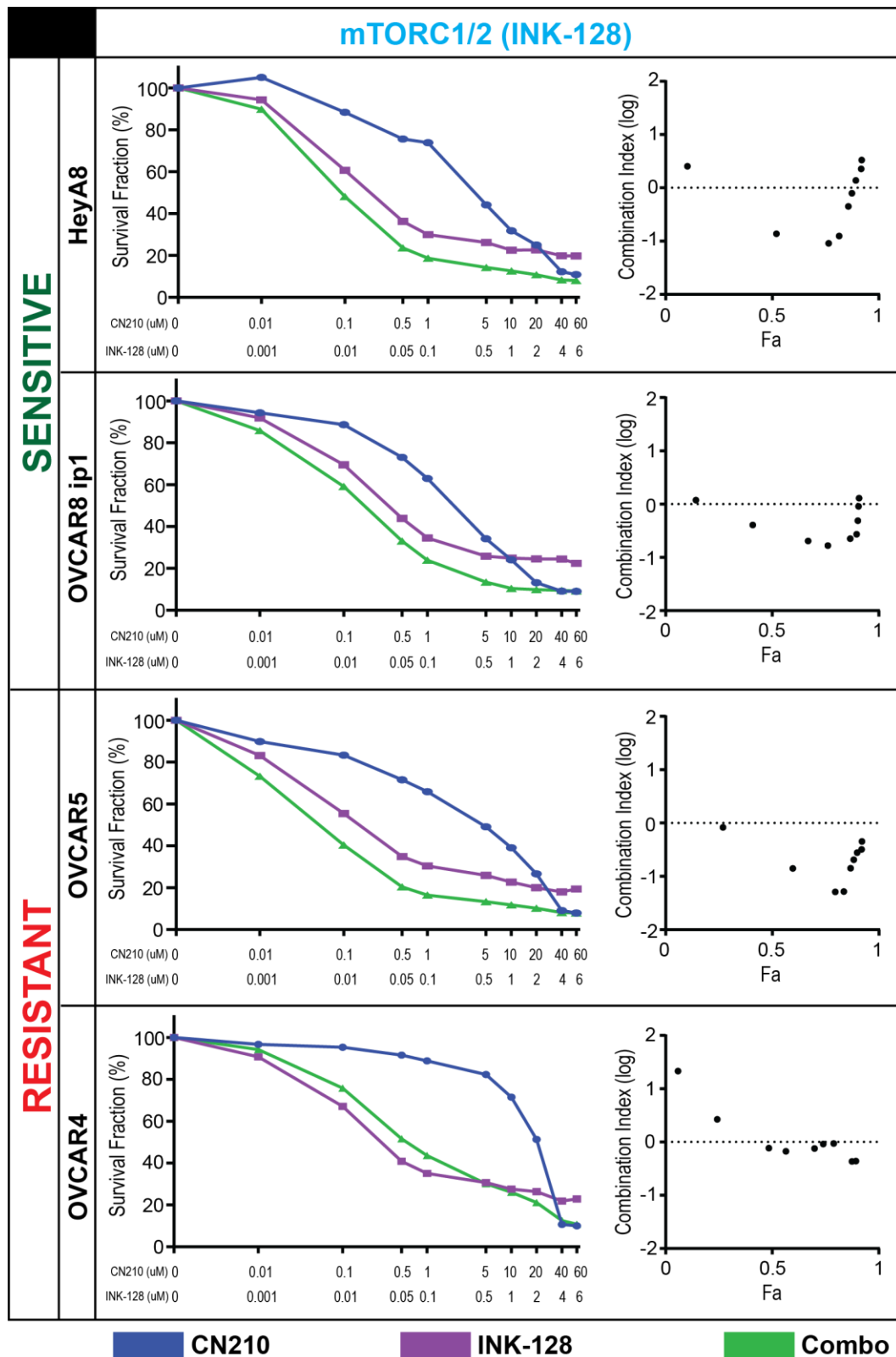
The combination of CN210 and INK-128 also led to more impressive results on apoptosis than combination with rapamycin (Figure 23). CN210 treatment alone resulted in a significant increase in apoptosis compared to DMSO in every cell line tested. Additionally, HeyA8 and OVCAR4 cell lines both showed a significant increase in apoptosis with INK-128 treatment alone compared to DMSO. The combination of CN210 and INK-128 produced a significant increase in apoptosis compared to DMSO in all four cell lines, similar to what was seen when combined with rapamycin (aside from OVCAR4). Although no meaningful interactions between CN210 and rapamycin were identified above, we show here that the CN210/INK-128 combination led to a significantly greater amount of apoptosis in OVCAR8 ip1 and OVCAR5 cells than either of the individual drugs alone. In fact, the results from the OVCAR8 ip1 cells suggest a true synergistic interaction between CN210 and INK-128 in this cell line.

Figure 23. **Combined effect of CN210 and INK-128 on apoptosis in CN210-resistant and sensitive cell lines.** Error bars represent the SD. Significance reported for each group compared to DMSO control, except where indicated. *, P <0.05; **, P <0.001; and ***, P <0.0001 as determined by the Student *t* test. ns, non-significant.
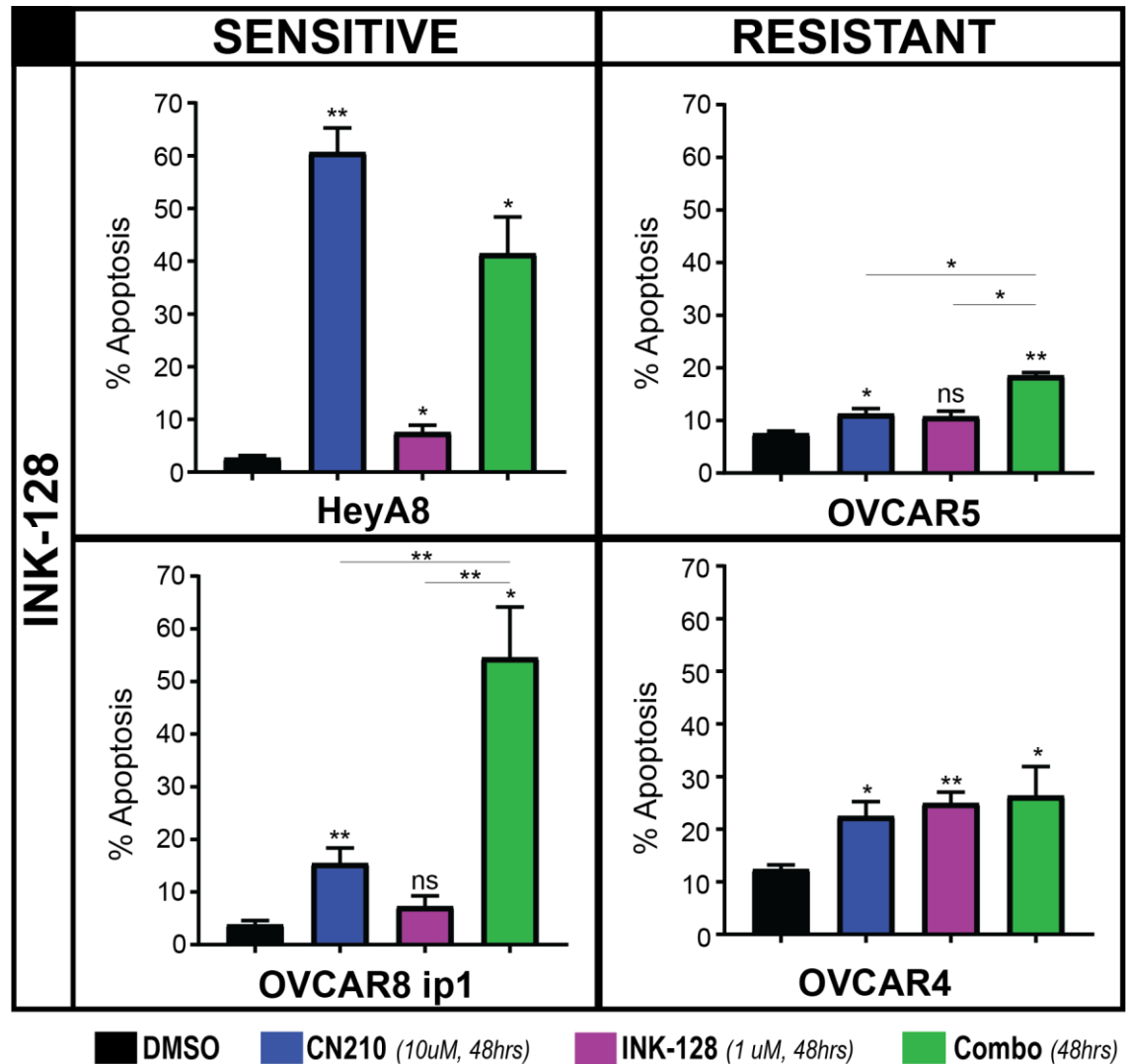
Combined effect BET and mTOR inhibition in a CN210-equivocal cell line

As the combined effect of CN210 with either rapamycin or INK-128 did not appear to be specific to either CN210-resistant or sensitive cells, we next determined the effect in the CN210-equivocal SKOV3 ip1 ovarian cancer cell line. As discussed above, the IC_{50} for CN210 in SKOV3 ip1 cells was 13.5 uM, falling in the middle between the CN210-sensitive and resistant cell lines originally selected. Combination treatment of CN210 and rapamycin resulted in a synergistic decrease in cell viability at the majority of concentrations tested per the log-CI graph. This same effect was also seen between CN210 and INK-128, however to a lesser extent (Figure 24).

Analysis of the combined effect on apoptosis demonstrated SKOV3 ip1 cells to be particularly sensitive to CN210 and mTOR inhibition. CN210 treatment alone resulted in a significant increase in apoptosis compared to DMSO. Both rapamycin and INK-128 treatment alone, as well as in combination with CN210 produced a significant increase in apoptosis when compared to DMSO. Interestingly, both CN210/rapamycin and CN210/INK-128 combinations resulted in significant increases in apoptosis compared to either CN210, rapamycin, or INK-128 alone (Figure 25). This finding demonstrated that the inherent sensitivity of an ovarian cancer cell line to CN210 does not predict its sensitivity to combined inhibition of both BET and mTOR proteins.

Figure 24. Combined effect of CN210 and either rapamycin or INK-128 on cell viability in a CN210-equivocal ovarian cancer cell line.
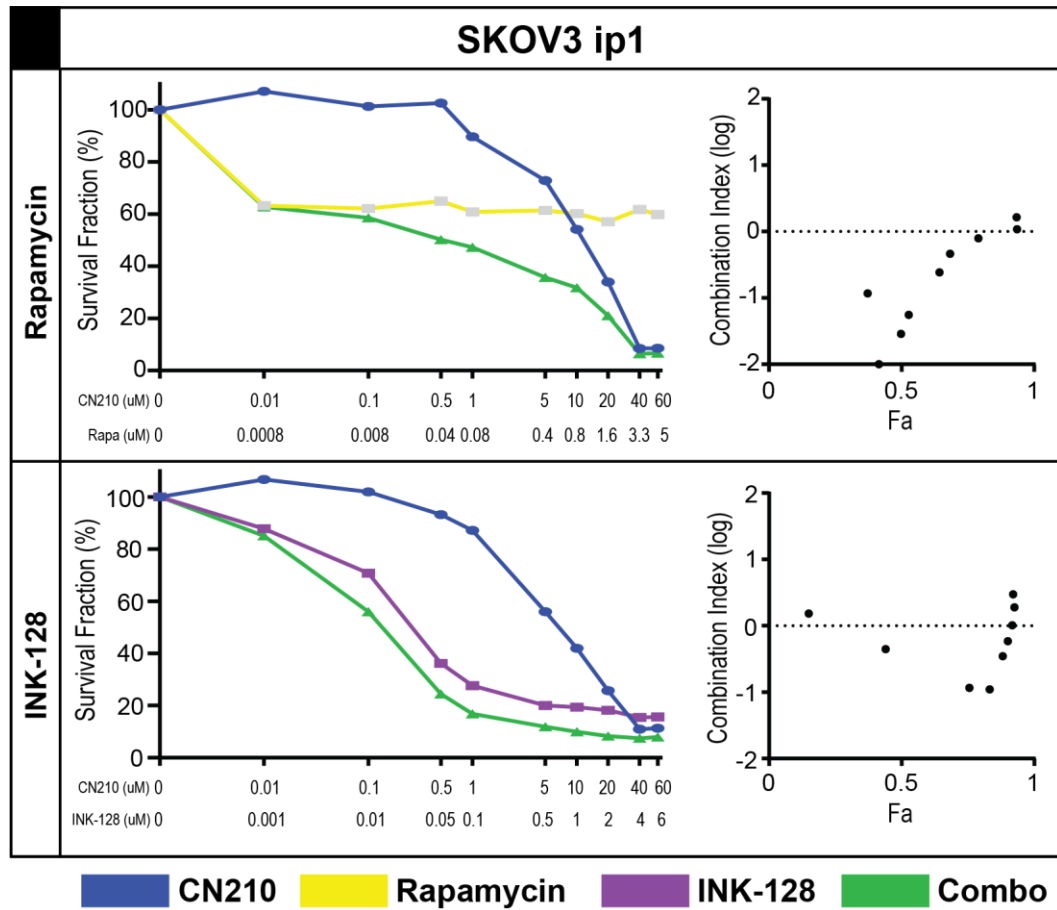
Figure 25. Combined effect of CN210 and either rapamycin or INK-128 on apoptosis in a CN210-equivocal ovarian cancer cell line. Error bars represent the SD. Significance reported for each group compared to DMSO control, except where indicated. *, P <0.05; **, P <0.001; and ***, P <0.0001 as determined by the Student *t* test. ns, non-significant.
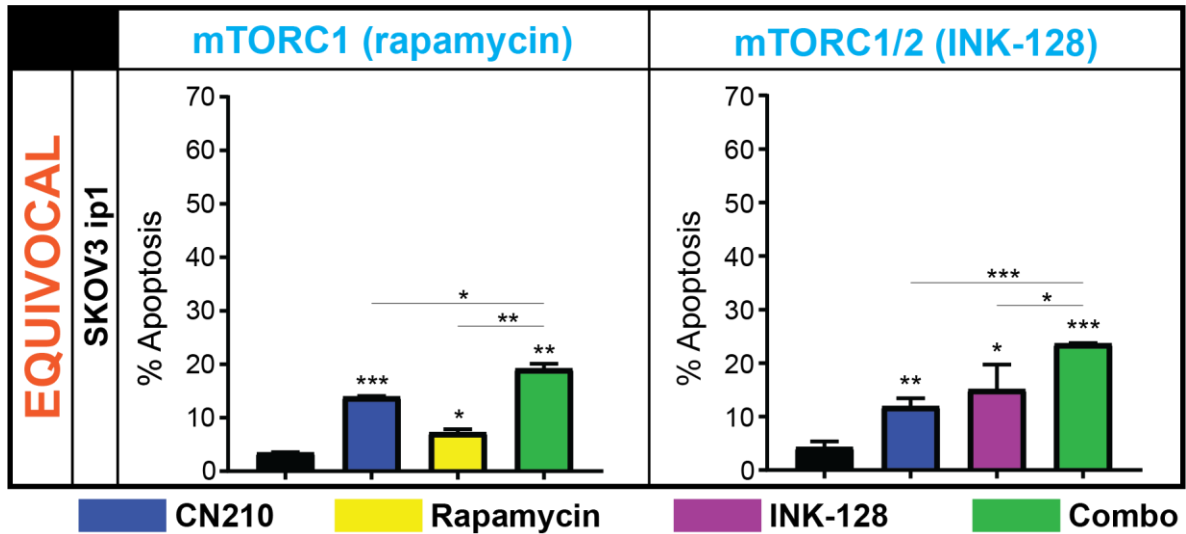
Validation of RPPA mTOR pathway changes after BET inhibition

To determine whether the RPPA results described above were reproducible, we next performed a series of Western blots to examine the protein expression changes after treatment with CN210. Notably, the RPPA data was generated from cell lysate after cells were treated with 1 uM CN210 treatment for 48 hours. As the RPPA platform allows for the detection of relatively small changes in protein expression, we chose to perform the validation experiments after treating cells with 10 uM of CN210 for 48 hours, in the hopes of amplifying the previously observed effects (Figure 26).

CN210 treatment resulted in activation of Rictor (measured from change in phosphorylated-Rictor) in all four cell lines, most notably in OVCAR8 ip1, OVCAR5, and OVCAR4 cells. Our heat maps in Figures 14 and 15 revealed phosphorylated-Rictor to be strongly upregulated in OVCAR8 ip1 and OVCAR5 cell lines, weakly upregulated in HeyA8 cells, and no significant fold change detected in OVCAR4 cells. CN210 treatment resulted in activation of Raptor in HeyA8 and OVCAR8 ip1 cell lines, with no change observed in OVCAR5 or OVCAR4 cells. Notably, the RPPA analysis did not include phosphorylated-Raptor. Our heat maps in Figures 14 and 15 did not register any significant changes of total Raptor in either HeyA8, OVCAR8ip1, or OVCAR5 cell lines, but did show upregulation in OVCAR4 cells. Furthermore, the additional heat map of only mTOR pathway proteins in Figure 19 showed a very miniscule decrease of total Raptor in HeyA8 and OVCAR8 ip1 cells, and a moderate increase in OVCAR4. None of the four cell lines showed any activation of mTOR at the 10 uM CN210 concentration using Western blot, however the RPPA data demonstrated significantly increased phosphorylated-mTOR in HeyA8, OVCAR8 ip1, OVCAR5, and OVCAR4 cell lines at the 1uM concentration. Using Western blot to examine the effect on a downstream target of mTORC1, we found increased activation of P70S6K in HeyA8, OVCAR8 ip1, and OVCAR5 cell lines with no change observed in OVCAR4 cells using 10 uM CN210. Our RPPA data demonstrated strong activation of P70S6K in HeyA8, OVCAR8ip1, and OVCAR4 cell lines with only slight activation in OVCAR5. Analysis of the effect on Akt activation at the 10 uM concentration of CN210 did not reveal any significant change, however the heat map in Figure 19 demonstrated a decrease in Akt activation. In general, RPPA data tends to identify only subtle changes in protein expression that can be used to generate hypotheses. Taking this into consideration, our validation experiments were able to aptly reproduce these trends in protein change after CN210 treatment.

Figure 26. mTOR pathway protein expression changes after CN210 treatment. Cells were treated with either 10 uM CN210 or DMSO in 10% FBS for 48 hours and harvested for cell lysate.
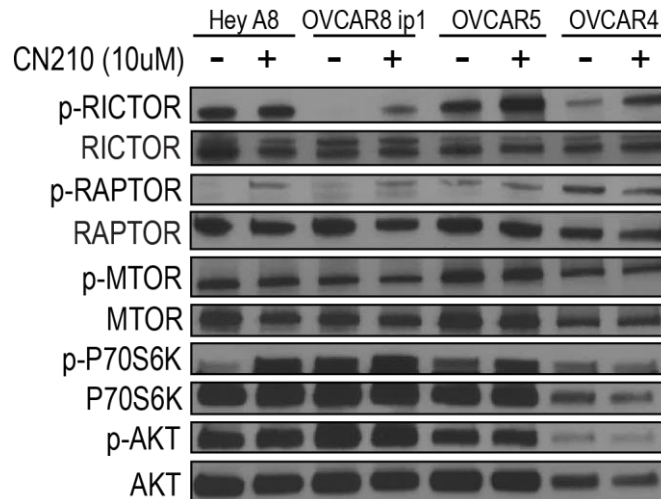
To determine if the fetal bovine serum (FBS) present in our cell culture media interfered with our assessment of protein expression changes, we next treated a select group of cells with 10 uM CN210 in serum free media (SFM) for 24 hours. In addition, untreated cells were grown in SFM for the same duration to serve as control. We selected OVCAR8 ip1, OVCAR5, and SKOV3 cells, to represent our CN210-sensitive, resistant, and equivocal cell lines, respectively. Interestingly, we found that Akt activation decreased in all three cell lines after CN210 treatment, a result that was consistent with our RPPA analysis and mTOR pathway specific heat map (Figure 27).

Figure 27. Akt protein expression change after CN210 treatment. Cells were treated with either 10 uM CN210 or untreated in SFM10 for 24 hours and harvested for cell lysate.
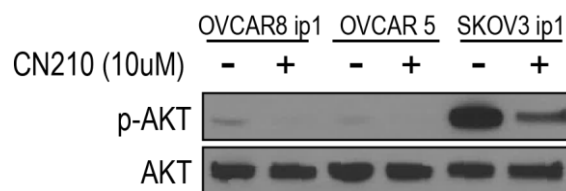
Effect of BET and dual mTOR inhibition In Vivo

To determine the effect of BET and mTOR inhibition *in vivo*, we selected the SKOV3 ip1 cell line as it demonstrated enhanced responses between BET and mTOR inhibitors. Furthermore, we chose to use the dual mTOR inhibitor INK-128 as it achieves a more robust blockade of the mTOR pathway than the mTORC1-specific rapamycin and other similar rapalogs. We injected 1×10^6 SKOV3 ip1 cells intraperitoneally into nude mice to emulate the normal growth environment of human ovarian cancer. Treatment began on day 8 and consisted of 100 mg/kg CN210, 1 mg/kg INK-128, a combination of both CN210 and INK-128, or control, each given daily via oral gavage. After 35 days of treatment, necropsy revealed that mice treated with either INK-128 alone or the combination CN210/INK-128, had a significantly decreased tumor weight compared to control (Figure 28A). Mice treated with CN210 also had a decreased tumor weight, although this was not statistically significant. Importantly however, we observed an enhanced effect at decreasing tumor weight when INK-128 was combined with CN210, as the CN210/INK-128 group had significantly decreased tumor weights compared to the CN210 group alone. Each treatment group (CN210, INK-128, or CN210/INK-128) also had a decrease in the total number of tumor nodules at necropsy compared to control, however these findings were not statistically significant (Figure 28B). It is important to mention that mice in the combination group displayed toxicity to CN210/INK-128 combination treatment at day 14. This was manifested primarily through decreased body weight and skin changes. All mice were given 4 days without intervention and then treatment was restarted for all groups on an every other day schedule. At final necropsy, there was no significant difference in mouse weight between the control and combination groups (Figure 28C). Mice in the control group developed bulky peritoneal tumors as well as diffuse nodular disease along the mesentery and intestines. Mice in the individual treatment groups still had some bulky peritoneal disease but far less diffuse nodular disease (Figure 28D). Although toxicity emerged in the combination group, once adjusted for and corrected, there was a

significant benefit to the mice receiving both CN210 and INK-128, compared to both control as well CN210 treatment alone.

Figure 28. Effect of CN210 and INK-128 combination treatment in SKOV3 ip1 ovarian cancer mouse model. (A-C) Mouse weight, tumor weight, and number of tumor nodules at necropsy across all treatment groups. (D) Representative mice images of tumor burden in each treatment group. Significance reported for each group compared to control, except where indicated. *, $P < 0.05$ as determined by the Student *t* test or Mann-Whitney test, depending on normality assumption. ns, non-significant.
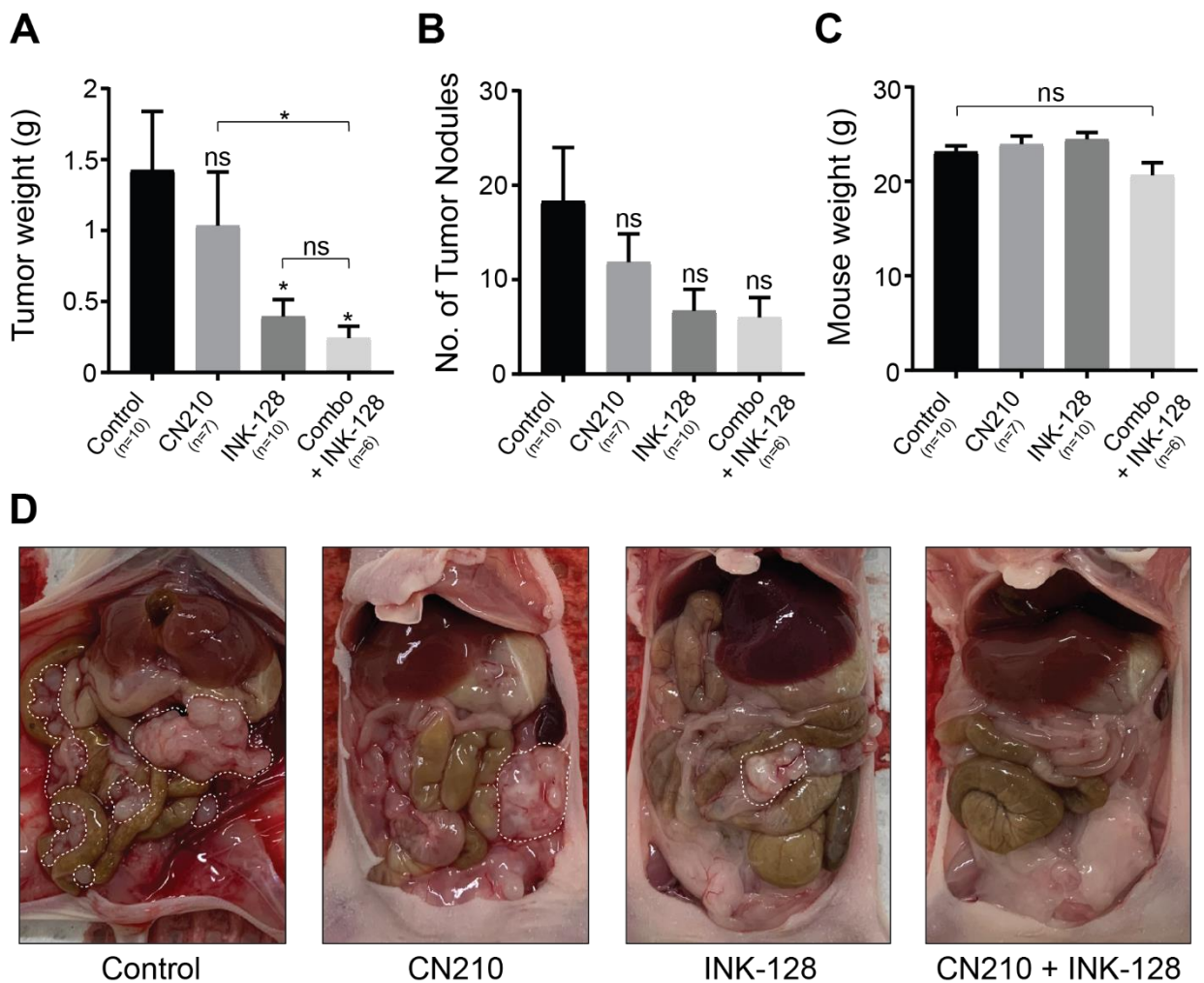
DISCUSSION

Key Findings

The key findings of the work presented above is that mTOR pathway activation is an early adaptive response to BET inhibition in ovarian cancer cells, and that targeting of both BET and mTOR proteins together can produce enhanced interactions. Specifically, we found that the use of a novel, clinical-trial ready BET inhibitor combined with a dual mTOR inhibitor produced synergistic decreases in cell viability, and significant increases in apoptosis. Furthermore, using an orthotopic mouse model, we showed that CN210/INK-128 combination therapy led to a significant decrease in tumor weight when compared to control or CN210 treatment alone.

Role of cMYC expression in CN210-treated ovarian cancer cells

Using the therapy prediction tool, we previously identified Brd4 to be upregulated in ovarian cancer compared to normal ovarian tissue and that there were multiple compounds being used in the phase 1 clinical setting to inhibit BET proteins. Although BET inhibitors had yet to be tested specifically in ovarian cancer patients, the data for cancer types it had been tested in demonstrated only modest response rates. In light of this, we decided to explore the use of combining additional anti-tumor agents with BET inhibition in the hopes of achieving an improved response that would ultimately translate into improved patient outcomes.

Previous reports have suggested that cancer cells which overexpress cMYC are the most sensitive to BET inhibition, predominantly due to an increased localization of BET proteins at the cMYC promoter and enhancer regions. After screening a panel of ovarian cancer cell lines with CN210, we selected two lines displaying CN210-sensitivity and two lines displaying CN210-resistance, as measured by IC_{50}. Interestingly, CN210 treatment led to substantially decreased cMYC expression in both HeyA8 and OVCAR4 cells, although HeyA8 cells demonstrated sensitivity to

CN210 and OVCAR4 cells demonstrated resistance. This finding suggests the presence of alternative mechanisms of cMYC regulation in ovarian cancer cells other than BET-related promoter interactions. Additionally, this shows that BET inhibitor-mediated cMYC expression change does not necessarily correlate with the effect on cell viability in ovarian cancer cells.

Examination of combined BET and PARP inhibition using in vitro and in vivo models

We next sought to examine the combined effect of BET and PARP inhibition in ovarian cancer models, as previous literature has reported a strong synergistic effect between the two compounds. While we did detect a synergistic effect at certain concentrations in some cell lines, our overall results were not consistent with the robust synergy between BET and PARP inhibition previously reported. One possible explanation for this could be that the majority of previous studies used JQ1 as the BET inhibitor. JQ1 produces a strong inhibition of BET proteins with an IC_{50} of ~100 nM, which is a 100-1000x fold difference in the IC_{50}s we identified with CN210. Furthermore, JQ1 has been shown to have multiple off-target effects, which limits its applicability in the clinical realm. Interestingly however, we did find that the addition of olaparib to CN210 increased apoptosis compared to CN210 alone in both HeyA8 and OVCAR4 cells, which were the two cell lines showing a downregulation of cMYC after CN210 treatment. This suggests that cells with decreased levels of cMYC might be more sensitive to BET/PARP inhibition than those with higher levels. We also examined the effect of altering the drug concentrations and treatment times in a CN210-resistant cell line to determine whether an enhanced effect could be produced. At every condition tested, the amount of apoptosis in the CN210/olaparib combination group essentially mirrored the amount in the CN210 only group, with no evidence of synergism observed. This suggests that the effect of the combination group was driven only by the CN210 with no additional contribution from olaparib. Notably, OVCAR5 is a *BRCA* wild-type (WT) cell line, which may explain the poor contribution from olaparib, however the OVCAR4 cell line is also *BRCA* WT and olaparib treatment produced 3x more apoptosis in OVCAR4 cells than in

OVCAR5 cells. Lastly, using an ovarian cancer orthotopic mouse model, we did not find any significant difference in tumor weight or number of tumor nodules between the control group and any of the treatment groups. As will be discussed in the limitations section, the choice of a CN210-resistant cell line, in addition to experimental technical difficulties, likely played a role in this result.

Considering that the two CN210-sensitive and resistant cell lines were *BRCA* WT, we explored the effect of BET and PARP inhibition in two *BRCA* mutated cell lines. Overall the results were far from expected given the efficacy of PARP inhibitors in ovarian cancer patients with *BRCA* mutations. Combined treatment with CN210/olaparib in these cell lines did not decrease cell viability to the extent that it did in any of the four *BRCA* WT cell lines. In fact, olaparib treatment did not even result in a significant increase in apoptosis in the *BRCA1* mutated cell line (COV362) compared to control. One possible explanation is that these cell lines have only one mutated copy of *BRCA* whereas tumor cells from patients have two mutated copies. Additionally, as neither of the *BRCA* mutated cell lines displayed synergy between CN210 and olaparib, this suggests a lack of involvement of BET proteins in the homologous recombination repair pathway.

Using RPPA analysis to identify adaptive changes to BET inhibition

Given that our findings using BET and PARP inhibitors were not as prominent as previously reported, we employed RPPA analysis to determine the adaptive changes to BET inhibition. RPPA is a valuable tool that can be used to identify subtle changes in protein expression after drug treatment at a high-throughput level. Importing our RPPA results into IPA revealed that multiple components of the mTOR pathway were upregulated after BETi treatment, suggesting that this pathway could be targeted to produce a synergistic effect with CN210. Furthermore, there did not appear to be a difference in this upregulation based on the cell lines' inherent sensitivity or resistance to CN210. Analysis of our raw data alone confirmed many of the findings from the IPA, including an interesting

finding of decreased activation of Akt in OVCAR8ip1 and OVCAR5 cells after CN210 treatment. One possible explanation for this is due to the multiple feedback loops present within the mTOR pathway, notably the negative feedback loop between mTORC1 and insulin/PI3K signaling (115).

In vitro assessment of the combined use of BET and mTOR inhibitors

The addition of mTOR inhibition (specifically INK-128) to BET inhibition in ovarian cancer cells produced a more substantial effect than the BETi/PARPi combination. We found that the addition of the mTORC1 inhibitor rapamycin to CN210 produced the greatest decrease in cell viability within HeyA8 and OVCAR5 cells, which again displayed different inherent sensitivity to BET inhibition. As a treatment alone, rapamycin was not effective in increasing the amount of apoptosis compared to DMSO. When combined with CN210 in the OVCAR8 ip1 cell line however, it did demonstrate a significant increase in the amount of apoptosis compared to CN210 or rapamycin alone, although the absolute amount was small. In addition, the overall effect of the combination group was weak with only ~20% of cells undergoing apoptosis. This is not surprising given the complexity of the mTOR pathway containing two main complexes that each have numerous interactions and feedback loops between various other components. Specifically, mTORC1 inhibition can actually increase Akt phosphorylation via a decrease in the negative feedback loop with the insulin/PI3K pathway. mTORC2 however, is still able to activate Akt and other downstream targets involved in cell survival when only mTORC1 is inhibited.

Combining CN210 with an inhibitor of both mTORC1 and mTORC2, rather than only mTORC1, produced significant *in vitro* and *in vivo* effects compared to CN210 by itself. We showed that CN210/INK-128 combination treatment produced a synergistic decrease in cell viability in HeyA8, OVCAR8 ip1, and OVCAR5 cell lines, with a negligible effect on OVCAR4 cells. Analysis of our apoptosis data revealed that INK-128 by itself was effective in significantly increasing apoptosis

compared to control in both OVCAR4 and HeyA8 cells, however the absolute differences were small. Importantly, we found that CN210/INK-128 combination treatment produced a significant increase in apoptosis in both OVCAR8 ip1 and OVCAR5 cells, with a likely synergistic increase in the OVCAR8 ip1 cell line. As both OVCAR8 ip1 and OVCAR5 cells were shown to have large decreases in Akt activation after CN210 treatment, this may explain why these two cell lines show an enhanced interaction between CN210 and INK-128. A major target of the dual mTOR inhibitors is Akt phosphorylation, so combining them with a compound that produces additional downregulation of Akt would likely lead to an enhanced effect. Similarly, CN210 treatment also resulted in decreased Akt expression in the SKOV3 ip1 cell line, as evidenced from Western blot data (SKOV3 ip1 cells were not included in RPPA analysis). Consistently, we also found a significant increase in apoptosis using the CN210/INK-128 combination in this cell line.

Perhaps an additional explanation for the observed anti-tumor effect of CN210 in SKOV3 ip1 cells lies in the fact that they possess an *ARID1A* gene mutation, resulting in a non-functioning protein (116). ARID1A is a member of the SWI/SNF chromatin remodeling complex which has been shown to function as a tumor suppressor through its role in the regulation of histone modification (117). Cells that contain *ARID1A* gene mutations have altered epigenetic regulation and may rely on epigenetic readers such as the BET family of proteins to drive oncogenesis. It therefore seems plausible that BET inhibition might be expected to produce a stronger anti-tumor effect in SKOV3 ip1 cells harboring an *ARID1A* mutation, compared to cell lines with functional ARID1A.

To understand why the synergistic response was so pronounced in the OVCAR8 ip1 cell line we examined the protein expression of mTOR pathway proteins using Western blot after 48hr treatment with 10 uM CN210. We found that DMSO-treated OVCAR8 ip1 cells had no expression of p-Rictor whereas the CN210 treated cells had a substantial expression of p-Rictor. As Rictor is only part of the mTORC2 complex, it corresponds that combining CN210 with rapamycin would not yield a synergistic effect, whereas combination with a dual mTORC1/2 inhibitor would. We believe that the

considerable increase in apoptosis after CN210/INK-128 treatment is due to the blockade of Akt signaling mediated by both CN210 and INK-128, as well as the decreased activation of Rictor using a dual mTORC1/2 inhibitor. Similarly, OVCAR8 ip1 cells also had an increase of Raptor activation after 10 uM CN210 treatment, which adds additional strength to the necessity of dual mTORC1/2 blockade. Although as single agents, mTORC1 and dual mTORC1/2 inhibitors did not display substantial effects *in vitro*, the addition of a dual mTORC1/2 inhibitor to a BET inhibitor produced significant effects deserving of further exploration.

Addition of mTORC1/2 inhibition to BET inhibition using an in vivo model

Lastly, we demonstrated using an orthotopic ovarian cancer mouse model that combined treatment of CN210 and INK-128 produced a significant decrease in tumor weight compared to control or CN210 only. In addition, mice treated with INK-128 alone also resulted in a significant decrease in tumor weight compared to control. Our *in vivo* results were consistent with our *in vitro* findings as the SKOV3 ip1 cell line demonstrated a significant interaction between both CN210/rapamycin and CN210/INK-128 compared to the individual drugs. Although toxicity emerged in the combination group, this was easily managed by altering the dosing schedule. Importantly, toxicity emerged early and the final results of the *in vivo* experiment reflected 21 days on the new treatment schedule. These findings suggest that if toxicity was carefully monitored, this drug combination can be moved into a phase 1 clinical trial to determine its anti-tumor effect in human patients.

Limitations

As eluded to above, there were multiple limitations to this study. One limitation lies in the usage of RPPA analysis as a tool to detect changes in protein expression after drug treatment. While

this platform is highly effective in determining subtle changes in protein expression, the results may not be reproducible, nor correspond to any meaningful effect on cell function. For example, there may be a 1.05 fold change in a specific protein after drug treatment, but this small degree of change may not have any actual effect on cellular cell function. It is important to keep these points in mind when using RPPA analysis as the results are more for hypothesis generation rather than hypothesis confirmation.

A second limitation of the study involved the orthotopic *in vivo* experiment using the combination of CN210 and olaparib. As the cell line chosen for the experiment (OVCAR5) did not demonstrate a uniformly synergistic interaction between the two compounds, it is no surprise that a significant interaction was not seen using an animal model. In hindsight, choosing a cell line that demonstrated a robust combined response between the two compounds would have been a more apt choice for the experiment. Furthermore, there were multiple technical issues with this experiment. Mice were treated daily via oral gavage with either control, CN210, olaparib, or CN210/olaparib. Multiple mice died across all four groups due difficulties administering the drug using the oral gavage technique. It was surprisingly easy to mistake the trachea for the esophagus and thus multiple mice died via accidental asphyxiation. Although these technical issues were extensively addressed and corrected prior to the conclusion of the experiment, a significant number of mice died which decreased the sample number in each group, certainly limiting the statistical significance.

A third limitation is the choice of BET inhibitor. As briefly mentioned above, CN210 was used for all experiments because it has been shown to have minimal off-target effects and is thus prepped for use in the clinical setting. Had JQ1 been used for the experiments, the results might have been more profound, particularly in combination with olaparib, however this would defeat the purpose of identifying additional drugs to combine with a compound that cannot be moved into human use.

Study Implications

Although ovarian cancer remains the deadliest gynecologic malignancy, the development of multiple new treatment options over the past decade has allowed women to live longer with the disease than ever before.

While the majority of clinical trials using mTOR inhibitors have been in the endometrial cancer arena, which are known to have frequent mutations in the PI3K/Akt/mTOR pathway, there have been multiple trials examining the use of mTORC1 inhibitors in ovarian cancer (NCT01196429, NCT 01065662, NCT01281514, NCT01256268). A phase 1 trial examining the addition of everolimus to carboplatin and pegylated liposomal doxorubicin in platinum-sensitive recurrent ovarian cancer revealed a response rate of 67% with tolerable toxicities consisting of mainly hematologic and gastrointestinal (118). Additionally, the mTORC1 inhibitor ridaforolimus was examined in combination with carboplatin and paclitaxel in a phase 1 trial of solid tumor cancers. Of the 6 women with ovarian cancer included in the study, 3 had partial responses according to RECIST criteria, 2 had stable disease, and 1 had progressive disease (119).

Dual mTOR inhibitors have also been examined in women with ovarian cancer. A phase I/II clinical trial examining the use of the dual mTOR inhibitor AZD2014 (vistusertib) in combination with paclitaxel in patients with HGSOC or squamous cell NSLC revealed a response rate of 64% in ovarian cancer patients, with well tolerated side effects (100). The combination of AZD2014 and olaparib has also been examined in patients with recurrent endometrial, ovarian, and breast cancers. The authors found that women with ovarian cancer had a 20% response rate with well tolerated toxicities (120).

The clinical testing of BET inhibitors is still in its infancy however, with only a few trials including women with ovarian cancer. As mentioned above, the majority of clinical trials examining BET inhibitors are in patients with hematologic malignancies and NMCs. There is currently an ongoing phase I/IIa clinical trial assessing the effect of the BET inhibitor BMS-986158 plus nivolumab in

patients with select advanced cancers. Importantly, the dual mTOR inhibitor used in this study (INK-128) has also recently been tested in patients with advanced solid tumors (121). Interestingly, patients receiving this oral drug daily had a 12% response rate, while those receiving it weekly had a 0% response rate. When combined with weekly paclitaxel, the response rate improved to 18%.

The clinical trials discussed above support the notion that both BET inhibitors and mTOR inhibitors are tolerable and have activity in the treatment of ovarian cancer. The implications from this current study suggest that the combination of BET inhibitors and dual mTOR inhibitors would likely produce enhanced anti-tumor activity in at least some patients. As many of these trials mature and progress into phase II and phase III studies, it will be interesting to see how durable the responses are. Additionally, we found moderate synergy between BET inhibition and PARP inhibition *in vitro*, yet our results differed from the previously published studies. This suggests a need for future biomarker development in order to determine which patients may achieve the best response to PARPi/BETi combination therapy. Our results also implicate Akt activation as possible biomarker for response to combination BET/mTOR inhibition. Although additional study is needed, we also propose that mTOR activation may be a mechanism of resistance in patients treated with BET inhibitors.

Future Directions

Future directions of the data presented here entail the development of a phase I clinical trial to test the safety profile and efficacy of combination CN210/INK-128 treatment. Toxicity will have to be closely monitored as discussed above in considering our *in vivo* experiment observations. It will also be important to carefully examine why some patients respond to combined treatment whereas others do not, in order to detect new biomarkers. Based on both the *in vitro* and *in vivo* work presented here, we found that the cancer cells which displayed either increased activation of Rictor or decreased activation of Akt in response to BETi treatment, were the most likely to gain benefit from the addition

of a dual mTOR inhibitor. In fact, OVCAR8 ip1 cells demonstrated both an increase in phosphorylated-Rictor and a decrease in phosphorylated-Akt, and remarkably they were the only cell line tested to demonstrate a true synergistic effect between BET and dual mTORC inhibition. To assess the role of these possible biomarkers, a clinical trial could be designed examining combination therapy in women with recurrent epithelial ovarian cancer. After obtaining a pre-treatment biopsy to measure Akt and Rictor expression, they would begin treatment with CN210 only. The patients would then be divided into three groups based on when a 2nd biopsy would be performed. One group would have an on-treatment biopsy at 1 month, another group at 2 months, and the last group at 3 months. Akt and Rictor expression would be assessed again on these 2nd biopsies and the change in expression of the biomarkers would be calculated. INK-128 would then be given to all patients across groups that demonstrated either an increase or decrease in Rictor or Akt activation, respectively. This design would not only assess the clinical activity of combination treatment vs. CN210 only within each group, but would also help determine the ideal time to perform the 2nd biopsy. The time point of the group that demonstrated the largest difference in outcomes between combination and CN210 therapy would then serve as the standard time to re-biopsy. This could then be further examined in a larger trial comparing CN210 (+/- INK-128 based on 2nd biopsy) against standard of care treatment for recurrent epithelial cancer ("dealer's choice" -- gemcitabine, PARPi, bevacizumab, pegylated doxorubicin)

In addition, as there are already multiple clinical trials testing BET inhibitors in humans, it is conceivable to design a trial wherein patients who have progressed through or recurred after BET inhibitor treatment are given dual mTOR targeting drugs to see if this mitigates or reverses the resistant phenotype.

Conclusions

Our preclinical data used RPPA analysis to identify mTOR activation as an early adaptive change to BET inhibition in ovarian cancer cells. mTOR activation after CN210 treatment was not specific to either CN210-resistant or sensitive cells. Cells that displayed either a decrease in Akt activation or an increase in Rictor activation after CN210 treatment had the largest combined effect of CN210/INK-128 dual treatment. We also determined that synergy between BETis and PARPis exists, but not to as large a degree as previously reported, suggesting the need for identification of additional markers to determine response. Lastly, we demonstrated that the combination of CN210 and INK-128 produces a significant decrease in tumor weight using an orthotopic mouse model, providing a strong rationale for incorporation into future clinical trial design.

Bibliography

1. Siegel, R. L., K. D. Miller, and A. Jemal. 2019. Cancer statistics, 2019. *CA Cancer J Clin* 69: 7-34.

2. Torre, L. A., B. Trabert, C. E. DeSantis, K. D. Miller, G. Samimi, C. D. Runowicz, M. M. Gaudet, A. Jemal, and R. L. Siegel. 2018. Ovarian cancer statistics, 2018. *CA Cancer J Clin* 68: 284-296.

3. Jacobs, I. J., U. Menon, A. Ryan, A. Gentry-Maharaj, M. Burnell, J. K. Kalsi, N. N. Amso, S. Apostolidou, E. Benjamin, D. Cruickshank, D. N. Crump, S. K. Davies, A. Dawnay, S. Dobbs, G. Fletcher, J. Ford, K. Godfrey, R. Gunu, M. Habib, R. Hallett, J. Herod, H. Jenkins, C. Karpinskyj, S. Leeson, S. J. Lewis, W. R. Liston, A. Lopes, T. Mould, J. Murdoch, D. Oram, D. J. Rabideau, K. Reynolds, I. Scott, M. W. Seif, A. Sharma, N. Singh, J. Taylor, F. Warburton, M. Widschwendter, K. Williamson, R. Woolas, L. Fallowfield, A. J. McGuire, S. Campbell, M. Parmar, and S. J. Skates. 2016. Ovarian cancer screening and mortality in the UK Collaborative Trial of Ovarian Cancer Screening (UKCTOCS): a randomised controlled trial. *Lancet* 387: 945-956.

4. Jacobs, I. J., S. J. Skates, N. MacDonald, U. Menon, A. N. Rosenthal, A. P. Davies, R. Woolas, A. R. Jeyarajah, K. Sibley, D. G. Lowe, and D. H. Oram. 1999. Screening for ovarian cancer: a pilot randomised controlled trial. *Lancet* 353: 1207-1210.

5. Pinsky, P. F., K. Yu, B. S. Kramer, A. Black, S. S. Buys, E. Partridge, J. Gohagan, C. D. Berg, and P. C. Prorok. 2016. Extended mortality results for ovarian cancer screening in the PLCO trial with median 15years follow-up. *Gynecol Oncol* 143: 270-275.

6. Heintz, A. P., F. Odicino, P. Maisonneuve, M. A. Quinn, J. L. Benedet, W. T. Creasman, H. Y. Ngan, S. Pecorelli, and U. Beller. 2006. Carcinoma of the ovary. FIGO 26th Annual Report on the Results of Treatment in Gynecological Cancer. *Int J Gynaecol Obstet* 95 Suppl 1: S161-192.

7.   Chen, S., and G. Parmigiani. 2007. Meta-analysis of BRCA1 and BRCA2 penetrance. *J Clin Oncol* 25: 1329-1333.

8.   Berek, J. S., S. T. Kehoe, L. Kumar, and M. Friedlander. 2018. Cancer of the ovary, fallopian tube, and peritoneum. *Int J Gynaecol Obstet* 143 Suppl 2: 59-78.

9.   Winter, W. E., 3rd, G. L. Maxwell, C. Tian, J. W. Carlson, R. F. Ozols, P. G. Rose, M. Markman, D. K. Armstrong, F. Muggia, W. P. McGuire, and S. Gynecologic Oncology Group. 2007. Prognostic factors for stage III epithelial ovarian cancer: a Gynecologic Oncology Group Study. *J Clin Oncol* 25: 3621-3627.

10.   Herzog, T. J., and B. Pothuri. 2006. Ovarian cancer: a focus on management of recurrent disease. *Nat Clin Pract Oncol* 3: 604-611.

11.   Matulonis, U. A., A. K. Sood, L. Fallowfield, B. E. Howitt, J. Sehouli, and B. Y. Karlan. 2016. Ovarian cancer. *Nat Rev Dis Primers* 2: 16061.

12.   Administration, F. D. 2019. Drugs@FDA.

13.   Kelland, L. 2007. The resurgence of platinum-based cancer chemotherapy. *Nat Rev Cancer* 7: 573-584.

14.   Aggarwal, S. 2010. Targeted cancer therapies. *Nat Rev Drug Discov* 9: 427-428.

15.   Villar-Prados, A., S. Y. Wu, K. A. Court, S. Ma, C. LaFargue, M. A. Chowdhury, M. I. Engelhardt, C. Ivan, P. T. Ram, Y. Wang, K. Baggerly, C. Rodriguez-Aguayo, G. Lopez-Berestein, S. Ming-Yang, D. J. Maloney, M. Yoshioka, J. W. Strovel, J. Roszik, and A. K. Sood. 2019. Predicting Novel Therapies and Targets: Regulation of Notch3 by the Bromodomain Protein BRD4. *Mol Cancer Ther* 18: 421-436.

16.   Consortium, G. T. 2013. The Genotype-Tissue Expression (GTEx) project. *Nat Genet* 45: 580-585.

17.   Filippakopoulos, P., J. Qi, S. Picaud, Y. Shen, W. B. Smith, O. Fedorov, E. M. Morse, T. Keates, T. T. Hickman, I. Felletar, M. Philpott, S. Munro, M. R. McKeown, Y. Wang, A. L. Christie, N. West, M. J. Cameron, B. Schwartz, T. D. Heightman, N. La Thangue, C. A.

French, O. Wiest, A. L. Kung, S. Knapp, and J. E. Bradner. 2010. Selective inhibition of BET bromodomains. *Nature* 468: 1067-1073.

18. Shi, J., and C. R. Vakoc. 2014. The mechanisms behind the therapeutic activity of BET bromodomain inhibition. *Mol Cell* 54: 728-736.

19. Stathis, A., and F. Bertoni. 2018. BET Proteins as Targets for Anticancer Treatment. *Cancer Discov* 8: 24-36.

20. Delmore, J. E., G. C. Issa, M. E. Lemieux, P. B. Rahl, J. Shi, H. M. Jacobs, E. Kastritis, T. Gilpatrick, R. M. Paranal, J. Qi, M. Chesi, A. C. Schinzel, M. R. McKeown, T. P. Heffernan, C. R. Vakoc, P. L. Bergsagel, I. M. Ghobrial, P. G. Richardson, R. A. Young, W. C. Hahn, K. C. Anderson, A. L. Kung, J. E. Bradner, and C. S. Mitsiades. 2011. BET bromodomain inhibition as a therapeutic strategy to target c-Myc. *Cell* 146: 904-917.

21. Whyte, W. A., D. A. Orlando, D. Hnisz, B. J. Abraham, C. Y. Lin, M. H. Kagey, P. B. Rahl, T. I. Lee, and R. A. Young. 2013. Master transcription factors and mediator establish super-enhancers at key cell identity genes. *Cell* 153: 307-319.

22. Hnisz, D., B. J. Abraham, T. I. Lee, A. Lau, V. Saint-Andre, A. A. Sigova, H. A. Hoke, and R. A. Young. 2013. Super-enhancers in the control of cell identity and disease. *Cell* 155: 934-947.

23. Winter, G. E., A. Mayer, D. L. Buckley, M. A. Erb, J. E. Roderick, S. Vittori, J. M. Reyes, J. di Iulio, A. Souza, C. J. Ott, J. M. Roberts, R. Zeid, T. G. Scott, J. Paulk, K. Lachance, C. M. Olson, S. Dastjerdi, S. Bauer, C. Y. Lin, N. S. Gray, M. A. Kelliher, L. S. Churchman, and J. E. Bradner. 2017. BET Bromodomain Proteins Function as Master Transcription Elongation Factors Independent of CDK9 Recruitment. *Mol Cell* 67: 5-18 e19.

24. Houzelstein, D., S. L. Bullock, D. E. Lynch, E. F. Grigorieva, V. A. Wilson, and R. S. Beddington. 2002. Growth and early postimplantation defects in mice deficient for the bromodomain-containing protein Brd4. *Mol Cell Biol* 22: 3794-3802.

25.   Shang, E., X. Wang, D. Wen, D. A. Greenberg, and D. J. Wolgemuth. 2009. Double bromodomain-containing gene Brd2 is essential for embryonic development in mouse. *Dev Dyn* 238: 908-917.

26.   Gyuris, A., D. J. Donovan, K. A. Seymour, L. A. Lovasco, N. R. Smilowitz, A. L. Halperin, J. E. Klysik, and R. N. Freiman. 2009. The chromatin-targeting protein Brd2 is required for neural tube closure and embryogenesis. *Biochim Biophys Acta* 1789: 413-421.

27.   Wang, F., H. Liu, W. P. Blanton, A. Belkina, N. K. Lebrasseur, and G. V. Denis. 2009. Brd2 disruption in mice causes severe obesity without Type 2 diabetes. *Biochem J* 425: 71-83.

28.   Marcotte, R., A. Sayad, K. R. Brown, F. Sanchez-Garcia, J. Reimand, M. Haider, C. Virtanen, J. E. Bradner, G. D. Bader, G. B. Mills, D. Pe'er, J. Moffat, and B. G. Neel. 2016. Functional Genomic Landscape of Human Breast Cancer Drivers, Vulnerabilities, and Resistance. *Cell* 164: 293-309.

29.   Baratta, M. G., A. C. Schinzel, Y. Zwang, P. Bandopadhayay, C. Bowman-Colin, J. Kutt, J. Curtis, H. Piao, L. C. Wong, A. L. Kung, R. Beroukhim, J. E. Bradner, R. Drapkin, W. C. Hahn, J. F. Liu, and D. M. Livingston. 2015. An in-tumor genetic screen reveals that the BET bromodomain protein, BRD4, is a potential therapeutic target in ovarian carcinoma. *Proc Natl Acad Sci U S A* 112: 232-237.

30.   Toyoshima, M., H. L. Howie, M. Imakura, R. M. Walsh, J. E. Annis, A. N. Chang, J. Frazier, B. N. Chau, A. Loboda, P. S. Linsley, M. A. Cleary, J. R. Park, and C. Grandori. 2012. Functional genomics identifies therapeutic targets for MYC-driven cancer. *Proc Natl Acad Sci U S A* 109: 9545-9550.

31.   Zuber, J., J. Shi, E. Wang, A. R. Rappaport, H. Herrmann, E. A. Sison, D. Magoon, J. Qi, K. Blatt, M. Wunderlich, M. J. Taylor, C. Johns, A. Chicas, J. C. Mulloy, S. C. Kogan, P. Brown, P. Valent, J. E. Bradner, S. W. Lowe, and C. R. Vakoc. 2011. RNAi screen identifies Brd4 as a therapeutic target in acute myeloid leukaemia. *Nature* 478: 524-528.

32. French, C. A., S. Rahman, E. M. Walsh, S. Kuhnle, A. R. Grayson, M. E. Lemieux, N. Grunfeld, B. P. Rubin, C. R. Antonescu, S. Zhang, R. Venkatramani, P. Dal Cin, and P. M. Howley. 2014. NSD3-NUT fusion oncoprotein in NUT midline carcinoma: implications for a novel oncogenic mechanism. *Cancer Discov* 4: 928-941.

33. French, C. A., C. L. Ramirez, J. Kolmakova, T. T. Hickman, M. J. Cameron, M. E. Thyne, J. L. Kutok, J. A. Toretsky, A. K. Tadavarthy, U. R. Kees, J. A. Fletcher, and J. C. Aster. 2008. BRD-NUT oncoproteins: a family of closely related nuclear proteins that block epithelial differentiation and maintain the growth of carcinoma cells. *Oncogene* 27: 2237-2242.

34. Mertz, J. A., A. R. Conery, B. M. Bryant, P. Sandy, S. Balasubramanian, D. A. Mele, L. Bergeron, and R. J. Sims, 3rd. 2011. Targeting MYC dependence in cancer by inhibiting BET bromodomains. *Proc Natl Acad Sci U S A* 108: 16669-16674.

35. Dawson, M. A., R. K. Prinjha, A. Dittmann, G. Giotopoulos, M. Bantscheff, W. I. Chan, S. C. Robson, C. W. Chung, C. Hopf, M. M. Savitski, C. Huthmacher, E. Gudgin, D. Lugo, S. Beinke, T. D. Chapman, E. J. Roberts, P. E. Soden, K. R. Auger, O. Mirguet, K. Doehner, R. Delwel, A. K. Burnett, P. Jeffrey, G. Drewes, K. Lee, B. J. Huntly, and T. Kouzarides. 2011. Inhibition of BET recruitment to chromatin as an effective treatment for MLL-fusion leukaemia. *Nature* 478: 529-533.

36. Amorim, S., A. Stathis, M. Gleeson, S. Iyengar, V. Magarotto, X. Leleu, F. Morschhauser, L. Karlin, F. Broussais, K. Rezai, P. Herait, C. Kahatt, F. Lokiec, G. Salles, T. Facon, A. Palumbo, D. Cunningham, E. Zucca, and C. Thieblemont. 2016. Bromodomain inhibitor OTX015 in patients with lymphoma or multiple myeloma: a dose-escalation, open-label, pharmacokinetic, phase 1 study. *Lancet Haematol* 3: e196-204.

37. Lewin, J., J. C. Soria, A. Stathis, J. P. Delord, S. Peters, A. Awada, P. G. Aftimos, M. Bekradda, K. Rezai, Z. Zeng, A. Hussain, S. Perez, L. L. Siu, and C. Massard. 2018. Phase Ib Trial With Birabresib, a Small-Molecule Inhibitor of Bromodomain and Extraterminal Proteins, in Patients With Selected Advanced Solid Tumors. *J Clin Oncol*: JCO2018782292.

38.   Stathis, A., E. Zucca, M. Bekradda, C. Gomez-Roca, J. P. Delord, T. de La Motte Rouge, E. Uro-Coste, F. de Braud, G. Pelosi, and C. A. French. 2016. Clinical Response of Carcinomas Harboring the BRD4-NUT Oncoprotein to the Targeted Bromodomain Inhibitor OTX015/MK-8628. *Cancer Discov* 6: 492-500.

39.   Hottinger, A. F., M. Sanson, E. Moyal, J. Delord, K. Rezai, A. Leung, S. Perez, M. Bekradda, N. Lachaux, and O. Chinot. 2016. P08.63 Dose optimization of MK-8628 (OTX015), a small molecule inhibitor of bromodomain and extra-terminal (BET) proteins, in patients with recurrent glioblastoma. *Neuro-Oncology* 18: iv56-iv56.

40.   Berthon, C., E. Raffoux, X. Thomas, N. Vey, C. Gomez-Roca, K. Yee, D. C. Taussig, K. Rezai, C. Roumier, P. Herait, C. Kahatt, B. Quesnel, M. Michallet, C. Recher, F. Lokiec, C. Preudhomme, and H. Dombret. 2016. Bromodomain inhibitor OTX015 in patients with acute leukaemia: a dose-escalation, phase 1 study. *Lancet Haematol* 3: e186-195.

41.   Abramson, J. S., K. A. Blum, I. W. Flinn, M. Gutierrez, A. Goy, M. Maris, M. Cooper, M. O'Meara, D. Borger, J. Mertz, R. J. Sims, S. Jeffrey, and A. Younes. 2015. BET Inhibitor CPI-0610 Is Well Tolerated and Induces Responses in Diffuse Large B-Cell Lymphoma and Follicular Lymphoma: Preliminary Analysis of an Ongoing Phase 1 Study. *Blood* 126: 1491-1491.

42.   O'Dwyer, P. J., S. A. Piha-Paul, C. French, S. Harward, G. Ferron-Brady, Y. Wu, O. Barbash, A. Wyce, M. Annan, T. Horner, N. J. Parr, R. K. Prinjha, C. Carpenter, G. Shapiro, A. Dhar, and C. Hann. 2016. Abstract CT014: GSK525762, a selective bromodomain (BRD) and extra terminal protein (BET) inhibitor: results from part 1 of a phase I/II open-label single-agent study in patients with NUT midline carcinoma (NMC) and other cancers. *Cancer Research* 76: CT014-CT014.

43.   Shapiro, G. I., A. Dowlati, P. M. LoRusso, J. P. Eder, A. Anderson, K. T. Do, M. H. Kagey, C. Sirard, J. E. Bradner, and S. B. Landau. 2015. Abstract A49: Clinically efficacy of the BET

bromodomain inhibitor TEN-010 in an open-label substudy with patients with documented NUT-midline carcinoma (NMC). *Molecular Cancer Therapeutics* 14: A49-A49.

44.   Walsh, C. S. 2015. Two decades beyond BRCA1/2: Homologous recombination, hereditary cancer risk and a target for ovarian cancer therapy. *Gynecol Oncol* 137: 343-350.

45.   Valerie, K., and L. F. Povirk. 2003. Regulation and mechanisms of mammalian double-strand break repair. *Oncogene* 22: 5792-5812.

46.   Sung, P., and H. Klein. 2006. Mechanism of homologous recombination: mediators and helicases take on regulatory functions. *Nat Rev Mol Cell Biol* 7: 739-750.

47.   Schorge, J. O., S. C. Modesitt, R. L. Coleman, D. E. Cohn, N. D. Kauff, L. R. Duska, and T. J. Herzog. 2010. SGO White Paper on ovarian cancer: etiology, screening and surveillance. *Gynecol Oncol* 119: 7-17.

48.   Alsop, K., S. Fereday, C. Meldrum, A. deFazio, C. Emmanuel, J. George, A. Dobrovic, M. J. Birrer, P. M. Webb, C. Stewart, M. Friedlander, S. Fox, D. Bowtell, and G. Mitchell. 2012. BRCA mutation frequency and patterns of treatment response in BRCA mutation-positive women with ovarian cancer: a report from the Australian Ovarian Cancer Study Group. *J Clin Oncol* 30: 2654-2663.

49.   Weissman, S. M., S. M. Weiss, and A. C. Newlin. 2012. Genetic testing by cancer site: ovary. *Cancer J* 18: 320-327.

50.   LaFargue, C. J., G. Z. Dal Molin, A. K. Sood, and R. L. Coleman. 2019. Exploring and comparing adverse events between PARP inhibitors. *Lancet Oncol* 20: e15-e28.

51.   LaFargue, C. J., and K. S. Tewari. 2016. Recent Patents for Homologous Recombination Deficiency Assays Among Women with Ovarian Cancer. *Recent Pat Biotechnol* 9: 86-101.

52.   Oncology, C. 2018. Full Prescribing Information for Rubraca® (rucaparib). In *www.rubraca.com*. C. Oncology, ed.

53.   AstraZeneca. 2018. Full Prescribing Information for Lynparza® (Olaparib). In *www.azpicentral.com*. AstraZeneca, ed.

54. Tesaro, I. 2017. Full Prescribing Information for Zejula® (niraparib). In *www.zejula.com/en/about*. I. Tesaro, ed.

55. Coleman, R. L., A. M. Oza, D. Lorusso, C. Aghajanian, A. Oaknin, A. Dean, N. Colombo, J. I. Weberpals, A. Clamp, G. Scambia, A. Leary, R. W. Holloway, M. A. Gancedo, P. C. Fong, J. C. Goh, D. M. O'Malley, D. K. Armstrong, J. Garcia-Donas, E. M. Swisher, A. Floquet, G. E. Konecny, I. A. McNeish, C. L. Scott, T. Cameron, L. Maloney, J. Isaacson, S. Goble, C. Grace, T. C. Harding, M. Raponi, J. Sun, K. K. Lin, H. Giordano, J. A. Ledermann, and A. investigators. 2017. Rucaparib maintenance treatment for recurrent ovarian carcinoma after response to platinum therapy (ARIEL3): a randomised, double-blind, placebo-controlled, phase 3 trial. *Lancet* 390: 1949-1961.

56. Pujade-Lauraine, E., J. A. Ledermann, F. Selle, V. Gebski, R. T. Penson, A. M. Oza, J. Korach, T. Huzarski, A. Poveda, S. Pignata, M. Friedlander, N. Colombo, P. Harter, K. Fujiwara, I. Ray-Coquard, S. Banerjee, J. Liu, E. S. Lowe, R. Bloomfield, P. Pautier, and S. O. E.-O. investigators. 2017. Olaparib tablets as maintenance therapy in patients with platinum-sensitive, relapsed ovarian cancer and a BRCA1/2 mutation (SOLO2/ENGOT-Ov21): a double-blind, randomised, placebo-controlled, phase 3 trial. *Lancet Oncol* 18: 1274-1284.

57. Mirza, M. R., B. J. Monk, J. Herrstedt, A. M. Oza, S. Mahner, A. Redondo, M. Fabbro, J. A. Ledermann, D. Lorusso, I. Vergote, N. E. Ben-Baruch, C. Marth, R. Madry, R. D. Christensen, J. S. Berek, A. Dorum, A. V. Tinker, A. du Bois, A. Gonzalez-Martin, P. Follana, B. Benigno, P. Rosenberg, L. Gilbert, B. J. Rimel, J. Buscema, J. P. Balser, S. Agarwal, U. A. Matulonis, and E.-O. N. Investigators. 2016. Niraparib Maintenance Therapy in Platinum-Sensitive, Recurrent Ovarian Cancer. *N Engl J Med* 375: 2154-2164.

58. Satoh, M. S., and T. Lindahl. 1992. Role of poly(ADP-ribose) formation in DNA repair. *Nature* 356: 356-358.

59.   Gogola, E., S. Rottenberg, and J. Jonkers. 2019. Resistance to PARP Inhibitors: Lessons from Preclinical Models of BRCA-Associated Cancer. *Annual Review of Cancer Biology* 3: 235-254.

60.   Lord, C. J., and A. Ashworth. 2013. Mechanisms of resistance to therapies targeting BRCA-mutant cancers. *Nat Med* 19: 1381-1388.

61.   Laplante, M., and D. M. Sabatini. 2012. mTOR signaling in growth control and disease. *Cell* 149: 274-293.

62.   Potter, C. J., L. G. Pedraza, and T. Xu. 2002. Akt regulates growth by directly phosphorylating Tsc2. *Nat Cell Biol* 4: 658-665.

63.   Sancak, Y., C. C. Thoreen, T. R. Peterson, R. A. Lindquist, S. A. Kang, E. Spooner, S. A. Carr, and D. M. Sabatini. 2007. PRAS40 is an insulin-regulated inhibitor of the mTORC1 protein kinase. *Mol Cell* 25: 903-915.

64.   Vander Haar, E., S. I. Lee, S. Bandhakavi, T. J. Griffin, and D. H. Kim. 2007. Insulin signalling to mTOR mediated by the Akt/PKB substrate PRAS40. *Nat Cell Biol* 9: 316-323.

65.   Wang, L., T. E. Harris, R. A. Roth, and J. C. Lawrence, Jr. 2007. PRAS40 regulates mTORC1 kinase activity by functioning as a direct inhibitor of substrate binding. *J Biol Chem* 282: 20036-20044.

66.   Ma, X. M., and J. Blenis. 2009. Molecular mechanisms of mTOR-mediated translational control. *Nat Rev Mol Cell Biol* 10: 307-318.

67.   Inoki, K., T. Zhu, and K. L. Guan. 2003. TSC2 mediates cellular energy response to control cell growth and survival. *Cell* 115: 577-590.

68.   Gwinn, D. M., D. B. Shackelford, D. F. Egan, M. M. Mihaylova, A. Mery, D. S. Vasquez, B. E. Turk, and R. J. Shaw. 2008. AMPK phosphorylation of raptor mediates a metabolic checkpoint. *Mol Cell* 30: 214-226.

69. Kim, D. H., D. D. Sarbassov, S. M. Ali, J. E. King, R. R. Latek, H. Erdjument-Bromage, P. Tempst, and D. M. Sabatini. 2002. mTOR interacts with raptor to form a nutrient-sensitive complex that signals to the cell growth machinery. *Cell* 110: 163-175.

70. Liu, P., W. Gan, Y. R. Chin, K. Ogura, J. Guo, J. Zhang, B. Wang, J. Blenis, L. C. Cantley, A. Toker, B. Su, and W. Wei. 2015. PtdIns(3,4,5)P3-Dependent Activation of the mTORC2 Kinase Complex. *Cancer Discov* 5: 1194-1209.

71. Yang, G., D. S. Murashige, S. J. Humphrey, and D. E. James. 2015. A Positive Feedback Loop between Akt and mTORC2 via SIN1 Phosphorylation. *Cell Rep* 12: 937-943.

72. Sarbassov, D. D., D. A. Guertin, S. M. Ali, and D. M. Sabatini. 2005. Phosphorylation and regulation of Akt/PKB by the rictor-mTOR complex. *Science* 307: 1098-1101.

73. Sarbassov, D. D., S. M. Ali, D. H. Kim, D. A. Guertin, R. R. Latek, H. Erdjument-Bromage, P. Tempst, and D. M. Sabatini. 2004. Rictor, a novel binding partner of mTOR, defines a rapamycin-insensitive and raptor-independent pathway that regulates the cytoskeleton. *Curr Biol* 14: 1296-1302.

74. Yu, Y., S. O. Yoon, G. Poulogiannis, Q. Yang, X. M. Ma, J. Villen, N. Kubica, G. R. Hoffman, L. C. Cantley, S. P. Gygi, and J. Blenis. 2011. Phosphoproteomic analysis identifies Grb10 as an mTORC1 substrate that negatively regulates insulin signaling. *Science* 332: 1322-1326.

75. Hsu, P. P., S. A. Kang, J. Rameseder, Y. Zhang, K. A. Ottina, D. Lim, T. R. Peterson, Y. Choi, N. S. Gray, M. B. Yaffe, J. A. Marto, and D. M. Sabatini. 2011. The mTOR-regulated phosphoproteome reveals a mechanism of mTORC1-mediated inhibition of growth factor signaling. *Science* 332: 1317-1322.

76. Feng, Z., H. Zhang, A. J. Levine, and S. Jin. 2005. The coordinate regulation of the p53 and mTOR pathways in cells. *Proc Natl Acad Sci U S A* 102: 8204-8209.

77.   Hietakangas, V., and S. M. Cohen. 2008. TOR complex 2 is needed for cell cycle progression and anchorage-independent growth of MCF7 and PC3 tumor cells. *BMC Cancer* 8: 282.

78.   Masri, J., A. Bernath, J. Martin, O. D. Jo, R. Vartanian, A. Funk, and J. Gera. 2007. mTORC2 activity is elevated in gliomas and promotes growth and cell motility via overexpression of rictor. *Cancer Res* 67: 11712-11720.

79.   Sabatini, D. M., H. Erdjument-Bromage, M. Lui, P. Tempst, and S. H. Snyder. 1994. RAFT1: a mammalian protein that binds to FKBP12 in a rapamycin-dependent fashion and is homologous to yeast TORs. *Cell* 78: 35-43.

80.   Brown, E. J., M. W. Albers, T. B. Shin, K. Ichikawa, C. T. Keith, W. S. Lane, and S. L. Schreiber. 1994. A mammalian protein targeted by G1-arresting rapamycin-receptor complex. *Nature* 369: 756-758.

81.   Oncology, P. 2018. Full Prescribing Information for TORISEL® (temsirolimus). In *https://www.pfizerpro.com/product/torisel/rcc*. P. Oncology, ed.

82.   Corporation, N. P. 2018. Full Prescribing information for Afinitor® (Everolimus). N. P. Corporation, ed, https://www.us.afinitor.com/.

83.   Janes, M. R., J. J. Limon, L. So, J. Chen, R. J. Lim, M. A. Chavez, C. Vu, M. B. Lilly, S. Mallya, S. T. Ong, M. Konopleva, M. B. Martin, P. Ren, Y. Liu, C. Rommel, and D. A. Fruman. 2010. Effective and selective targeting of leukemia cells using a TORC1/2 kinase inhibitor. *Nat Med* 16: 205-213.

84.   Thoreen, C. C., S. A. Kang, J. W. Chang, Q. Liu, J. Zhang, Y. Gao, L. J. Reichling, T. Sim, D. M. Sabatini, and N. S. Gray. 2009. An ATP-competitive mammalian target of rapamycin inhibitor reveals rapamycin-resistant functions of mTORC1. *J Biol Chem* 284: 8023-8032.

85.   Garcia-Martinez, J. M., J. Moran, R. G. Clarke, A. Gray, S. C. Cosulich, C. M. Chresta, and D. R. Alessi. 2009. Ku-0063794 is a specific inhibitor of the mammalian target of rapamycin (mTOR). *Biochem J* 421: 29-42.

86.   Falcon, B. L., S. Barr, P. C. Gokhale, J. Chou, J. Fogarty, P. Depeille, M. Miglarese, D. M. Epstein, and D. M. McDonald. 2011. Reduced VEGF production, angiogenesis, and vascular regrowth contribute to the antitumor properties of dual mTORC1/mTORC2 inhibitors. *Cancer Res* 71: 1573-1583.

87.   Feldman, M. E., B. Apsel, A. Uotila, R. Loewith, Z. A. Knight, D. Ruggero, and K. M. Shokat. 2009. Active-site inhibitors of mTOR target rapamycin-resistant outputs of mTORC1 and mTORC2. *PLoS Biol* 7: e38.

88.   Yu, K., C. Shi, L. Toral-Barza, J. Lucas, B. Shor, J. E. Kim, W. G. Zhang, R. Mahoney, C. Gaydos, L. Tardio, S. K. Kim, R. Conant, K. Curran, J. Kaplan, J. Verheijen, S. Ayral-Kaloustian, T. S. Mansour, R. T. Abraham, A. Zask, and J. J. Gibbons. 2010. Beyond rapalog therapy: preclinical pharmacology and antitumor activity of WYE-125132, an ATP-competitive and specific inhibitor of mTORC1 and mTORC2. *Cancer Res* 70: 621-631.

89.   Yu, K., L. Toral-Barza, C. Shi, W. G. Zhang, J. Lucas, B. Shor, J. Kim, J. Verheijen, K. Curran, D. J. Malwitz, D. C. Cole, J. Ellingboe, S. Ayral-Kaloustian, T. S. Mansour, J. J. Gibbons, R. T. Abraham, P. Nowak, and A. Zask. 2009. Biochemical, cellular, and in vivo activity of novel ATP-competitive and selective inhibitors of the mammalian target of rapamycin. *Cancer Res* 69: 6232-6240.

90.   Obata, K., S. J. Morland, R. H. Watson, A. Hitchcock, G. Chenevix-Trench, E. J. Thomas, and I. G. Campbell. 1998. Frequent PTEN/MMAC mutations in endometrioid but not serous or mucinous epithelial ovarian tumors. *Cancer Res* 58: 2095-2097.

91.   Levine, D. A., F. Bogomolniy, C. J. Yee, A. Lash, R. R. Barakat, P. I. Borgen, and J. Boyd. 2005. Frequent mutation of the PIK3CA gene in ovarian and breast cancers. *Clin Cancer Res* 11: 2875-2878.

92.   Philp, A. J., I. G. Campbell, C. Leet, E. Vincan, S. P. Rockman, R. H. Whitehead, R. J. Thomas, and W. A. Phillips. 2001. The phosphatidylinositol 3'-kinase p85alpha gene is an oncogene in human ovarian and colon tumors. *Cancer Res* 61: 7426-7429.

93.   Cheng, J. Q., A. K. Godwin, A. Bellacosa, T. Taguchi, T. F. Franke, T. C. Hamilton, P. N. Tsichlis, and J. R. Testa. 1992. AKT2, a putative oncogene encoding a member of a subfamily of protein-serine/threonine kinases, is amplified in human ovarian carcinomas. *Proc Natl Acad Sci U S A* 89: 9267-9271.

94.   Carpten, J. D., A. L. Faber, C. Horn, G. P. Donoho, S. L. Briggs, C. M. Robbins, G. Hostetter, S. Boguslawski, T. Y. Moses, S. Savage, M. Uhlik, A. Lin, J. Du, Y. W. Qian, D. J. Zeckner, G. Tucker-Kellogg, J. Touchman, K. Patel, S. Mousses, M. Bittner, R. Schevitz, M. H. Lai, K. L. Blanchard, and J. E. Thomas. 2007. A transforming mutation in the pleckstrin homology domain of AKT1 in cancer. *Nature* 448: 439-444.

95.   http://www.cbioportal.org/public-portal/., c. f. C. G.

96.   Montero, J. C., X. Chen, A. Ocana, and A. Pandiella. 2012. Predominance of mTORC1 over mTORC2 in the regulation of proliferation of ovarian cancer cells: therapeutic implications. *Mol Cancer Ther* 11: 1342-1352.

97.   Mabuchi, S., H. Kuroda, R. Takahashi, and T. Sasano. 2015. The PI3K/AKT/mTOR pathway as a therapeutic target in ovarian cancer. *Gynecol Oncol* 137: 173-179.

98.   Behbakht, K., M. W. Sill, K. M. Darcy, S. C. Rubin, R. S. Mannel, S. Waggoner, R. J. Schilder, K. Q. Cai, A. K. Godwin, and R. K. Alpaugh. 2011. Phase II trial of the mTOR inhibitor, temsirolimus and evaluation of circulating tumor cells and tumor biomarkers in persistent and recurrent epithelial ovarian and primary peritoneal malignancies: a Gynecologic Oncology Group study. *Gynecol Oncol* 123: 19-26.

99.   Fu, S., B. T. Hennessy, C. S. Ng, Z. Ju, K. R. Coombes, J. K. Wolf, A. K. Sood, C. F. Levenback, R. L. Coleman, J. J. Kavanagh, D. M. Gershenson, M. Markman, K. Dice, A. Howard, J. Li, Y. Li, K. Stemke-Hale, M. Dyer, E. Atkinson, E. Jackson, V. Kundra, R. Kurzrock, R. C. Bast, Jr., and G. B. Mills. 2012. Perifosine plus docetaxel in patients with platinum and taxane resistant or refractory high-grade epithelial ovarian cancer. *Gynecol Oncol* 126: 47-53.

100. Basu, B., M. G. Krebs, R. Sundar, R. H. Wilson, J. Spicer, R. Jones, M. Brada, D. C. Talbot, N. Steele, A. H. Ingles Garces, W. Brugger, E. A. Harrington, J. Evans, E. Hall, H. Tovey, F. M. de Oliveira, S. Carreira, K. Swales, R. Ruddle, F. I. Raynaud, B. Purchase, J. C. Dawes, M. Parmar, A. J. Turner, N. Tunariu, S. Banerjee, J. S. de Bono, and U. Banerji. 2018. Vistusertib (dual m-TORC1/2 inhibitor) in combination with paclitaxel in patients with high-grade serous ovarian and squamous non-small-cell lung cancer. *Ann Oncol* 29: 1918-1925.

101. Zhang, Z., P. Ma, Y. Jing, Y. Yan, M. C. Cai, M. Zhang, S. Zhang, H. Peng, Z. L. Ji, W. Di, Z. Gu, W. Q. Gao, and G. Zhuang. 2016. BET Bromodomain Inhibition as a Therapeutic Strategy in Ovarian Cancer by Downregulating FoxM1. *Theranostics* 6: 219-230.

102. Cancer Genome Atlas Research, N. 2011. Integrated genomic analyses of ovarian carcinoma. *Nature* 474: 609-615.

103. Landen, C. N., Jr., B. Goodman, A. A. Katre, A. D. Steg, A. M. Nick, R. L. Stone, L. D. Miller, P. V. Mejia, N. B. Jennings, D. M. Gershenson, R. C. Bast, Jr., R. L. Coleman, G. Lopez-Berestein, and A. K. Sood. 2010. Targeting aldehyde dehydrogenase cancer stem cells in ovarian cancer. *Mol Cancer Ther* 9: 3186-3199.

104. Yokoyama, Y., H. Zhu, J. H. Lee, A. V. Kossenkov, S. Y. Wu, J. M. Wickramasinghe, X. Yin, K. C. Palozola, A. Gardini, L. C. Showe, K. S. Zaret, Q. Liu, D. Speicher, J. R. Conejo-Garcia, J. E. Bradner, Z. Zhang, A. K. Sood, T. Ordog, B. G. Bitler, and R. Zhang. 2016. BET Inhibitors Suppress ALDH Activity by Targeting ALDH1A1 Super-Enhancer in Ovarian Cancer. *Cancer Res* 76: 6320-6330.

105. Zhu, H., F. Bengsch, N. Svoronos, M. R. Rutkowski, B. G. Bitler, M. J. Allegrezza, Y. Yokoyama, A. V. Kossenkov, J. E. Bradner, J. R. Conejo-Garcia, and R. Zhang. 2016. BET Bromodomain Inhibition Promotes Anti-tumor Immunity by Suppressing PD-L1 Expression. *Cell Rep* 16: 2829-2837.

106. Jing, Y., Z. Zhang, P. Ma, S. An, Y. Shen, L. Zhu, and G. Zhuang. 2016. Concomitant BET and MAPK blockade for effective treatment of ovarian cancer. *Oncotarget* 7: 2545-2554.

107. Sun, C., J. Yin, Y. Fang, J. Chen, K. J. Jeong, X. Chen, C. P. Vellano, Z. Ju, W. Zhao, D. Zhang, Y. Lu, F. Meric-Bernstam, T. A. Yap, M. Hattersley, M. J. O'Connor, H. Chen, S. Fawell, S. Y. Lin, G. Peng, and G. B. Mills. 2018. BRD4 Inhibition Is Synthetic Lethal with PARP Inhibitors through the Induction of Homologous Recombination Deficiency. *Cancer Cell* 33: 401-416 e408.

108. Karakashev, S., H. Zhu, Y. Yokoyama, B. Zhao, N. Fatkhutdinov, A. V. Kossenkov, A. J. Wilson, F. Simpkins, D. Speicher, D. Khabele, B. G. Bitler, and R. Zhang. 2017. BET Bromodomain Inhibition Synergizes with PARP Inhibitor in Epithelial Ovarian Cancer. *Cell Rep* 21: 3398-3405.

109. Yang, L., Y. Zhang, W. Shan, Z. Hu, J. Yuan, J. Pi, Y. Wang, L. Fan, Z. Tang, C. Li, X. Hu, J. L. Tanyi, Y. Fan, Q. Huang, K. Montone, C. V. Dang, and L. Zhang. 2017. Repression of BET activity sensitizes homologous recombination-proficient cancers to PARP inhibition. *Sci Transl Med* 9.

110. Kurimchak, A. M., C. Shelton, K. E. Duncan, K. J. Johnson, J. Brown, S. O'Brien, R. Gabbasov, L. S. Fink, Y. Li, N. Lounsbury, M. Abou-Gharbia, W. E. Childers, D. C. Connolly, J. Chernoff, J. R. Peterson, and J. S. Duncan. 2016. Resistance to BET Bromodomain Inhibitors Is Mediated by Kinome Reprogramming in Ovarian Cancer. *Cell Rep* 16: 1273-1286.

111. Center, T. U. o. T. M. A. C. 2019. Functional Proteomics RPPA Core Facility -- Education and References.

112. de Hoon, M. J., S. Imoto, J. Nolan, and S. Miyano. 2004. Open source clustering software. *Bioinformatics* 20: 1453-1454.

113. Saldanha, A. J. 2004. Java Treeview--extensible visualization of microarray data. *Bioinformatics* 20: 3246-3248.

114. Institute, B. 2019. Cancer Cell Line Encyclopedia.

115.   Saxton, R. A., and D. M. Sabatini. 2017. mTOR Signaling in Growth, Metabolism, and Disease. *Cell* 169: 361-371.

116.   Domcke, S., R. Sinha, D. A. Levine, C. Sander, and N. Schultz. 2013. Evaluating cell lines as tumour models by comparison of genomic profiles. *Nat Commun* 4: 2126.

117.   Wu, J. N., and C. W. Roberts. 2013. ARID1A mutations in cancer: another epigenetic tumor suppressor? *Cancer Discov* 3: 35-43.

118.   Martin, L. P., A. Jain, C. Chu, G. Mantia-Smaldone, S. C. Rubin, E. A. Ross, and R. J. Schilder. 2018. Phase I study of carboplatin (C), pegylated liposomal doxorubicin (PLD) and everolimus (E) in platinum-sensitive epithelial ovarian, Fallopian tube or primary peritoneal cancer in first relapse (NCT01281514). *Journal of Clinical Oncology* 36: 5580-5580.

119.   Chon, H. S., S. Kang, J. K. Lee, S. M. Apte, M. M. Shahzad, I. Williams-Elson, and R. M. Wenham. 2017. Phase I study of oral ridaforolimus in combination with paclitaxel and carboplatin in patients with solid tumor cancers. *BMC Cancer* 17: 407.

120.   Westin, S. N., J. K. Litton, R. A. Williams, C. J. Shepherd, W. Brugger, E. J. Pease, P. T. Soliman, M. M. Frumovitz, C. F. Levenback, A. Sood, L. Meyer, S. L. Moulder, V. Valero, S. Saleem, A. M. Rodriguez, A. Cyriac, L. Engerman, C. Samuel, G. B. Mills, and R. L. Coleman. 2018. Phase I trial of olaparib (PARP inhibitor) and vistusertib (mTORC1/2 inhibitor) in recurrent endometrial, ovarian and triple negative breast cancer. *Journal of Clinical Oncology* 36: 5504-5504.

121.   Moore, K. N., T. M. Bauer, G. S. Falchook, S. Chowdhury, C. Patel, R. Neuwirth, A. Enke, F. Zohren, and M. R. Patel. 2018. Phase I study of the investigational oral mTORC1/2 inhibitor sapanisertib (TAK-228): tolerability and food effects of a milled formulation in patients with advanced solid tumours. *ESMO Open* 3: e000291.

Vita

Christopher John LaFargue was born in Oakland, California, the only son of Craig and Linda LaFargue. He was raised in the California Bay Area and graduated from De La Salle High School in Concord, California, in 2002. He then moved to Boston, Massachusetts where he began his undergraduate studies at Boston University. He received a Bachelor of Arts in biochemistry and molecular biology with a minor in music composition. He then began work in the prostate cancer research field under the mentorship of Dr. Mark A. Rubin at the Brigham and Women's Hospital in Boston, Massachusetts. After Dr. Rubin was offered a vice-chairman position at Weill Cornell Medical School in New York City, New York, he asked Chris to accompany him to continue his research and help Dr. Rubin setup the new lab. Chris spent two additional years at Weill Cornell Medical School before matriculating at New York Medical College in Valhalla, New York, in 2009. He received his medical degree from this institution in 2013 and then moved back to California where he entered the Obstetrics and Gynecology residency program at the University of California – Irvine, in Orange, California. He completed his training in 2017 and then began a fellowship in Gynecology Oncology at the University of Texas M.D. Anderson Cancer Center. His two year Master's program during this fellowship was mentored by Dr. Anil Sood and focused on novel therapeutic development in ovarian cancer.

Permanent Address:

8910 Sungate Drive

Pearland, TX 77584